

A mis padres y mi hermana
A Iván

A la memoria de Alberto Serrano,
que nos dejó la misma semana de comenzar el trabajo de esta tesis.

Acknowledgements

I would like to deeply thank Susana Marcos for her the guidance and support in the development of this thesis. And further thanks to my colleagues from the laboratory.

I would like to acknowledge to Frank Schaeffel for his interest, help and useful recommendations during these experiments and their members from Frank Schaeffel' lab for their support during the visit to Department of Pathophysiology of Vision and Neuroophthalmology in University Eye Hospital in Tuebingen in January of 2003.

I would like to thank the Instituto de Oftalmobiología Aplicada (IOBA) Universidad de Valladolid to provide resources and expertise to conduct this project, particularly Jesús Merayo and Guadalupe Rodríguez. Their help has been extraordinary in all the procedures with the Faculty of Medicine animal facilities. Guadalupe Rodríguez also contributed enormously in data collection and laboratory support. All members of the refractive surgery unit have been extremely supportive to conduct refractive surgery in the chicks. And Rodrigo Torres and Tomás Blanco Mezquita for chick surgery treatments.

I also thank people from Visual Optics and Biophotonics lab, Lourdes Llorente, for her great help in the preparation and validation of the aberrometer, her collaboration in mice measurements and their advices on image processing routines, Sergio Barbero, Carlos Dorronsoro and Patricia Rosales for their great help and advices during Hartmann Shack building and a lot of features in relation with this work, Sergio Ortiz for implementation of automatic shutter in the Hartmann Shack system, and Alberto de Castro for developing the keratometer.

Thank you very much.

Grants and fundings:

- CSIC Predoctoral fellowship Unidad Asociada IOBA/Universidad de Valladolid – Instituto de Optica/ CSIC to Elena García de la Cera.
- Grant # BFM2002-02638, Ministerio de Ciencia y Tecnología, Spain. “Role of ocular aberrations in the development and compensation of refractive errors”, 2002-2005.
- Grants #CAM08.7/004.1/2003, Consejería de Educacion Comunidad Autónoma de Madrid to Susana Marcos. “Optical and visual quality in patients after cataract surgery: study of new aspheric and multifocal IOL designs”,2003-2004, and GR/SAL/0387/2004, "Development and application of new technologies to the evaluation of cataract surgery", 2005.
- FIS2005-04382, Ministerio de Educación y Ciencia, Spain, “Optical Properties of the anterior segment of the eye. Application to the correction of refractive errors and presbyopia”, 2005-2008.
- Integrated Action Germany-Spain #HA-2003-02638 to Susana Marcos and # D/03/40332 ,DAAD, Deutscher Akademischer Austausch Dienst, to Frank Schaeffel., Ministerio de Educación y Ciencia, España, “Optical Quality in an experimental animal model", 2003-2005.
- European Young Investigator Award, European Science Foundation to Susana Marcos, Physical and Technological approaches to the understanding and correction of myopia and presbyopia, 2005-2011.

Agradecimientos

2 de Octubre 2007

Desde la oportunidad que me brinda esta página de agradecimientos de mi tesis doctoral es mi intención recordar a todas y cada una de las personas que, de algún modo, me han ayudado, corregido, animado, confiado o, simplemente acompañado, en todos estos años de formación.

Me siento infinitamente agradecida a Dra. Susana Marcos, directora de esta tesis y principal responsable de todo mi trabajo durante estos años en el Instituto de Óptica del Consejo Superior de Investigaciones Científicas. No fue sólo su gran formación y vocación, que le hacen entregarse a algo tan altruista como el mundo científico, lo que más me animó a realizar esta tesis bajo su dirección, sino su confianza en mi trabajo y el tiempo que me dedicó que, hasta en los momentos de dudas, no dejó de mostrarme. He aprendido mucho de ella, desde el punto de vista científico y de la investigación, pero lo que más me llevo de estos años es el ejemplo de Susana, de que con trabajo y esfuerzo se puede conseguir mucho, y que la confianza que otros depositan en lo que haces es casi más importante. Esto lo he asumido como algo fundamental para mi labor docente. Gracias además por su infinidad de correcciones y creer que yo era capaz de sacar este trabajo adelante.

Gracias, Susana, por esa primera entrevista en la que conseguiste transmitirme el entusiasmo por el mundo de la investigación y aquella reunión más adelante, en la que volviste a hacerlo cuando no tenía las cosas muy claras y supiste adaptarte a mi nueva situación, quizá fue el momento más importante para mí. Gracias.

Gracias a mis padres y a mi hermana. Mi educación, formación y posterior dedicación al mundo científico y docente no habría sido posible sin su esfuerzo y, en ocasiones, sacrificio personal. De ellos recibí ánimos y total confianza en mis decisiones, y con algo que me ha sido muy útil durante mi vida y también el trabajo de esta tesis: su ejemplo de entrega, esfuerzo y de dedicación.

Gracias a Iván, por estar cerca, por ayudarme en todo lo que ha podido y por ser la principal “víctima” de mis últimos meses de tesis.

A mis compañeros del laboratorio del CSIC. A Lourdes, por sus conversaciones científicas y no tan científicas que compartimos y que personalmente me ayudaron tanto. Con ella y Patricia pasé muchas horas de “sótano”, les tengo que agradecer todo lo que me escucharon y ayudaron. A Sergio Barbero, Carlos Dorronsoro, Daniel Cano, Sergio Ortiz, Alberto Castro gracias por ayudarme siempre que lo he necesitado. Y a las últimas incorporaciones: Lucie, Jose, Enrique y Alfonso, que me pillaron en mi época más “autista”, mil gracias por tener siempre una palabra agradable al pasar por el laboratorio. Y a Carlos Meneses por solucionar todos los problemas “informáticos” sobre la marcha.

Un agradecimiento especial merece el Profesor Frank Schaeffel, por su acogida en su laboratorio de Tübingen, Alemania, en Enero de 2003 y todo lo que a lo largo de esta tesis me enseñó sobre el manejo de pollos y ratones.

Quiero agradecer al IOBA y al Dr. Jesús Merayo (Instituto de Oftalmobiología Aplicada de Valladolid) el permitirme realizar el programa de doctorado interdisciplinar en “Ciencias de la Visión” y la programación de los experimentos con modelos animales en sus instalaciones. Muchísimas gracias a Guadalupe, óptico optometrista del IOBA, que colaboró todo lo que pudo y más. Muchas gracias por su disponibilidad, mucho de este trabajo se lo debo a ella. Quiero agradecer también a Rodrigo Torres y Tomás Blanco, por su colaboración en las cirugías.

Es justo acordarme de mis amigos que han “padecido” mi falta de tiempo. Gracias a Santi, por estar tan pendiente y tener tanto interés en todo lo que hacía. También a Bea, Alberto, BB, Mercedes, Alfonso, Jose Luís, Luís y Pablo por estar siempre tan cerca.

A mis compañeros de trabajo en el colegio por su interés y por estar siempre dispuestos a sustituirme cuando iba a congresos, charlas etc... y por tratar de entender “eso de los pollos”.

Anterior a esta tesis, pero que también influyó en mi formación, mis profesores, personas que con su trabajo y ejemplo me dirigieron hacia una formación científica. Y a los profesores de la Escuela de Óptica de la Universidad Complutense, a Margarita Mallol, con quien escribí mi primer artículo; y de la Facultad de Ciencias de la Universidad Autónoma de Madrid, a Mercedes Carrascosa con quien hice mis primeros pinitos en un proyecto de investigación, por hacerme sentir el gusanillo por una tesis doctoral. A Cris, Ele, David, Tres, Iván, Nela, Esme... y tantos otros, compañeros de la Facultad de Física, que hicieron tan importante esos años de decisiones en la Facultad.

Al personal de administración del Instituto de Óptica del CSIC, sobre todo a Eloy, Chari y Encarnita, ¡todavía recuerdo la carrera que se dio Encarnita con todos mis papeles para la solicitud de la beca!, ¡llegó!, y a M^aPaz que nunca pierde la sonrisa. Y al del Instituto de Oftalmobiología Aplicada de Valladolid, especialmente a Yolanda y a Lurdes, por facilitar todos los trámites “a distancia” y su disponibilidad.

Y a Gloria Fuertes, por dedicarle un cuento a “Piopio Lope, el pollito miope”.

26 de Abril de 2008

Después de casi un año de espera para la defensa de esta tesis debido a problemas de salud, quiero agradecer a Susana y al tribunal de tesis su paciencia e interés.

Y a todos los que durante este tiempo os habéis interesado por mí, mil gracias. Ha sido muy importante sentirme acompañada. Creo que mucho de lo que he sido capaz de afrontar durante este tiempo ha sido gracias al apoyo de tantísimas personas que os habéis hecho sentir cerca.

Ahora he vivido más de cerca la importancia de avanzar en el conocimiento científico y en la investigación, y la necesidad de un esfuerzo de la sociedad para apoyar a aquellas personas que hoy en día trabajan en los distintos campos científicos, y que cuya motivación es dar mayor conocimiento, calidad y esperanza de vida.

Gracias a los investigadores, sea cual sea su campo científico, que han tenido que sacrificarse personal y económicamente para poder abrirse camino en el campo de la investigación. Nunca se podrá recompensar ese esfuerzo.

Índice

Capítulo 1: Introducción	1
1.1. Miopía	3
1.1.1. <i>Prevalencia</i>	4
1.1.2. <i>Etiología</i>	7
1.1.3. <i>Genética</i>	7
1.1.4. <i>Trabajo de cerca y factores relacionados</i>	8
1.1.5. <i>Proceso de emetropización</i>	11
1.1.6. <i>Modelos animales de miopía</i>	12
1.1.6.1. <i>Modelo de pollo</i>	12
1.1.6.2. <i>Modelo de ratón</i>	14
1.1.7. <i>Relación con la miopía humana</i>	15
1.2. Calidad óptica ocular	16
1.2.1. <i>Polinomios de Zernike</i>	19
1.2.2. <i>Métricas de calidad óptica</i>	20
1.2.2.1. <i>RMS</i>	20
1.2.2.2. <i>PSF, MTF y OTF</i>	20
1.2.2.3. <i>Strehl ratio</i>	21
1.2.3. <i>Técnicas de medidas de aberraciones</i>	21
1.2.4. <i>Aberraciones oculares en humanos</i>	23
1.2.5. <i>Aberraciones de alto orden y miopía</i>	24
1.2.6. <i>Aberraciones: Modelos animales</i>	25
1.2.7. <i>¿Por qué es relevante encontrar la relación entre aberraciones oculares y miopía?</i>	26
1.3. Hipótesis y objetivos	27
Capítulo 2: Métodos	29
2.1. Medida de aberraciones oculares	32
2.1.1. <i>Montaje Hartmann Shack</i>	33
2.1.1.1. <i>Canal de iluminación</i>	34
2.1.1.2. <i>Canal de detección</i>	35
2.1.1.3. <i>Monitorización de pupila</i>	36
2.1.2. <i>Control automático y procesado de datos</i>	36
2.1.3. <i>Alineamiento y calibración del sistema</i>	38
2.1.3.1. <i>Colocación de microlentes y cámaras</i>	39
2.1.3.2. <i>Ojo artificial</i>	40
2.1.3.3. <i>Calibración del Sistema de Badal</i>	40
2.1.4. <i>Validación de medida de aberraciones</i>	41
2.1.4.1. <i>Medidas esféricas y cilíndricas</i>	41
2.1.4.2. <i>Aberraciones de alto orden</i>	42
2.2. Medida de parámetros biométricos	43
2.2.1. <i>Error refractivo</i>	43
2.2.1.1. <i>Retinoscopía de mano</i>	43

2.2.1.2. <i>Equivalente esférico a partir de aberrometría</i>	44
2.2.2. <i>Longitud axial: Biometría</i>	44
2.2.3. <i>Radio corneal: Keratometría</i>	45
Capítulo 3: Cambios longitudinales de las aberraciones ópticas en ojos de pollo normales y miopes	49
3.1. Resumen	53
3.2. Introducción	54
3.3. Métodos	57
2.1.1. <i>Sujetos y procedimientos experimentales</i>	57
2.1.2. <i>Refracción y ultrasonidos</i>	58
2.1.3. <i>Aberrometría Shack-Hartmann</i>	58
2.1.4. <i>Análisis estadístico</i>	59
3.4. Resultados	60
3.4.1. <i>Biometría por ultrasonidos y refracción</i>	60
3.4.2. <i>Aberraciones ópticas</i>	61
3.4.3. <i>MTF</i>	63
3.5. Discusión	67
3.5.1. <i>Comparación con estudios previos</i>	67
3.5.2. <i>¿Emetropización de las aberraciones?</i>	69
3.5.3. <i>Aberraciones ópticas y emetropización</i>	71
Capítulo 4: Emetropización y aberraciones ópticas tras PRK en pollos	73
4.1. Resumen	77
4.2. Introducción	78
4.3. Métodos	80
4.3.1. <i>Sujetos y protocolos experimentales</i>	80
4.3.2. <i>Cirugía refractiva</i>	81
4.3.3. <i>Aberrometría Hartmann-Shack y refracción</i>	82
4.3.4. <i>Queratometría</i>	83
4.3.5. <i>Biometría por ultrasonidos</i>	83
4.3.6. <i>Análisis estadístico</i>	83
4.4. Resultados	84
4.4.1. <i>Error refractivo</i>	84
4.4.2. <i>Aberraciones ópticas</i>	85
4.4.3. <i>Radio corneal de curvatura</i>	89
4.4.4. <i>Longitud axial</i>	90
4.5. Discusión	92
Capítulo 5: Aberraciones ópticas del ojo del ratón	97
5.1. Resumen	102
5.2. Introducción	104
5.3. Métodos	108

5.3.1.	<i>Sujetos</i>	108
5.3.2.	<i>Aberrometría de Hartmann-Shack</i>	108
5.3.3.	<i>Protocolos experimentales</i>	108
5.3.4.	<i>Análisis de datos</i>	109
5.4.	Resultados	112
5.4.1.	<i>Imágenes de Hartmann-Shack</i>	112
5.4.2.	<i>Estado refractivo</i>	112
5.4.3.	<i>Aberraciones de alto orden</i>	113
5.4.4.	<i>MTF</i>	114
5.4.5.	<i>Profundidad de foco</i>	115
5.5.	Discusión	117
5.5.1.	<i>El efecto de la anestesia</i>	117
5.5.2.	<i>Comparación con otros estudios</i>	118
5.5.3.	<i>Consecuencias de los resultados</i>	120
Capítulo 6: Ajustando la biometría ocular a las aberraciones		123
6.1	Resumen	128
6.2.	Introducción	129
6.2.1.	<i>Recopilación de datos biométricos de ojo de pollo</i>	130
6.2.2.	<i>Recopilación de datos biométricos de ojo de ratón</i>	145
6.3	Métodos	148
6.4	Resultados	151
6.5	Discusión	155
Capítulo 7: Conclusiones		159
Publicaciones		169
Referencias		171

Table of contents

	Page
Chapter 1: Introduction	1
1.1. Myopia	3
1.1.1. <i>Prevalence of myopia</i>	4
1.1.2. <i>Etiology of myopia</i>	7
1.1.3. <i>Genetic factors</i>	7
1.1.4. <i>Near work and related factors</i>	8
1.1.5. <i>Emmetropization process</i>	11
1.1.6. <i>Animal models of myopia</i>	12
1.1.6.1. <i>Chick model</i>	12
1.1.6.2. <i>Mouse model</i>	14
1.1.7. <i>Relating experimental myopia to human myopia</i>	15
1.2. Ocular optical quality	16
1.2.1. <i>Zernike polynomials</i>	19
1.2.2. <i>Optical quality metrics</i>	20
1.2.2.1. <i>RMS</i>	20
1.2.2.2. <i>PSF, MTF & OTF</i>	20
1.2.2.3. <i>Strehl ratio</i>	21
1.2.3. <i>Aberration measurement techniques</i>	21
1.2.4. <i>Human ocular aberrations</i>	23
1.2.5. <i>High order aberrations and myopia</i>	24
1.2.6. <i>Aberrations: Animal models</i>	25
1.2.7. <i>Why is it relevant to test relationships between aberration and myopia?</i>	26
1.3. Hypothesis and goals	27
 Chapter 2: Methods	 29
2.1. Measurement of ocular aberrations	32
2.1.1. <i>Hartmann Shack set-up</i>	33
2.1.1.1. <i>Illumination channel</i>	34
2.1.1.2. <i>Detection channel</i>	35
2.1.1.3. <i>Pupil monitoring</i>	36
2.1.2. <i>Automatic control and data processing</i>	36
2.1.3. <i>Alignment and calibration of the system</i>	38
2.1.3.1. <i>Placing the micro array and CCD cameras.</i>	39
2.1.3.2. <i>Artificial eye</i>	40
2.1.3.3. <i>Calibration of the Badal System</i>	40
2.1.4. <i>Validation of aberration measurements</i>	41
2.1.4.1. <i>Sphere and cylinder measurements</i>	41
2.1.4.2. <i>High order aberrations</i>	42
2.2. Measurement of biometric parameters	43
2.2.1. <i>Refractive error</i>	43
2.2.1.1. <i>Streak Retinoscopy</i>	43

2.2.1.2. <i>Spherical equivalent from aberrometry</i>	44
2.2.2. <i>Axial length: Biometry</i>	44
2.2.3. <i>Corneal radius: Keratometry</i>	45
Chapter 3: Longitudinal changes of optical aberrations in normal and form-deprived myopic chick eyes	49
3.1. Abstract	53
3.2. Introduction	54
3.3. Methods	57
3.1.1. <i>Subjects and experimental protocols.</i>	57
3.1.2. <i>Refraction and ultrasound biometry</i>	58
3.1.3. <i>Shack-Hartmann aberrometry</i>	58
3.1.4. <i>Statistical analysis</i>	59
3.4. Results	60
3.4.1. <i>Ultrasound biometry and refraction</i>	60
3.4.2. <i>Optical aberrations.</i>	61
3.4.3. <i>Modulation transfer function.</i>	63
3.5. Discussion	67
3.5.1. <i>Comparison with previous studies in experimental models</i>	67
3.5.2. <i>An emmetropization of the optical aberrations?</i>	69
3.5.3. <i>Optical aberrations and emmetropization</i>	71
Chapter 4: Emmetropization and optical aberrations in a myopic corneal refractive surgery chick model	73
4.1. Abstract	77
4.2. Introduction	78
4.3. Methods	80
4.3.1. <i>Subjects and experimental protocols</i>	80
4.3.2. <i>Refractive surgery</i>	81
4.3.3. <i>Hartmann-Shack aberrometry and refraction</i>	82
4.3.4. <i>Keratometry</i>	83
4.3.5. <i>Ultrasound biometry</i>	83
4.3.6. <i>Statistical analysis</i>	83
4.4. Results	84
4.4.1. <i>Refractive error</i>	84
4.4.2. <i>Optical aberrations</i>	85
4.4.3. <i>Corneal radius of curvature</i>	89
4.4.4. <i>Axial length</i>	90
4.5. Discussion	92
Chapter 5: Optical aberrations in the mouse eye	97
5.1. Abstract	102
5.2. Introduction	104
5.3. Methods	108
5.3.1. <i>Subjects</i>	108
5.3.2. <i>Hartmann-Shack aberrometer</i>	108

5.3.3. <i>Experimental protocols</i>	108
5.3.4. <i>Data analysis</i>	109
5.4. Results	112
5.4.1. <i>Hartmann-Shack images and wave aberrations</i>	112
5.4.2. <i>Refractive state</i>	112
5.4.3. <i>High order aberrations</i>	113
5.4.4. <i>Modulation Transfer Functions</i>	114
5.4.5. <i>Depth-of-focus</i>	115
5.5. Discussion	117
5.5.1. <i>The effect of anaesthesia</i>	117
5.5.2. <i>Comparisons with other studies: refraction, MTF and depth-of-focus</i>	118
5.5.3. <i>Implications of the results</i>	120
Chapter 6: Matching ocular biometry to optical aberrations	123
6.1. Abstract	128
6.2. Introduction	129
6.2.1. <i>A compilation of chick biometric data</i>	130
6.2.2. <i>A compilation of mice biometric data</i>	145
6.3. Methods	148
6.4. Results	151
6.5. Discussion	155
Chapter 7: Conclusions	159
Publications	169
References	171

Chapter 1. Introduction

The cornea and the lens of the eye project the images of the external world onto the retina. For adequate visual perception, this image should be focused on the photoreceptor layer (the cells that are responsible for light capture). One of the most extraordinary processes of ocular development in vertebrates is the coordination to adjust the axial length of the eye to the focal plane of the ocular optics (an active process called emmetropization). This tuning mechanism fails in a significant percentage of the population, who develop refractive errors (30% of the population in Europe and up to 85% in some Asian countries suffers from myopia) (Saw 2003; Kempen et al. 2004; Jorge et al. 2007). Despite its high prevalence, the etiology of myopia is not fully understood, although there is clear evidence that environmental factors play a major role (Saw 2003). Other high order aberrations, which are typically not measured in the optometry practice also contribute to retinal image degradation. In the young normal eye, the total aberrations of the eye are lower than those of the individual optical components, and whether this is a result of an active or a passive mechanism has been debated (Artal et al. 2001; Kelly et al. 2004; Tabernero et al. 2007; Marcos et al. 2008). In this thesis we investigated the potential role of ocular aberrations in myopia development, as well as the change of ocular aberrations during development, using experimental models of myopia.

1.1. Myopia

Myopia is a refractive error that allows detecting near objects clearly, but not distant objects. Images formed by a myopic eye from distant objects are perceived as blurred. This is due to the fact that parallel rays coming from infinite (distant objects) are focused in front of the retina, instead of on the retinal plane as occurs in the emmetropic eye when the accommodation is relaxed. The focus distance of the eye lenses is insufficient relative to eye dimensions, more specifically to axial length, which is the distance between the cornea and retinal photoreceptor layer. Figure 1.1 shows a scheme of a myopic eye, projecting distant objects in front of the retina and an emmetropic eye, perceiving distant objects in focus on the retina. Many studies around the world

suggest that myopia is associated mainly with a longer axial length due to enlargement of the vitreous chamber (Schaeffel et al. 1988; Hung et al. 1995; McBrien and Adams 1997; Gilmartin 2004) and secondly to greater corneal power (Grosvenor and Goss 1999).

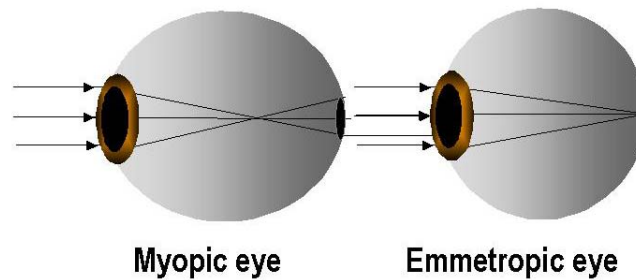


Figure 1.1 Image from a distant object is perceived as blurred and in an myopic eye, in contrast with emmetropic eye that focuses on the retinal plane.

1.1.1. Prevalence of myopia

Myopia in humans is a very common condition and has typically been associated to age and genetic factors (familiar antecedents, ethnic heritage...) as well as environmental factors (near work, social status, occupation...). Newborn eyes show commonly hyperopic errors: the cornea and lens are steeply curved, compared with their adult values, and the focal plane is short. During postnatal development, the focal plane moves away from the cornea (Chan and Edwards 1993; Pennie et al. 2001). This hyperopic shift toward emmetropia during development is inherent to the emmetropization process (Chan and Edwards 1993). During emmetropization two major changes occur in ocular growth: an increase of the vitreous chamber depth and a decrease of the cornea and lens power.

The fine tuning between power of ocular components of the eye and axial length is directed by a control mechanism to achieve an emmetropic eye. In emmetropic eyes the axial length matches the focal plane, allowing focusing of distant objects without accommodation. Often the emmetropization process is interfered by some reason, disrupting adequate ocular development, and resulting in hyperopic or, more frequently, myopic errors (e.g. (Zadnik and Mutti 1987; McBrien and Adams 1997)). An increased axial length, relative to the focal plane results in myopia. This relative increased length to eye power lenses

depends on several conditions and occurs in different situations. The prevalence of myopia changes across countries and types of society (Saw 2003). Myopia in the first stages of life is associated to immature eyes and usually reduces to emmetropia by one year of age (e.g (Fletcher 1955; Fledelius 1981; Varughese et al. 2005; Ziylan et al. 2006) although pre-term children have higher probability of developing myopia in later years (Larsson et al. 2003). At age five myopia is inexistent in some populations such as in rural china, 3% in Chile, 1-3% in North American and European societies, 4% in Japan and 3% in South Africa. But significantly higher prevalences are found in Taiwan or Singapore (12-28% in six and seven year old children), and the amounts of myopia as well as prevalence increase with age at a faster rate than in rural china, in suburban Chilean or north American and European primary school populations (Grosvenor 1987; Lin et al. 1999; Maul et al. 2000; Zhao et al. 2000; Morgan and Rose 2005; Saw et al. 2005). Also, it is common to find significant levels of myopia in school years in children who entered school as emmetropes (Quek et al. 2004; Morgan and Rose 2005). This general increasing tendency of the myopia prevalence continues to adult years, with prevalence of myopia in adults of 25.4% in USA, 26.6 % in West Europe , 30.01 % in Spain, 16.4% in Australia and again higher values in Asian populations: 80% in Singapore male school leavers or 82.2% in Chinese military conscripts (Grice et al. 1997; Montés-Micó and Ferrer-Blasco 2000; Kempen et al. 2004; Saw et al. 2005; Thorn et al. 2005; Anera et al. 2006). The prevalence rates of myopia are rising and is considered epidemic in some Asian populations (Saw 2003). Figure 1.2 shows myopia prevalence and progression in several Asian and Western populations. Other studies found different myopia prevalences associated to different conditions: Females and males (Krause et al. 1982; Kempen et al. 2004; Wickremasinghe et al. 2004), caucasian and African-american (Sperduto et al. 1983; Kleinstein et al. 2003; Hyman et al. 2005), years of school assistance (Rosner and Belkin 1987), high educational demands over several years (Lin et al. 1996; Kinge and Midelfart 1999; Kinge et al. 1999; Jorge et al. 2007), greater daily reading time (Angle and Wissmann 1980), higher near work demand (Goldschmith 1968; Curtin 1985; Ong and Ciuffreda 1995; McBrien and Adams 1997; Saw et al. 2002), place of residence (urban vs. rural) (Morgan and Rose 2005).

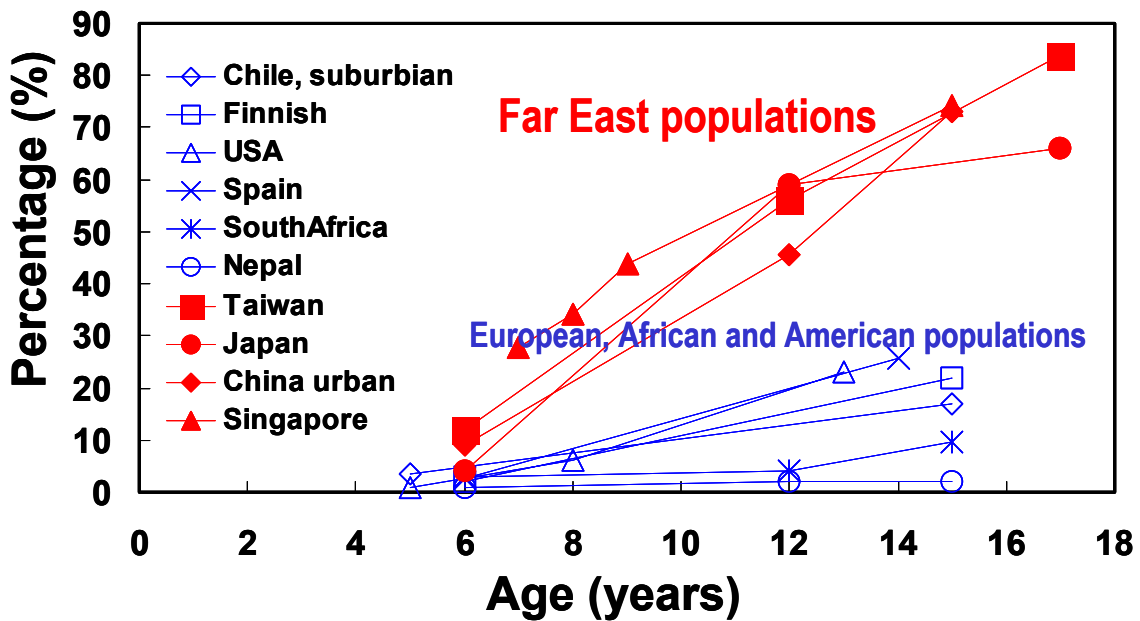


Figure 1.2 Prevalence (%) of myopia around the world as a function of age.

Myopia has been classified in several categories according to different etiological factors: simple myopia, characterized by normal visual acuity with optical correction and absence of other structural anomalies; night myopia at low illumination conditions due to the lack of accommodation stimulus; pseudomyopia produced by an apparent myopia due to unrelaxed accommodation and pathologic myopia, which is related to high myopia associated degenerative changes in the posterior segment of the eye and it is a pathologic disease more than a high refractive error (Ursekar 1983; Tokoro 1988). Grosvenor (Grosvenor 1987) proposed a system for classification of myopia on the basis of age-related prevalence and age of onset: congenital, youth-onset, early adult-onset, and late adult-onset.

1.1.2. Etiology of myopia

Myopia has been associated to different factors, both genetic and environmental (Pacella et al. 1999; Thorn et al. 1999; Saw 2003). It is often stated that whether myopia development is affected primarily by visual experience is a consequence of genetic background. Understanding the

physiological mechanism involved in myopia development is critical in for potential interventions, and consequently myopia prevention.

1.1.3. Genetic factors

Genetic factors are reported as a risk factor for myopia. The high prevalence of myopia found in specific ethnic groups suggests a role of the genes in this refractive error. On the other hand, the increase rate of myopia prevalence over the last generations in the same ethnic groups indicates that this effect can not be attributed to genes and environmental factors are also important (Lin et al. 1999; Saw 2003; Morgan and Rose 2005). Ocular growth involves several biological process (tissues, biochemical pathways...) since several genes are associated to eye growth (Feldkämper and Schaeffel 2003; McBrien and Gentle 2003; Schaeffel et al. 2003), indicating that there should be a biological basis for a contribution of genetic variation to refractive error (Morgan and Rose 2005). Several chromosomal localisations for inherited high myopia have been reported in genome-wide scans at least for high myopia, (Young et al. 1998; Young et al. 2001; Naiglin et al. 2002; Paluru et al. 2003; Gilmartin 2004; Young et al. 2005), but not for other more frequent types of myopia such as juvenile myopia (Mutti et al. 2002; Ibay et al. 2004).

Parental history studies show that myopia is more likely to occur when both parents are myopic and least when neither parent is myopic (Goss and Jackson 1996; Pacella et al. 1999; Mutti et al. 2002; Khandekar et al. 2005; Saw et al. 2005; Kurtz et al. 2007), although not all types of myopia have been related to parental history (Zadnik et al. 1994; Iribarren et al. 2005). However there are other factors present in these parental studies such as common environment and lifestyle similar in parents and children (Iribarren et al. 2002; Morgan and Rose 2005). Although heredity seems to be the most important factor in juvenile myopia when parents are myopes, other environmental factors such as increased near work, higher school achievement, and less time in sports activity are thought to play a role (Mutti et al. 2002). Therefore refractive error is affected with a set of variables and their interactions, with genetic and environmental being involved to various extents in the emmetropization process

(Saw 2003). An inappropriate visual stimulation may induce different ocular growth patterns and amounts of myopia depending on the individual's genetic predisposition. Twin studies show higher concordance for monozygotic twins than dizygotic (Chen et al. 1985; Hammond et al. 2001), and higher concordance in myopia values in twins with similar reading habits than discordant ones (Chen et al. 1985). The feedback (visual information which eye interprets for a correct eye growing signal in the emmetropization process) may be interfered by inherited metabolic conditions, developing myopia in predisposed subjects (Feldkämper and Schaeffel 2003).

1.1.4. Near work and related factors

The most relevant clinical environmental factor typically associated with myopia in humans is near work. Donders in 1864 (Donders 1864), associated near work requirements with refractive errors. Several studies show a greater prevalence of myopia and prevalence rates are highest among people who have occupations requiring near work (microscopists, visual display terminal workers...) (Tokoro 1988; Zylbermann et al. 1993; Simensen and Thorud 1994; McBrien and Adams 1997; Saw et al. 2002; Saw et al. 2007). In addition myopia is less common in populations where school is not compulsory (Young et al. 1969), as opposed to the high prevalence of myopia found in some Asian cities, such as Singapore, where school tasks are very demanding and require high levels of reading (Saw 2003). According to this hypothesis, the emmetropization process that results in myopia could be a consequence to improve focus in frequent readers (Mutti et al. 1996; Goss 2000), a sort of "near emmetropization". Higher progression rates are associated with earlier onset of myopia and with greater time spent on near work and less time spent outdoors, shorter reading distance, higher IOP, and esophoria at near. Although the question on how near work may trigger myopia and even the hypothesis is itself still under debate, ongoing clinical trials explore the effect of prescribing addition (positive refraction) for relaxing accommodative response with the aim of decreasing progression of myopia (Fulk et al. 2000; Gwiazda et al. 2003; Kurtz et al. 2007). However, not all studies have associated myopia progression with reading, short reading distance and close work or a reduction of myopia

progression by a decrease of the myopia by reading without glasses or positive refraction (Grosvenor et al. 1987; Hemminki and Parssinen 1987; Parssinen et al. 1989; Saw et al. 2002).

An old hypothesis is that intraocular pressure in the vitreous chamber is increased by sustained accommodation during near work requirements. Van Alphen in 1961 (Van Alphen 1961) proposed that the eye adjusts axial length to match the refractive power of the eye, the ciliary muscle and choroids control the intraocular pressure. When choroidal tension is insufficient to resist intraocular pressure, the ocular posterior segment would be stretched resulting in axial myopia. Higher values of intraocular pressure in myopic chicks than in hyperopic chicks have been reported, but this relationship between intraocular pressure and myopia is not clear (Schmid et al. 2003) and some studies (Goss and Caffey 1999) did not find statistical differences in IOP between myopic and emmetropic children. Other studies suggest that the ciliary muscle contraction during accommodation could influence scleral growth and eye shape directly, without involving intraocular pressure (Drexler et al. 1998). Greene (Greene 1980) proposed that stretching of the posterior sclera due to influence of extraocular muscles and pressure during ocular convergence could be the mechanism relating near work and myopia development, while others reject the idea of a mechanically stretching of sclera preceding myopia development (Ong and Ciuffreda 1995). Wildsoet & Wallman (Wallman et al. 1995) proposed a change choroidal thickness for compensating defocus in a chick model. In avian and mammalian models the sclera creep rate increased and decreased in order to modify axial length (Phillips et al. 2000).

Several studies have attempted to relate accommodative response differences with refractive state. It seems well established that myopes tend to have a smaller accommodative responses than non-myopes (Rosenfield 1998; Jiang 2000). The amount of accommodative convergence is elevated relative to accommodative response (AC/A ratios) in myopic children, therefore showing reduced accommodation, enhanced accommodative convergence and esophoria. Some have suggested increased tension in the crystalline lens increasing the effort to accommodate and enlarging the eye (Mutti et al. 2000).

The most extended hypothesis relating near work and myopia refers to the presence of a hyperopic blur associated to an accommodation lag (Gwiazda et al. 2005). Accommodative lag has been shown to be higher in myopes than hyperopes (Bullimore et al. 1992; He et al. 2005). Whether increased accommodation lag in myopes is a cause (due to the presence of hyperopic blur) or a consequence of myopia (due to decreased blur cues in myopia) is a question under debate. Some studies (Mutti et al. 2002) found that accommodative lag was not significantly different in children who became myopic compared with emmetropes previously to onset myopia. Higher accommodative lag was measured in children after the onset of their myopia, suggesting that increased accommodative lag could be a consequence rather than a cause of myopia. Whether accommodation is used as a signal to direct eye growth remains therefore unclear. In fact, intact accommodation is not necessary for proper emmetropization in experimental animal models, as it has been shown that some species are able to properly emmetropize and recover from induced refractive errors after lesion of the Edinger-Westphal nucleus or ciliary muscle (Wallman and Adams 1987; Troilo 1990).

1.1.5. Emmetropization process

The presence of an active mechanism during development that controls a fine tuning between the focal length of ocular components and axial length (known as emmetropization) is well established (Wallman 1993; Wildsoet 1997), although, as discussed above, it is not fully understood. It appears as if the eye was programmed to achieve optimal focus and a clear retinal image, with the process being visually guided. When retinal image quality gets degraded by some reason, the process gets disrupted, the eye continues to grow in the axial dimension (seeking best focus), therefore resulting in myopia. Several pathologies that affect the quality of the retinal image during development (congenital cataracts, lid haemangioma, palpebral ptosis, vitreous haemorrhage...) are typically associated with significant amounts of myopia (Robb 1977; Hoyt et al. 1981; Rabin et al. 1981). The requirement of a clear

retinal image for a proper emmetropization has been extensively demonstrated using animal models.

Blur in the peripheral retina has also been considered to be an important factor in myopia development with potential interactions between the defocus at the fovea and peripheral retina (Wallman and Winawer 2004; Smith et al. 2005). Differences in ocular globe shape have been found across refractive errors in humans. Myopic eyes have been shown to exhibit larger axial length than equatorial diameter (Gilmartin 2006) and a hyperopic retinal periphery relative to the fovea (Drexler et al. 1998; Atchison et al. 2004; Singh et al. 2006). The eye has been proposed to grow axially as a result of interactive effects between foveal image and blurred peripheral retinal image (Ciuffreda et al. 2007). Also, recent experiments in monkeys (Smith et al. 2005) suggest that deprivation, imposed only in the periphery of the visual field, can induce foveal myopia, raising the hypothesis that peripheral refractive errors imposed by the spectacle lens correction could influence foveal refractive development also in humans (Smith et al. 2006). On the other hand, this effect has not been found in chicks, where defocus imposed on local retinal areas produce local changes in eye growth (Diether and Schaeffel 1997; Schippert and Schaeffel 2006).

1.1.6. *Animal models of myopia*

Animal models have allowed systematic investigations of the role of the visual environment in the regulation of the axial length and myopia. Visual form deprivation experiments in animals have shown that visual experience plays a major role in normal emmetropization and myopia development. By altering visual experience in new born animals, myopia can be artificially developed, and the role of different factors (type of treatment, duration, age of treatment, etc...) in the outcomes of refractive error can be systematically studied. Many different animals have been used as models for myopia: Chicks (Wallman et al. 1978; Yinon et al. 1980; Schaeffel and Howland 1988; Schaeffel and Howland 1991; Irving et al. 1992; Wildsoet and Wallman 1995; Schaeffel and Diether 1999), tree shrews (Sherman et al. 1977; Norton 1990), monkeys (Wiesel and Raviola 1977; Hung et al. 1995; Smith and Hung 2000), marmosets (Troilo and

Judge 1993; Whatham and Judge 2001; Troilo and Nickla 2002), cats (Ni and Smith 1989; Wilson et al. 2002), mice (Beuerman et al. 2003; Tejedor and de la Villa 2003; Schaeffel et al. 2004), fish (Kroger and Wagner 1996; Shen et al. 2005), etc.

1.1.6.1. Chick model

Chick (*Gallus gallus domesticus*) has been used more than any other model in myopia research. Although chicks are phylogenetically distant from humans it has proved to be an excellent model for myopia. The chicken eye is flat, i.e. with a shorter anterior posterior axis than other meridians. A scleral plate, a ring with ossicles, provides ocular support and shape. In addition, the chicken retina does not have blood vessels (Schuck et al. 2000) and is provided with a vascular projection from the retina into the vitreous chamber called pecten. The function of the pecten is not well known (Wolburg et al. 1999). Avian pecten arises from the optic nerve (Schuck et al. 2000) and it seems to play a role in the retina nutrition (Kiama et al. 1997; Wolburg et al. 1999), but other functions have also been suggested: intraocular PH regulation (Brach 1975), blood-retina barrier (Wolburg et al. 1999) (Schuck et al. 2000), regulation of intraocular pressure (Seaman and Himelfar.Tm 1963), and reduction of intraocular glare (Barlow and Ostwald 1972).

Additionally the chick retina does not show a fovea but an area centralis (Morris 1982) a high ganglion-cell-density area (Straznicky and Chehade 1987) and contains cone opsins red, green, blue, and violet, as well as the rod-specific opsin rhodopsin (Bruhn and Cepko 1996). Accommodation in chicks is achieved, apart from the lens, by the cornea. Ciliary muscle alters the corneal curvature for corneal accommodation and moving the ciliary body anteriorly as a part of the lenticular accommodative mechanism (Schaeffel and Howland 1987; Schaeffel et al. 1988; Glasser et al. 1995). The ciliary muscle also may serves in the regulation of aqueous dynamics within the eye (Murphy et al. 1995). Accommodation occurs independently in the two eyes. Figure 1.3 shows a section of an enucleated chick eye.

Chicks are easily available animals, and their breeding and feeding requirements are not demanding. They mature rapidly, so changes occur within days, making them very appropriate for lab experiments. One of the first techniques for depriving chicks from visual forms was eyelid closure (Yinon 1984), or using either occluders or plastic diffusers over the eye, avoiding

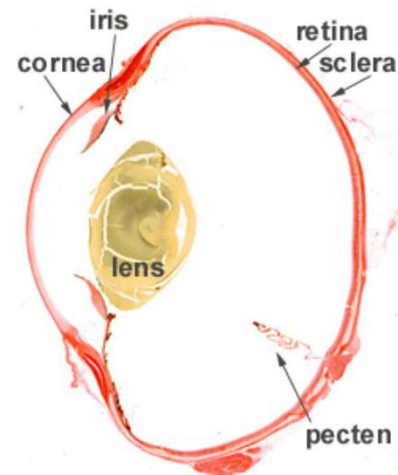


Figure 1.3 Sagittal section of an enucleated chick eye. (Adapted from www.lsi.usp.br.txt)

alterations in the cornea and allowing light entrance in the eye but not forms (Wallman et al. 1978; Hodos and Kuenzel 1984; Schaeffel et al. 1988; Beresford et al. 2001; Guggenheim et al. 2002; Choh et al. 2006). Myopia induced by treatments involving eye lid closure, occluders or plastic goggles in young chickens, is called form-deprivation myopia. Myopia can also be achieved by defocusing retinal image with negative lenses. It has been shown that the chick eye emmetropizes to the new condition, by matching the axial length to the focal plane (which with a negative lens is placed posteriorly to the retina), i.e. producing a compensatory elongation of the eye (Schaeffel et al. 1988; Schaeffel and Howland 1991; Wildsoet and Wallman 1995; Park et al. 2003; Choh and Sivak 2005). The same effect has been found in the absence of accommodation, i.e. Edinger-Westphal nucleus ablation or ciliary nerve section (Schaeffel et al. 1990), and having removed a connection with the brain in optic nerve sectioned animals (Schmid and Wildsoet 1996; Diether and Wildsoet 2005). Evidence that the mechanism happens at the retina is further supported by observations in chicks that the axial elongation process is spatially local so that one portion of the eye may elongate while another portion remains normal. This has been observed in eyes exposed to translucent diffusers or to minus lenses that cover only a partial visual field or cylindrical lenses (Wallman and Adams 1987; Troilo and Wallman 1991; Irving et al. 1995; Diether and Schaeffel 1997), or in chicks raised in cages with low roof which results in a myopic shift in the inferior retina (Miles and Wallman 1990). Other way for altering visual experience in chick myopia models has been restricting image

contrast or spatial frequencies during post-natal development (Bartmann and Schaeffel 1994; Schmid and Wildsoet 1997).

Axial length and choroid thickness seem to be driven by circadian rhythms (Nickla et al. 1998; Nickla et al. 2001; Nickla 2006). Chicks can recover from myopia in intermittent form depriving treatments. When the visual restriction is briefly removed, ocular growth returns to normal rates (Wallman and Adams 1987; Troilo and Wallman 1991; Zhu et al. 2003), showing the existence of a regulatory mechanism driven by a visual cue.

1.1.6.2. Mouse model

There is a special interest in developing a myopia model in mice because the mouse genome has been completely sequenced and it can be manipulated. A mouse myopia model could reveal genetic and environmental factors for the same animal model. While a bright retinal reflection can be found in mice (Schmucker and Schaeffel 2004), their optical quality is believed to be low (Artal et al. 1998; Prusky et al. 2004). Several authors have investigated whether refraction can be induced with visual deprivation as in other animal models, but response to treatments are not so evident as in chick models. Tejedor et al. (Tejedor and de la Villa 2003) reported induced form deprivation myopia in mice, while Schaeffel et. al suggested technical difficulties in measuring changes in form deprived mice (Schaeffel and Burkhardt 2002). A difficulty of this model is to measure refractive error by retinoscopy. Mice eyes have pupil diameters smaller than 1.5 mm, and it is very difficult to observe retinal reflection shifts. It has been suggested that at least some mice strains, could not respond very efficiently to visual deprivation by ocular elongation (Schaeffel and Howland

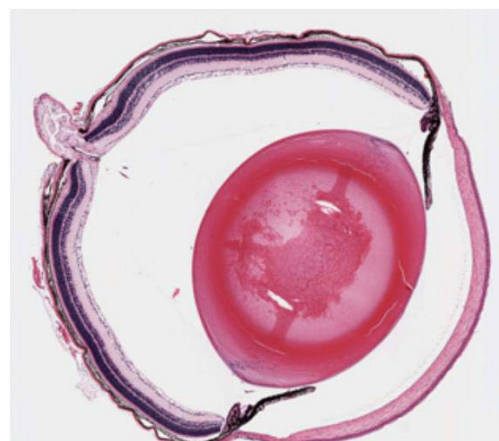


Figure 1.4 Section of an enucleated mouse eye (Adapted from www.uhnres.utoronto.ca)

2003; Schaeffel et al. 2004). Reports of refractive error obtained in form deprived mice eyes by photoretinoscopy indicate the development of low amounts of myopia and inhomogeneous distribution of the pupil brightness, indicating the presence of high order aberrations (Schaeffel et al. 2004). Figure 1.4 shows a section of an enucleated mouse eye.

1.1.7. Relating experimental myopia to human myopia

The normal refractive development in most animals appears to parallel human refractive development (Norton 1999): the distribution of refractive values, the progression toward emmetropia, the decrease of variability of refractive values (Norton and McBrien 1992; Pickett-Seltner et al. 1988; Prusky et al. 2004), the vitreous chamber elongation (Wallman et al. 1981), and the thinning of the choroid (McBrien 1998) are similarly found in myopic humans (Curtin 1985). Other changes are specific to each species: corneal curvature and increased variability in lens power in chicks (Troilo et al. 1995; Priolo et al. 2000), reduced lens thickness in tree shrews (McKanna and Casagrande 1978; Norton and Rada 1995). Infants with congenital cataracts, corneal opacities or retinopathy of prematurity typically develop myopia (Robb 1977; Hoyt et al. 1981; Gee and Tabbara 1988) suggesting that form deprivation early in life also results in myopia development in humans.

The hyperopic defocus in the accommodated eye during near tasks has been related to the hyperopic defocus imposed with negative lenses in animal models, which results in myopia development. However, findings in animal models showing that brief exposures to normal viewing counteract the effect of hyperopic defocus and prevent from myopia development questions that substantial near work is the major cause for myopia development, since that would only occur if near work was conducted continuously. Results from animal studies have consequences for possible myopia treatment in humans. For example, myopic defocus has been shown to have a protective role in myopia development (Flitcroft 1998), as it has been shown to protect against myopia in a chick model (Zhu et al. 2003) , and therefore it could be a possible treatment for myopia in humans.

In summary, animal models have revealed the existence of an active emmetropization mechanism controlled by visual experience. Experiments on animal models help to understand the role played by the visual environment in the development of myopia and to separate causal relationships from changes which are consequence of axial elongation and could explain some clinical observations in myopic humans. Studies are therefore needed to investigate which physiological properties of myopic eyes are a cause or a consequence of myopia, and to explore the causes of retinal degradation and their impact on myopia development, and the interactions between the different factors (genetic, environmental) involved in this process.

1.2. Ocular optical quality: Aberrations

Although in humans the most important refractive defects are spherical and cylindrical refractive errors, high order aberrations are also present, which also degrade retinal image quality. If the lenses of the eye (cornea and lens) were perfect, light from a point source at infinity would converge on the focal point at the retina. In the opposite sense, a point of light in the retina would emit a spherical wavefront, exiting the eye as a plane wave front. Phase deviations from these perfect wavefront, measured at the pupil plane, are known as wave aberrations.

Figure 1.5 represents a non-aberrated (top) and an aberrated (bottom) eye. In the non-aberrated eye images are only limited by diffraction. In aberrated eye, forms distorted images of an object; rays entering the eye through different pupil positions get deviated from the chief ray at the retinal plane, and a distorted wavefront travels toward the retina. Figure 1.6 also represents a non-aberrated and an aberrated eye. A point of light in the retina is emitted as a spherical wavefront in non-aberrated eye, but as an aberrated spherical wavefront in aberrated eye.

Wave aberrations are typically estimated from local ray aberrations, by either measuring the deviations of incoming beams from the principal ray

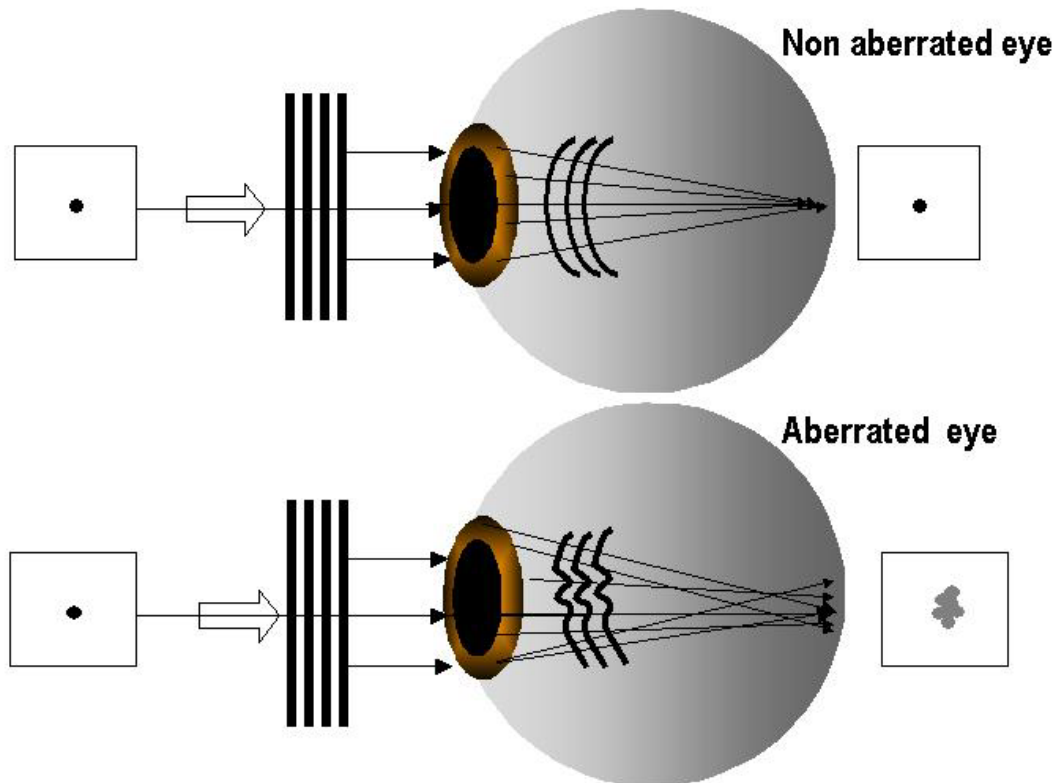


Figure 1.5 Image of a point source formed by a non-aberrated and an aberrated eye. For an incoming wavefront, rays entering the eye through different pupil positions converge on the same retinal location, and a spherical wavefront travels toward the retina.

(ingoing aberrometers such as spatially resolved refractometer or laser ray tracing, Figure 1.5) or sampling the wavefront as it exits the eye (such as Hartmann-Shack wavefront sensor, Figure 1.6). The magnitude of ray aberration for each pupil position is proportional to the local slope (derivatives) of the wavefront aberration, where α , β are the horizontal and vertical coordinates of the ray aberration, R_p is the pupil radius, and $W(x,y)$ is the wave aberration.

$$\alpha = \frac{1}{R_p} \frac{\partial W(x,y)}{\partial x}$$

$$\beta = \frac{1}{R_p} \frac{\partial W(x,y)}{\partial y} \quad \text{Eq (1.1)}$$

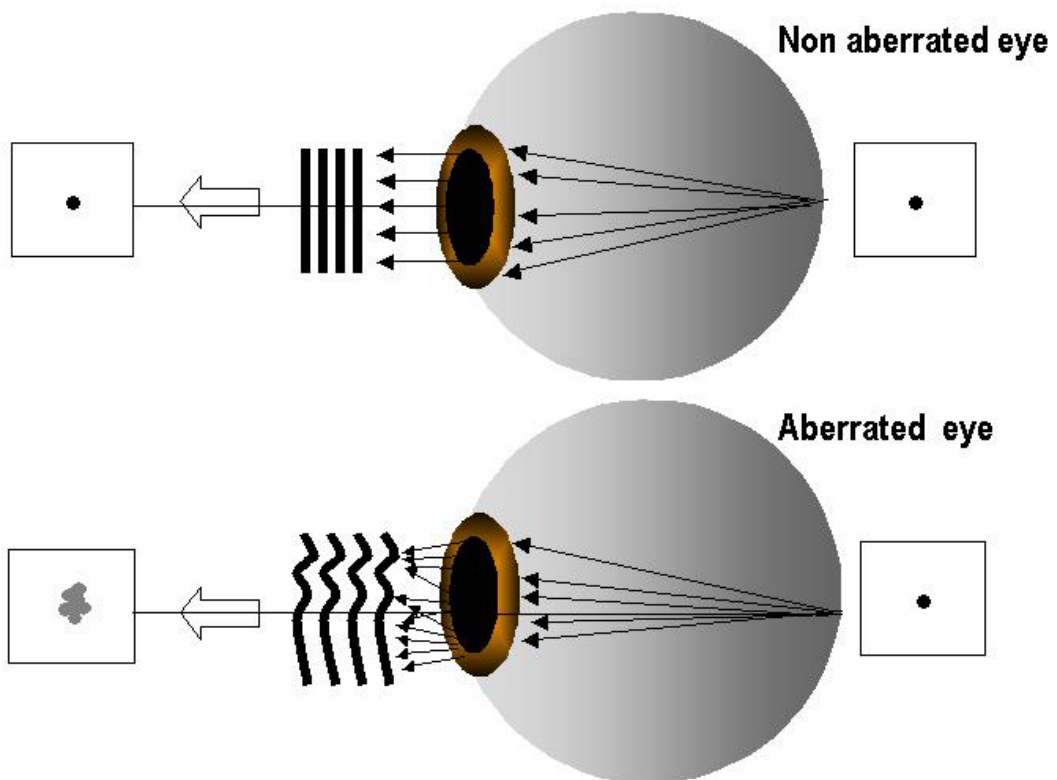


Figure 1.6 A light spot projected by the retina exiting the eye (non-aberrated, top, and aberrated eye, bottom).

1.2.1. Zernike polynomials

A Zernike polynomial expansion (ISO, "Standard 10110.A3 - The Zernike polynomials.") is the recommended basis for describing wave aberrations over circular pupils (Thibos et al. 2000), and will be the one used in this thesis. Among other advantages, Zernike polynomials are an orthogonal basis over the unit circle, and the lower orders represent typical refractive errors. Normally, Zernike coefficients are indexed using a double-index scheme: Z_0^0 , Z_1^{-1} , Z_1^1 ... The subindex indicates the aberration type (order) and the upper index the individual aberrations in each order. Second order aberrations include defocus and astigmatism; third order aberrations include coma, and fourth order aberrations include spherical aberration. Figure 1.7 represents a set of Zernike polynomials up the 4th order.

$$W = \sum_n^m C_n^m Z_n^m$$

$$Z_1^{-1} = x$$

$$Z_1^1 = y$$

$$Z_2^{-2} = x^2 - y^2$$

$$Z_2^0 = 2x^2 + 2y^2 - 1$$

$$Z_2^2 = 2yx$$

$$Z_3^{-3} = x^3 - 3y^2x$$

$$Z_3^{-1} = 3x^3 + 3xy^2 - 2x$$

$$Z_3^1 = 3yx^2 + 3y^3 - 2y$$

$$Z_3^3 = 3yx^2 - y^3$$

$$Z_4^0 = 1 - 6y^2 - 6x^2 + 6y^4 + 12x^2y^2 - 6x^4$$

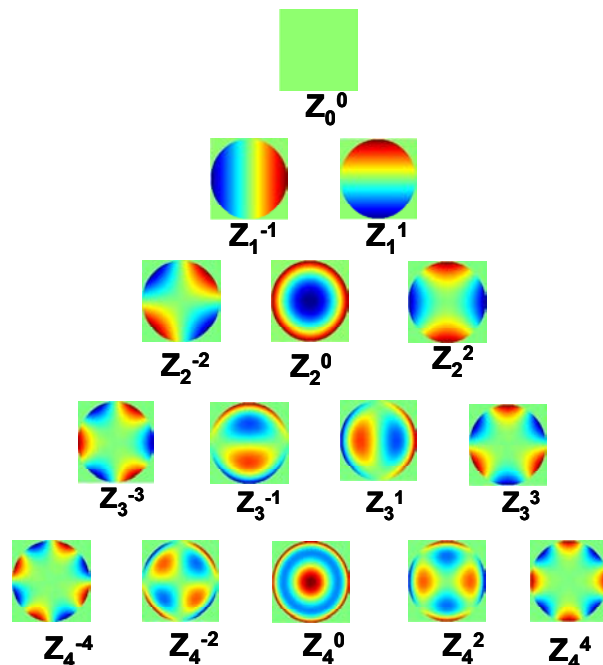


Figure 1.7 Zernike polynomial pyramid up to the 4th order

Aberrations (both magnitude and distribution) have been shown to vary widely across the population. Ocular aberrations in humans have been shown

to increase with age and change with accommodation (He et al. 1998; Mclellan et al. 2001; Artal et al. 2002; Fujikado et al. 2004; Wang and Koch 2004; Plainis et al. 2005; Chen et al. 2006). High order aberrations have been shown to increase with standard LASIK refractive surgery (Campbell et al. 1999; Moreno-Barriuso et al. 2001) and, as will be later shown, higher amounts of aberrations tend to be more associated with higher amounts of myopia.

1.2.2. Optical quality metrics

Several metrics estimated from the wave aberration have been proposed to describe the optical quality of the eye, with particular attention to those that correlate best with visual function (Thibos et al. 2000). For the purposes of this thesis, we will use metrics computed directly from the Zernike coefficients, as well as retinal image plane metrics.

1.2.2.1. RMS

The root-mean-squared (RMS) value of a particular term or mode is the RMS contribution of that term or the individual coefficients of that mode. The RMS expresses the deviation averaged over the entire wavefront. Making use of the orthogonality and normalization properties of the Zernike coefficients, the wavefront variance (RMS squared) can be simply derived from the squared coefficients.

1.2.2.2. Point Spread Function (PSF), MTF and OTF.

The point spread function is the image of a point object through the optical system. It is calculated as the squared magnitude of the inverse Fourier transform of the pupil function $P(x,y)$:

$$P(x,y) = A(x,y)e^{ikW(x,y)} \quad (\text{Eq. 1.2})$$

Where k is the wave number ($2\pi/\text{wavelength}$), $A(x,y)$ is an apodization function (when the waveguide nature of cones is considered) and $W(x,y)$ is the wave

aberration. $P(x,y)$ is zero outside the pupil. The Optical Transfer Function (OTF) is the Fourier transform of the point-spread function (PSF) and the modulation transfer function (MTF) is the modulus of the OTF. The MTF represents the contrast loss as a function of spatial frequency, and accounts for the optical degradation imposed by both diffraction and high order aberrations.

1.2.2.3. Strehl ratio

Strehl ratio represents the maximum value of the PSF, normalized to the maximum of the diffraction-limited PSF, or equivalently, the volume under the OTF normalized by the diffraction-limited OTF.

1.2.3. Aberration measurement techniques

Aberrometers measure the ray aberration as a function of pupil position. This is proportional to the local slope (derivative) of the wave aberration, from which the wave aberration can be easily retrieved. Ocular aberrations are measured using different techniques (Spatially Resolved Refractometer –SRR- (He et al. 1998; Burns and Marcos 2000; Burns and Marcos 2001), Laser Ray Tracing –LRT-(Moreno-Barriuso et al. 2001), Hartmann-Shack –HS- (Liang et al. 1994; Thibos et al. 1999; Moreno-Barriuso et al. 2001), among others. Although all techniques measure ray aberrations, differences across instruments rely on either the psychophysical (requiring the participation of the subject) or objective (based on light reflected off the retina) nature of the technique; “ingoing” (aberrations measured as the test beam goes into the eye) or “outgoing” (as the wavefront emerges from the eye) direction of the measurement. For example, the SRR is a psychophysical and “ingoing” technique, as a test beam enters the eye through a series of entry pupil positions while a fixation cross is perceived through a centered pupil. The subject aligns the spot with the reference cross-target. The tilted angle is proportional to the derivative of the wave aberration at each entry pupil. The LRT is an objective “ingoing” technique based on the same principle, but now the deviation of the test ray from the principal ray is detected by a CCD camera placed on a plane conjugate to the retina. An x-y scanner synchronized to the

CCD camera allows to sample sequentially a series of pupil positions in a brief period of time. The Hartmann-Shack (HS) is an “outgoing” aberrometry technique based on the measurement of ray deviations at different pupil positions of a wave reflected by the retina from a light point source. A microlens array, placed on a pupil conjugate plane, focuses multiple spots (one per lenslet) onto a CCD camera. Each lenslet samples a small part of the wave-front corresponding to a certain pupil location. A regular pattern of spots would be obtained for an ideal non aberrated eye, while ocular aberrations produce an irregular pattern of spots. The deviation of each spot from the ideal position is proportional to the local derivative of the wave aberration. Figure 1.8 shows a schematic diagram of the Hartmann-Shack spot image capture in a non aberrated eye (regular pattern) and an aberrated eye (distorted pattern).

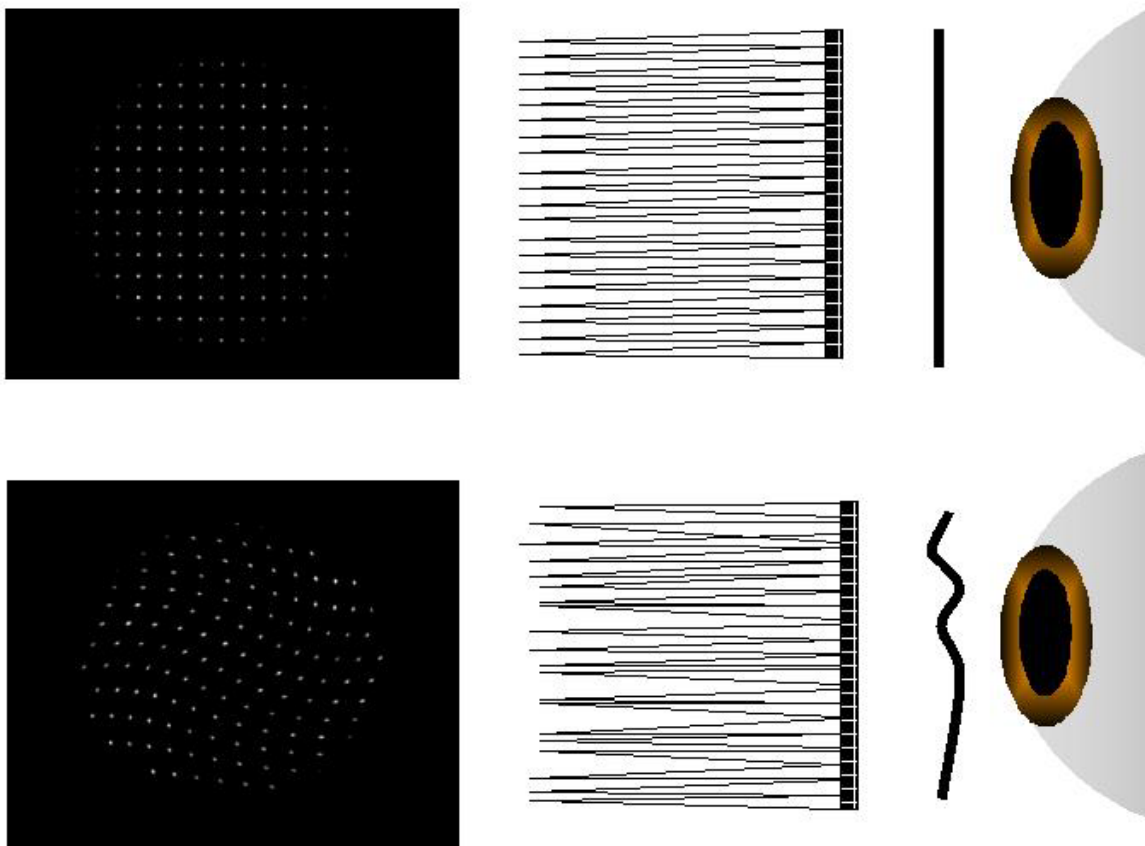


Figure 1.8 Hartmann Shack pattern from non aberrated (upper) and aberrated eye (lower).

The advantage of this technique over the others described is that only one snapshot is necessary to obtain the wave aberration for the entire pupil. HS aberrometry is therefore an objective and fast technique. For normal human eyes it has been shown that the SRR, LRT and HS provide similar measurements of wave aberrations (Moreno-Barriuso et al. 2001; Marcos et al. 2002; Llorente et al. 2003).

In this thesis we developed a Hartmann-Shack aberrometer, which we considered to be the most adequate approach to measure aberrations in animal models, because it allows faster measurements and does not require a great collaboration from the subject.

1.2.4. Human ocular aberrations

The aberrations of the human eye have received increased attention in recent years. The availability of more efficient and reliable aberrometers, has allowed large population studies in normal subjects (Porter et al. 2001; Castejon-Mochon et al. 2002; Thibos et al. 2002), as well as the study of the relationship of ocular aberrations with different conditions (refractive error (Marcos et al. 2000; Marcos et al. 2001; Cheng et al. 2003; Llorente et al. 2004), aging (McLellan et al. 1999; Mclellan et al. 2001; Marcos et al. 2004), accommodation (He et al. 2000), keratoconus (Barbero et al. 2002), Hios (Barbero 2003; Marcos et al. 2005; Marcos et al. 2007), refractive surgery (Moreno-Barriuso et al. 2000; Marcos 2001; Marcos et al. 2001; Marcos et al. 2001; Moreno-Barriuso et al. 2001; Llorente et al. 2004) etc. The ocular aberration pattern is the result of the contribution of corneal and crystalline lens aberrations and their interactions. The geometrical shapes (curvatures and asphericity) of the corneal and crystalline lens surface, and very likely the gradient index distribution of the crystalline lens, contribute to spherical aberration. Irregularities of the cornea, as well as the relative position of the optical elements (i.e. off-axis location of the fovea, pupil displacement) contribute to high order aberrations (Marcos et al. 2001).

Total ocular aberrations in the young normal eye are typically higher than corneal aberrations alone, indicating that internal optics (mainly crystalline lens) compensates part of the aberrations of the cornea. This interaction produces a balance of astigmatism and high order aberrations (Artal and Guirao 1998; Kelly et al. 2004). With age, the loss of this compensation due to changes primarily in the crystalline produces degradation of the ocular optics (McLellan et al. 2001; Artal et al. 2002). This balance between corneal and internal aberrations has been debated to arise from either an active or a passive mechanism. An active and visually guided process would require a plasticity of the eye to reduce total aberrations and improve retinal image, i.e. an emmetropization of high order aberrations by fine tuning of ocular surface geometry and positioning, somewhat similar to the fine tuning between optical power and axial length occurring in the emmetropization for refractive error. On the other hand, passive mechanism would result from purely geometrical factors (Artal et al. 2006; Marcos et al. 2008). In humans, some cross-sectional studies including infants and children report a decrease in aberrations with age, and suggest an emmetropization of high order aberrations. However, other studies of ocular aberrations in infants have been shown relatively low amounts of aberrations, suggesting that if there is a compensating process (visually guided or not) this is likely not very important (Wang and Candy 2005).

1.2.5. High order aberrations and myopia

Several studies have reported that (high) myopes have significantly higher amount of higher order aberrations than emmetropes, and shown significant correlations between spherical error and myopia (Collins et al. 1995; He et al. 2002; Marcos et al. 2002; Paquin et al. 2002). Spherical aberration is low in low myopes (<6 D) because there is a balance between corneal and internal (lens and others) aberrations. Marcos et al. (2002) showed several changes as a function of myopia: corneal spherical aberration increase toward more positive values and internal spherical aberration changed toward more negative values, keeping total spherical aberration constant. Cross-sectional as well as longitudinal studies show increased asphericity in higher myopic eyes

(Carney et al. 1997; Horner et al. 2000). Applegate (Applegate 1991) found coma and spherical aberrations in myopic eyes. Llorente et al. (Llorente et al. 2004) found significant differences in the optical and structural properties (corneal asphericity, corneal and ocular spherical aberration, apart from axial length) between hyperopes and myopes. While other studies did not found significant differences in myopes than emmetropic eyes (Cheng et al. 2003; He et al. 2005), there is a general agreement that high myopic eyes tend to be more aberrated.

1.2.6. Aberrations: Animal models.

As described before, defocus and astigmatism (second order aberrations) have been widely studied in a large number of species, particularly those used as experimental models for myopia. However, despite the fact that high order aberrations can degrade substantially the retinal image, and retinal image quality plays a role in emmetropization little is known on the optical quality and aberrations in animal models.

The first reports on chick eye is optical quality are controversial. A conference abstract reported that chicks showed worse optical quality and higher amounts of aberrations than humans (Thibos et al. 2002). However, this is in contrast with the good retinal image quality reported by Coletta et al. (Coletta et al. 2000; Coletta et al. 2003) using a double-pass technique. During this thesis, and posterior to the publication of our papers, measurements of ocular aberrations in chicks (Kisilak et al. 2006) were presented, confirming an improvement of optical quality with age in chicks, and excellent optical quality at 2-weeks of age.

To our knowledge, no report of the aberrations and optical quality in the mouse eye has been presented before. The observations of inhomogeneous photoretinoscopic reflexes (Schmucker and Schaeffel 2004) and very recent reports of retinal imaging in mice using adaptive optics (Biss et al. 2007) confirm our results of poor optical quality in the mouse. In general, the rodent eye optical quality is believed to be highly degraded, according to double-pass

estimates (Artal et al. 1998) and ray tracing simulations using parameters from enucleated eyes (Hughes 1979) in rats. Huxlin et al. measured ocular aberrations in cats and found similar amounts than in humans (Huxlin et al. 2004). In primates, measurements of optical aberrations in marmosets showed that levels of higher-order aberrations of the marmoset eye are higher than in humans eyes but significantly lower than in anaesthetized animals, emphasizing the importance of measuring aberrations under awake conditions (Coletta et al. 2001; Coletta et al. 2003). Also in the marmoset, wavefront aberrations were shown to decrease with age and to be higher in myopic eyes (Coletta et al. 2004). Very recently, aberrations have been reported in the Rhesus Monkeys (Ramamirtham et al. 2004; Ramamirtham et al. 2006).

1.2.7. Why is it relevant to test relationships between aberrations and myopia?

There is evidence for potential relations between aberrations and myopia:

1. A degraded retinal image quality during ocular development produces myopia. As aberrations affect the visual experience degrading retinal images they could play a role in myopia development (Wilson et al. 2002).
2. There is a correlation between aberrations and myopia. Myopes seem to have higher aberrated eyes (Atchison et al. 1995; Marcos et al. 2002; Paquin et al. 2002).
3. An increase of corneal aberrations have been shown to occur for substantial time after extended reading, particularly in myopes and Asian subjects. This could represent a mechanism explaining the relationship between myopia development, near tasks and higher prevalence in Asian populations (Buehren et al. 2003).
4. There are clinical evidences of slower myopia progression in RGP (Rigid Gas Permeable) contact lens users, although there is controversy whether

this is purely a consequence of corneal shaping (Perrigin et al. 1990; Khoo et al. 1999). On the other hand, it has been shown that high order aberrations decrease when RGP contact lenses are worn (Dorronsoro et al. 2003).

5. The effect of form deprivation and lens treatments in myopia animal models will be limited by the tolerance to blur. Depth of focus is highly affected by ocular aberrations. However, the ocular aberrations in widely used animal models for myopia (such as the chick) or potential animal models for myopia (such as the mouse) have not been studied.
6. Longitudinal measurements of ocular aberrations during normal development and during development of myopia have never been studied. Those measurements will allow to test the hypothesis of active (visually guided) or passive (geometrical) mechanisms for the fine tuning of ocular components, particularly in animal models whose visual experience can be altered.

1.3. Hypothesis and goals.

The main goal of this thesis is to test relationships between ocular aberrations and myopia development in animal models (chicks and mice), which allow longitudinal measurements in relatively short periods of time and manipulation of visual experience. We will test the hypothesis that aberrations are a consequence of myopia, and that aberrations are a cause for myopia. We will also investigate the sources of optical aberrations in the normal and myopic eye of these models.

The specific goals of this thesis are:

1. Development of custom technology to measure optical aberrations and ocular biometry in animal model eyes. We developed a Hartmann-Shack wavefront sensor to measure total eye aberrations, a corneal keratometer to measure corneal radius of curvature, and adapted an

ultrasound biometer and streak retinoscopy to in vivo measurements in animal models (Chapter 2).

2. Measurement of optical quality in the normal chick eye, and changes of optical aberrations with development. We will address the question whether aberrations follow an emmetropization process, similar to refractive error (Chapter 3).
3. Measurement of optical aberrations and ocular biometry during myopia development in a form-deprived chick model. With these measurements we will assess if increased aberrations are associated with myopic eyes, i.e. if aberrations are a consequence of myopia (Chapter 3).
4. Development of a refractive surgery myopic chick model. We will investigate the potential of altering the emmetropization process by reshaping the cornea (nominally imposing a hyperopic defocus). We will study optical aberrations and ocular biometry in this model and will assess if increased aberrations can result in increased ocular elongation, i.e. if aberrations can be a cause of myopia (Chapter 4).
5. Measurement of optical aberrations in the wildtype mouse eye. We will assess relationships between the refractive error in the mouse and retinal image quality, as well as the impact of optical depth of focus on the possibilities to induce myopia (Chapter 5).
6. Development of computer eye models for the chick and mouse eye. We will explore the relationships between biometry and structure of the ocular components and the measured optical aberrations to understand the sources of aberrations in the developing (1-14 days) chick eye (normal and myope) and the 28-day old mouse eye (Chapter 6).

Chapter 2. Methods

Resumen capítulo 2:

Métodos

En este capítulo se describen todas las técnicas empleadas para medir los distintos parámetros oculares en los modelos animales implementados en esta tesis. En particular, se diseñó y construyó un sensor de frente de onda Hartmann-Shack para medir las aberraciones oculares de pollos y ratones adaptados a las características propias de cada modelo. Además un biómetro de ultrasonidos fue adaptado para las medidas de longitud axial en ojos de pollo y se construyó un queratómetro (en colaboración con Alberto de Castro) adaptándolo a las pequeñas dimensiones del ojo del pollo para una medida correcta de la curvatura corneal. El error refractivo fue medido mediante retinoscopía de mano o bien por aberrometría en algunos estudios de pollos o ratones donde la retinoscopía no era posible.

In this chapter we describe all the techniques to measure different ocular parameters in animal model eyes implemented in this thesis. In particular we designed and built a Hartmann-Shack wavefront sensor to measure ocular aberrations in chicks and mice, adapted to the particular features of these models. We also adapted an ultrasound biometer to measure axial length in the chick eye, and built (in collaboration with Alberto de Castro) a keratometer adapted to small eye dimensions to measure corneal curvature in the chick eye. Refractive error was obtained by streak retinoscopy or from aberrometry in some chick and mice studies where retinoscopy was not possible.

2.1. Measurement of ocular aberrations

We measured ocular monochromatic aberrations in animal models using a custom-developed Hartmann-Shack wavefront sensor, built specifically in this thesis for this application.

In the Hartmann-Shack technique a light point source is projected on the retina, and the light reflected is focused by a microlens array on a CCD camera (see Figure 1.8 on the introduction). Deviations of each retinal spot with respect to the ideal location are obtained in order to reconstruct the wave aberration in the pupil plane. In this section we present the design, set up, calibration and computer routines for automatic control and data processing developed in this thesis. The system was built with the following specifications: 1) It should be adapted to the animal eye dimensions (chick and mouse); 2) It should be compact and easily portable (for example, to an animal facility) and installable on any computer.

2.1.1. Hartmann Shack set-up

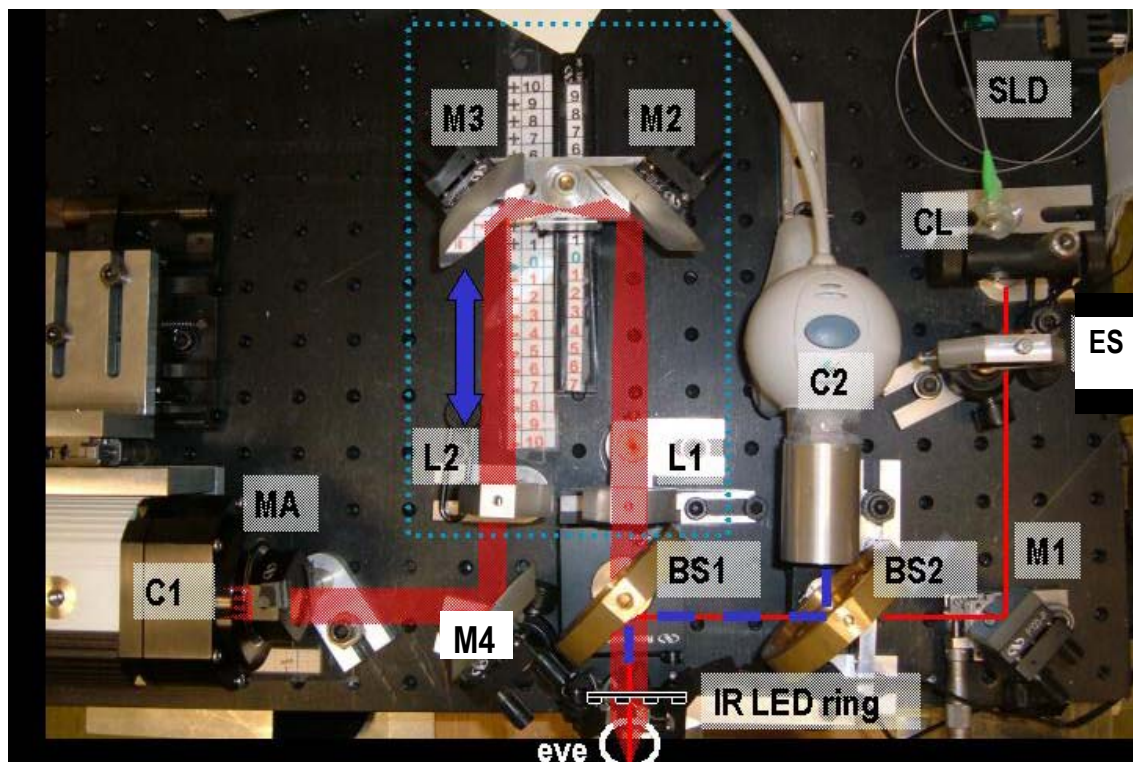
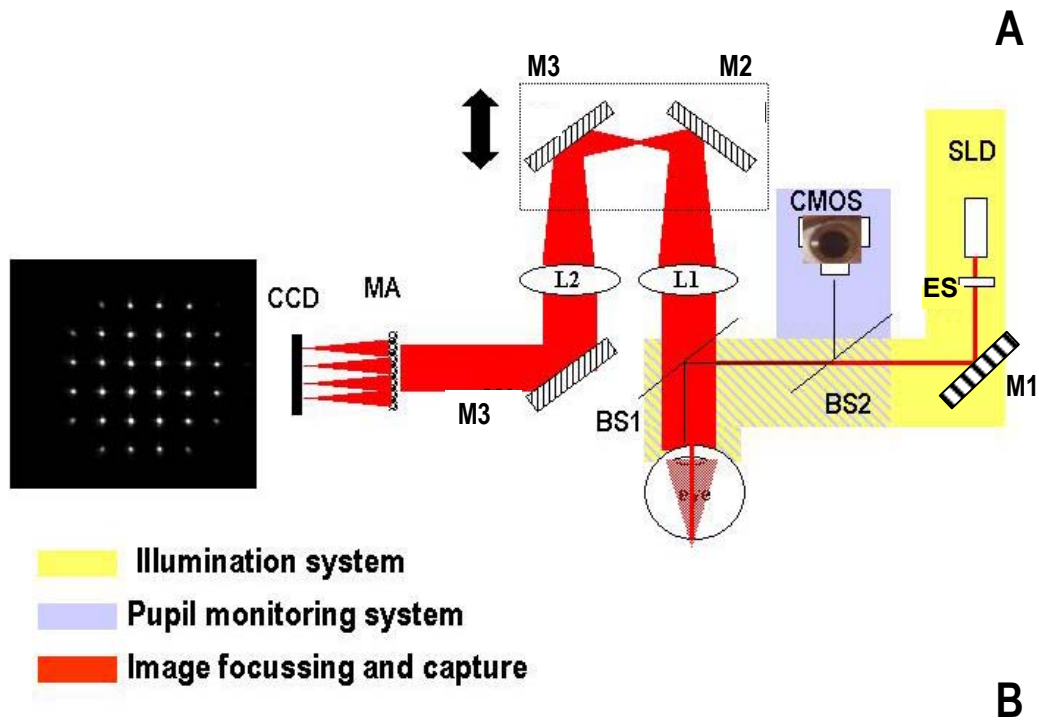


Figure 2.1 Schematic diagram (A) and photograph (B) of the custom-built Hartmann-Shack system.

We developed a Hartmann-Shack aberrometer with three channels: Illumination channel, detection channel, and pupil monitoring channel. The system was mounted on an aluminium optic table (AOSA, Madrid, Spain) and the physical dimensions of the optical set up were 35 x 50 mm. The optical table was mounted on a x-y-z stage, so that the entire platform (rather than the animal) was moved for pupil centration (x-y) and pupil focus (z). Figure 2.1 A & B shows a schematic diagram and photograph of the system.

2.1.1.1. *Illumination channel*

The illumination channel projects a light spot onto the retina. The light source consists of a Superluminescent Diode (SLD) (Superlum Diodes Ltd. Moscow, Russia) with an emission wavelength of 676 ± 14.6 nm. A module driving set for current and temperature control for the SLD allowed light intensity adjustment. The SLD was coupled to fibre optic attached to a collimator lens (CL) (Thorlabs, Munich, Germany) (see Figure 2.2). At the exit of the lens, the light beam has a 0.22° half angle of divergence and 6.2 mm diameter. The beam is blocked by an electronic shutter (ES) (Densitron technologies, London, United Kingdom) to control light exposure. The device consisted on a single blade shutter driven by a solenoid plunger. When power was applied the shutter was closed and it opened when the power was turned off. The shutter open and close time was less than 16 ms. The shutter was controlled from the computer by data acquisition modules (ADAM).

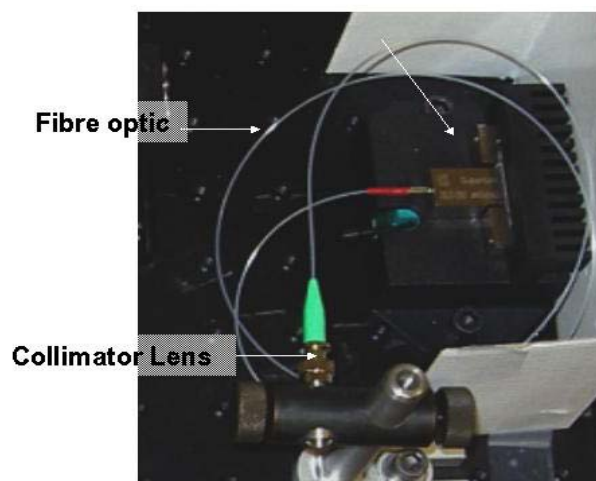


Figure 2.2 Super Luminescent Diode (SLD)

When the shutter was opened, the light beam from the SLD was directed into the eye by reflections on a square silver mirror (M1) (Newport

Corporation, Irving, California, USA) and a plate beam splitter (BS1) (Melles Griot, Rochester, New York, USA). Exposure levels and times were below maximum values for human eyes, following ANSI safety standards.

2.1.1.2. Detection channel

The detection channel consisted of: 1) a 25-mm circular lenslet array (MA) (Adaptive Optics Associates, Inc, Cambridge MA, USA) with a square pattern of microlenses (65 columns x 65 rows) of 400 microns aperture and 24-mm focal length on a epoxy substrate. 2) A cooled high resolution (1280 x 1024 pixels) 12 bit CCD camera (C1) (Retiga 1300. Qimaging, Burnaby, Canada), with high signal to noise ratio (60 dB)). The camera was provided with a firewire interface, plug and play capabilities and high speed data transfer rate. 3). A focusing block (FB) that consisted of a Badal system with two elliptical mirrors (M2 & M3) of 33.02 and 46.70 mm

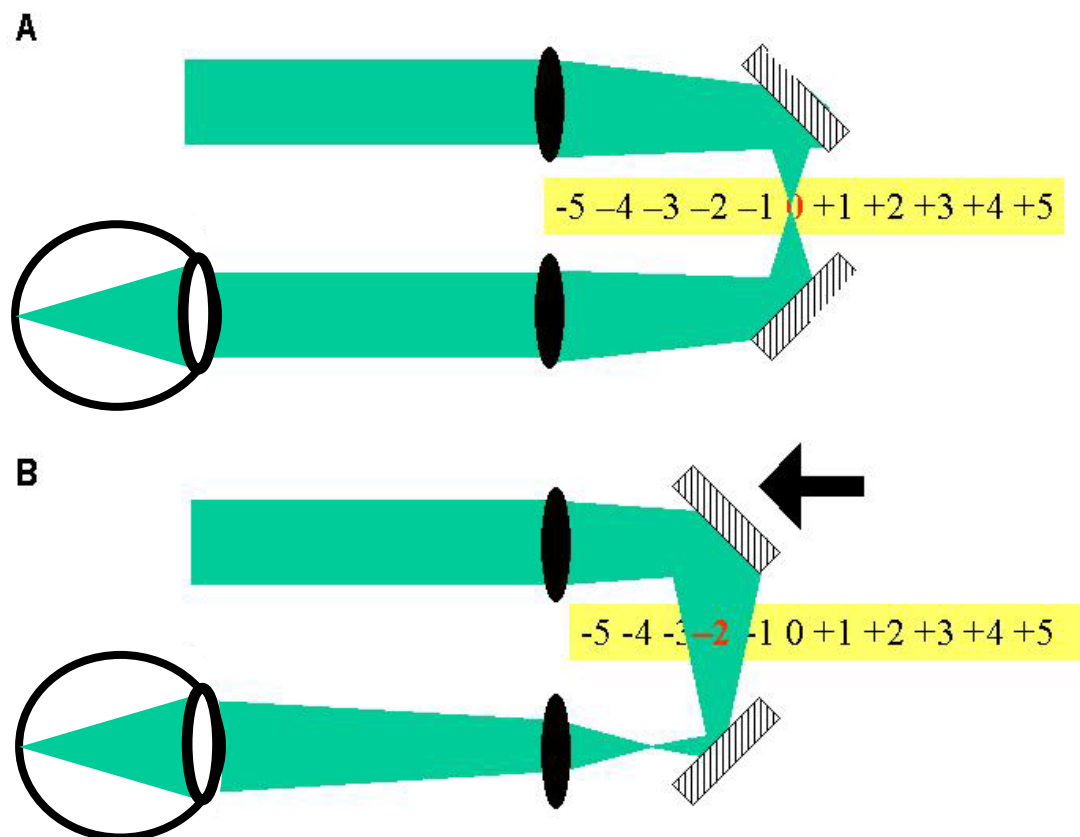


Figure 2.3 A- Badal position for an emmetropic eye. B-Badal position to correct a myopic eye.

vertical and horizontal axes lengths (Newport, 13E20-ER2 with reflectivity more than 98.5%) and two lenses (L1 & L2) (Newport, PAC055, 125 mm of focal length and a diameter of 25.4 mm). The mirrors were mounted on a rail and they were displaced to compensate for refractive errors. A displacement of 7.81 mm on the rail was equivalent to a focus shift of 1 D. The system could correct from -10 D to +10 D. Figure 2.3 shows an scheme of Badal position for emmetropic eye (A) and the position for correction of a myopic eye (B).

2.1.1.3. Pupil monitoring

The pupil monitoring channel was inserted in the system by means of two plate beam splitters (BS1 & BS2, Newport). The pupil was illuminated by 8 LEDs (Luminiscent Electric Diode) mounted on a 48-mm diameter ring (LR) placed in front of the eye and a camera (C2). The camera (Qcam, Logitech, Romanel-sur-Morges, Switzerland) has a color CMOS sensor of 1/5" size, a resolution of 352 x 288 pixels and 43° of field of view. The USB interface permitted an easy and fast communication with the computer. The camera lens was replaced by a custom-built system with an objective built with two concentric aluminium cylinders and a lens (50.8mm focal length and diameter= 25.4mm lens diameter) (Newport, PAC040). Images of the pupil plane were magnified by a factor of x2. The camera allowed continuous viewing of the pupil and was used to center the eye immediately before the image capture.

2.1.2. Automatic control and data processing

Cameras, shutter and image capture were controlled by a program developed in Visual Basic. The Interface program permitted grabbing pupillary images, closing and opening the shutter and capturing the Hartmann-Shack retinal images. When the eye appeared aligned in the pupil monitoring camera, the software allowed rapid opening of the shutter, Hartmann-Shack image capture and saving and shutter closing. Figure 2.4 shows a typical screen capture of the control software.

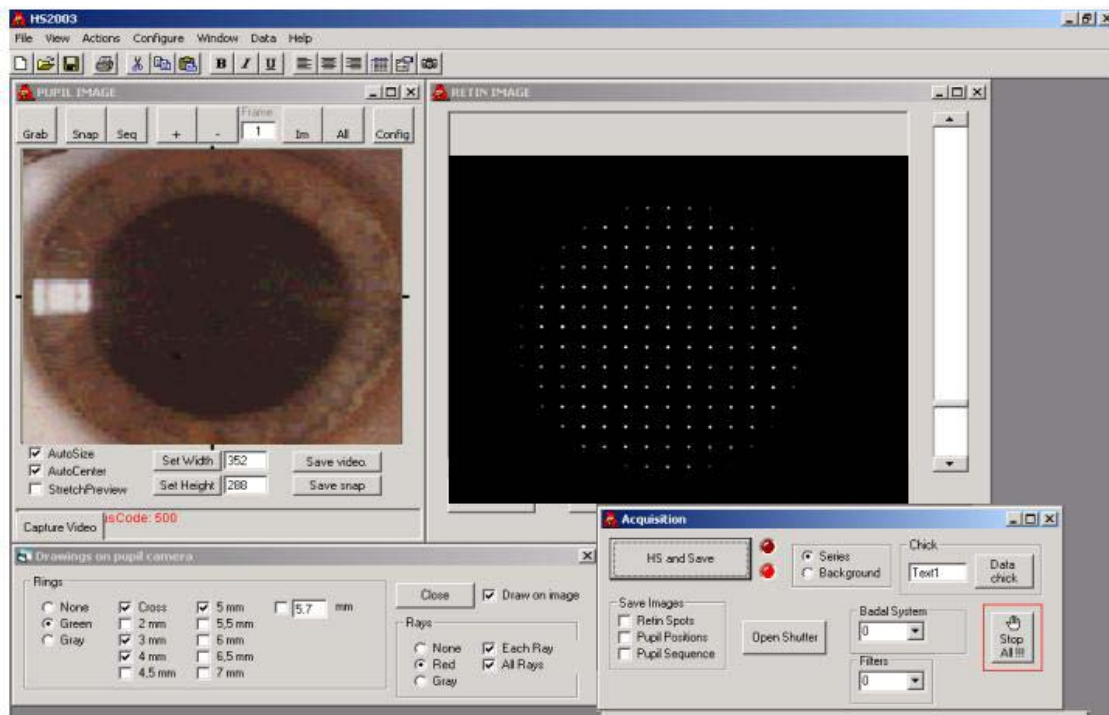


Figure 2.4 Screen capture from the control software.

The Hartmann-Shack spot images were processed using custom routines written in Matlab. The processing routines comprise the following steps, described graphically in Figure 2.5: 1) The retinal image was automatically divided in cells, each cell corresponding to the field of view of each microlens. For an ideal optical system (with no aberration) each HS spot should lie in the center of the cell. 2) Each spot image was detected automatically and fitted to a 2-dimensional gaussian function. The centroid was estimated as the peak location of the gaussian function. 3) The goodness of the fit to a gaussian function was estimated and a rejection criterion for eliminating spots corresponding to cells were the fitting parameter was below a threshold.

Typical situations in which the goodness of the fit was below threshold corresponded to situations in which there was light leakage from an adjacent cell, two spots in a cell, saturated images with non gaussian intensity profile, cells with no spots etc...4) From the centroids the aberration ray of each pupil position was estimated as the angular distance between the centroid of the

corresponding aerial image and the ideal location. The calibrated scale at the retinal image plane is 1 mrad = 0.024 mm. 5) The wave aberration was reconstructed from ray aberrations by a polynomial Zernike modal fitting.

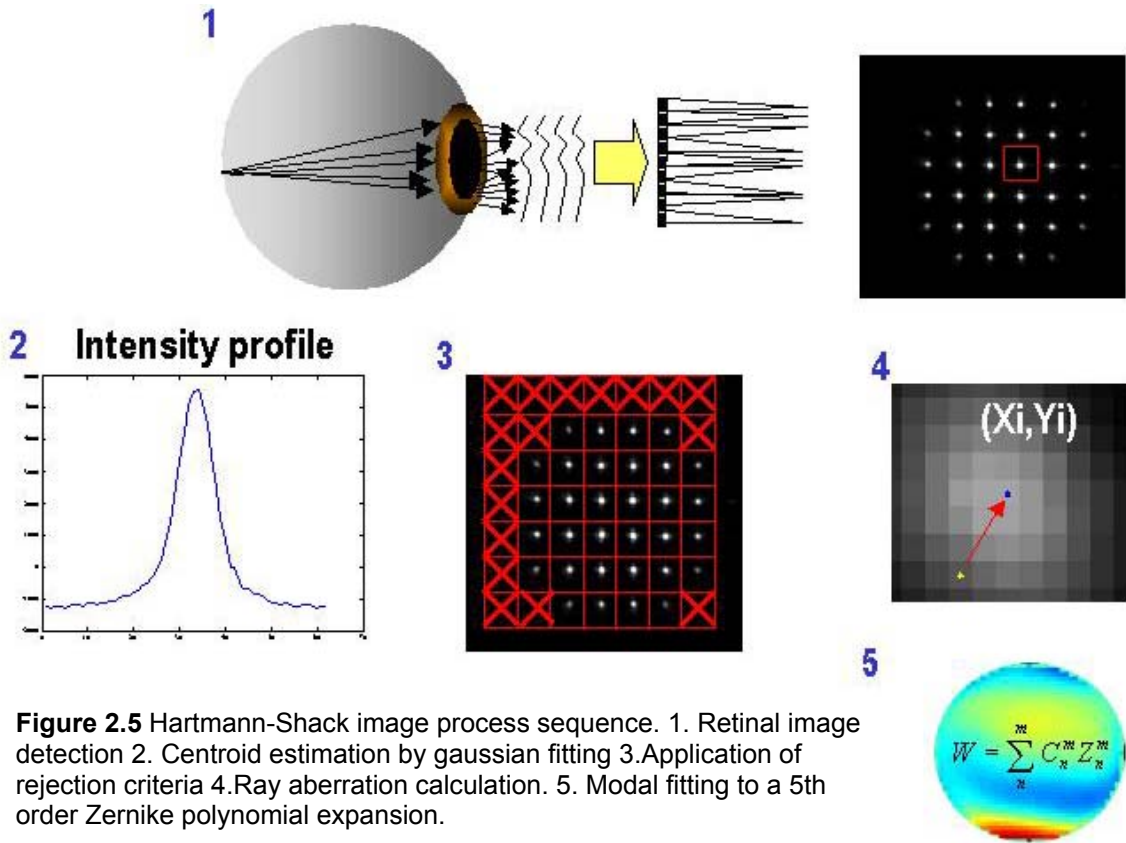


Figure 2.5 Hartmann-Shack image process sequence. 1. Retinal image detection 2. Centroid estimation by gaussian fitting 3. Application of rejection criteria 4. Ray aberration calculation. 5. Modal fitting to a 5th order Zernike polynomial expansion.

2.1.3. Alignment and calibration of the system

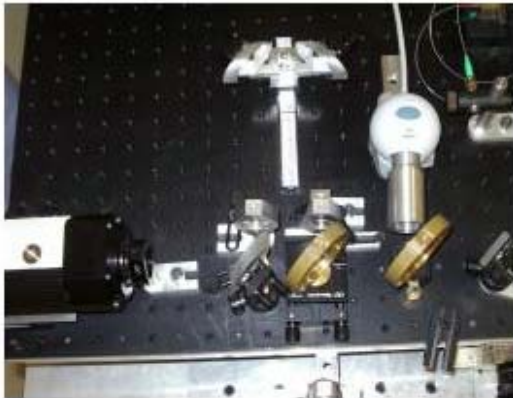
A systematic alignment was performed to ensure proper centration (at any position of the Badal system), and accurate location of pupil and retinal conjugate planes. Also, the system was calibrated using trial lenses, phase plates and artificial eyes with known aberrations.

2.1.3.1. Placing the micro array and CCD cameras

CCD camera C1 was placed on a x-y micrometer stage. First, the optical axis of the system was identified, and centered on the CCD chip. The location of the microlens array (a pupil conjugate plane) was found using a calibrated grid, the CCD camera and the focusing block, as the plane where

the magnification of the images of the grid captured by the CCD was constant

Badal: +10D



Badal: -10D

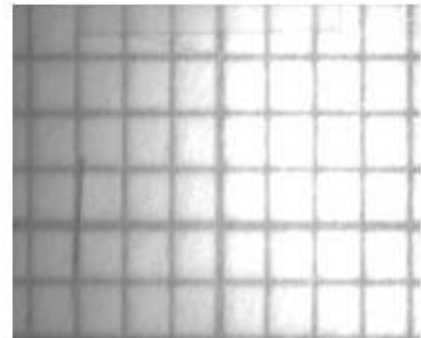
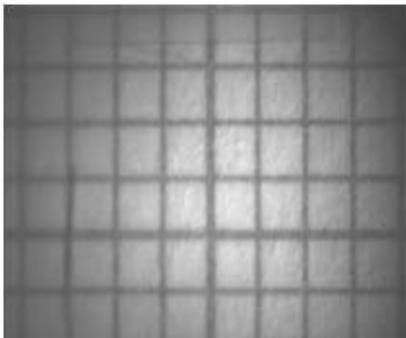
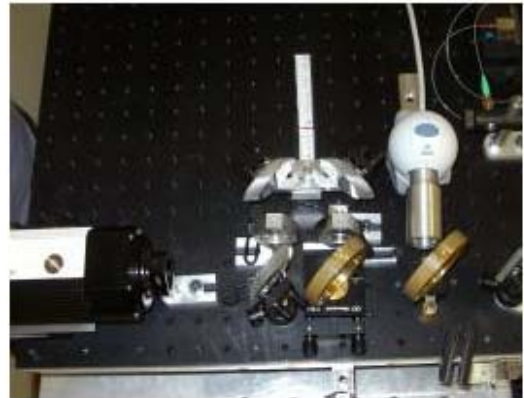


Figure 2.6 Images of the calibrated grid from two different positions of the Badal system during the set-up alignment.

regardless the position of the focusing block.

Figure 2.6 shows two images of the calibrated grid placed at the pupil plane, for two different positions of the focusing Block (0D and -10 D). Once this position was found, the pupil camera (C2) was placed in the pupil monitoring channel in such a way that both cameras captured the same test images and were collinear

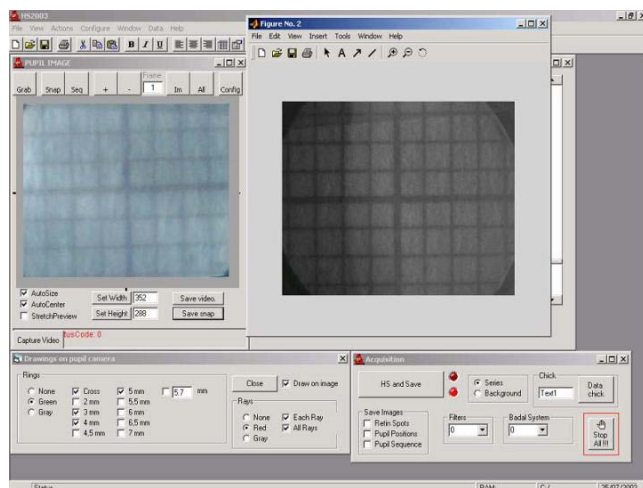


Figure 2.7 Images of simultaneous test grid by the retinal camera (C2, left) and the pupil camera (C1, right).

with the optical axis of the system (see Figure 2.7). Finally, we moved the CCD camera back 24 mm (i.e., the focal distance of the microlens array) along the optical axis, and placed the microlens array on the pupil conjugate plane. The alignment of the system was checked again, with an artificial eye (described in the next section), ensuring that the central spot of the retinal grid image (which is collinear with the optical axis of the camera) did not move across different positions of the Badal system.

2.1.3.2. Artificial eye

An artificial eye was built for validations and calibrations of the system. It consisted of an achromatic lens of 12.7 mm of diameter and 50.8 mm focal length (Newport, PAC028) and an aluminium cylinder. At the end of the cylinder a diffuser acted as a retinal back-reflector. A screw allowed to move the “retina” in the axial dimension. to simulate different refractive conditions. All Zernike terms measured for this eye were significantly different from zero. In particular, at best focus Z_{20} and Z_{40} were <0.01 microns.

2.1.3.3. Calibration of the Badal System

We checked that the Badal system did not introduce magnification errors in the system and that the defocus corrections matched the theoretical predictions. The calibration of the Badal system involved the following steps: 1) We measured the separation between spots when the Badal lenses L1 and L2 were removed. The measured distance was 400 microns, the nominal separation between the centers of the microlenses. 2) With the lenses back in the system, we used the artificial eye described in section 2.1.3.2. to set up the zero position of the Badal system (where the spot separation is 400 microns). 3) We estimated the second order wave aberrations for the artificial eye and 10 different positions of the Badal optometer. We verified with equation 2.1 (Thibos et al. 2002):

$$M = \frac{-Z_{20}4\sqrt{3} + Z_{40}12\sqrt{5} - \dots}{r^2} \quad \text{Eq (2.1)}$$

that the mirror displacement was 7.81 mm/diopter, which matched the theoretical estimation

2.1.4. Validation of aberration measurements

We checked that the Hartmann-Shack system measured low and high order aberrations accurately. We used the artificial eye described in Section 2.1.3.2, provided with spherical and cylindrical trial lenses, as well as three Polymethyl methacrylate (PMMA) test eyes with known high order aberrations (Campbell 2005).

2.1.4.1. Sphere and cylinder measurements

Data were obtained for the artificial eye described in section 2.1.3.2 with spherical trial lenses placed in a pupil conjugate plane. Defocus was obtained from Zernike coefficients using equation (2.1). Figure 2.8 (A) shows defocus for the different trial lenses under test ranging from -3.25 D to $+4$ D. Additional measurements were performed using cylindrical lenses with the non-aberrated artificial eye, which were used to check that the measured amount of astigmatism and axis were correct (examples for $+2$ and $+3$ D cylindrical lenses are shown in Figure 2.8 (B)). Average differences between measured cylinder and nominal values were: -0.21 ± 0.22 D, and average difference in the axis was 3.5 ± 3.1 degrees.

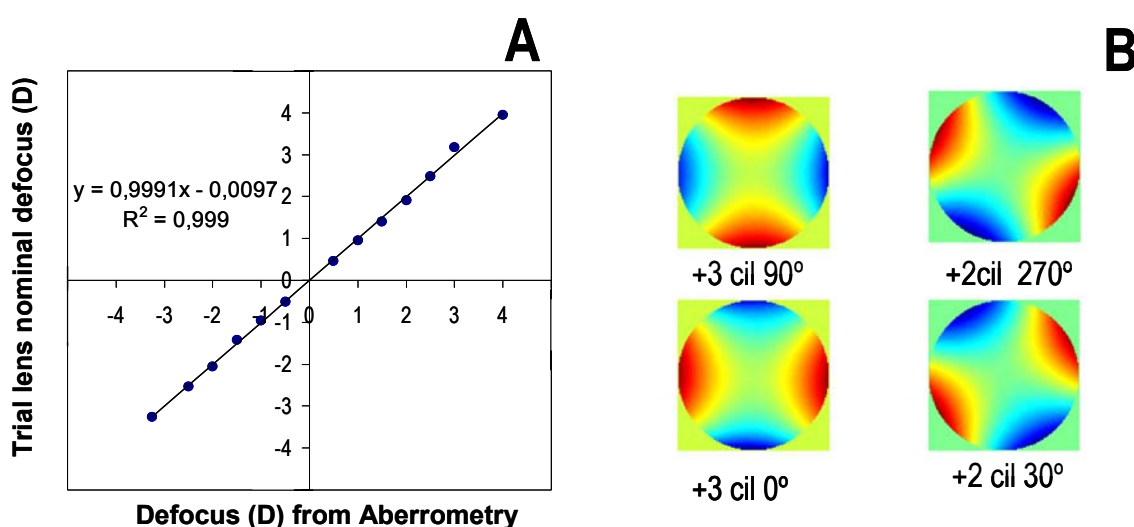


Figure 2.8 A. Trial lens defocus vs. defocus obtained by Zernike coefficients. B. Aberration maps for several cylindrical trial lenses.

2.1.4.2. High order aberrations

The accuracy of our Hartmann Shack system in measuring high order aberrations was studied using PMMA artificial eyes with known aberrations provided by Charles Campbell (Berkeley, CA, USA). These test eyes were designed as rods with a convex front surface with a radius of curvature similar to the human cornea (7.8 mm) and 12.7 mm of diameter (Campbell 2005). The back surface (“retinal plane”) is polished and painted with black paint. Three eyes were tested: A4 with a simple spherical front surface, and nominally only with coefficients Z_{20} and Z_{40} significantly different from zero; A3 (cast) and L2 (extruded) lathed with significant amounts of high order aberrations in terms Z_{20} , Z_{40} , Z_{51} and Z_{62} . The eyes had been calibrated using numerical ray tracing on the surface elevation maps, and measured by different commercial aberrometry techniques in a published multi-site study by Campbell (Campbell 2005). The reference values were obtained by averaging results from the different instruments. Figure 2.9 shows a comparison of Zernike coefficients from the average reported values and those obtained with or our Hartmann Shack system.

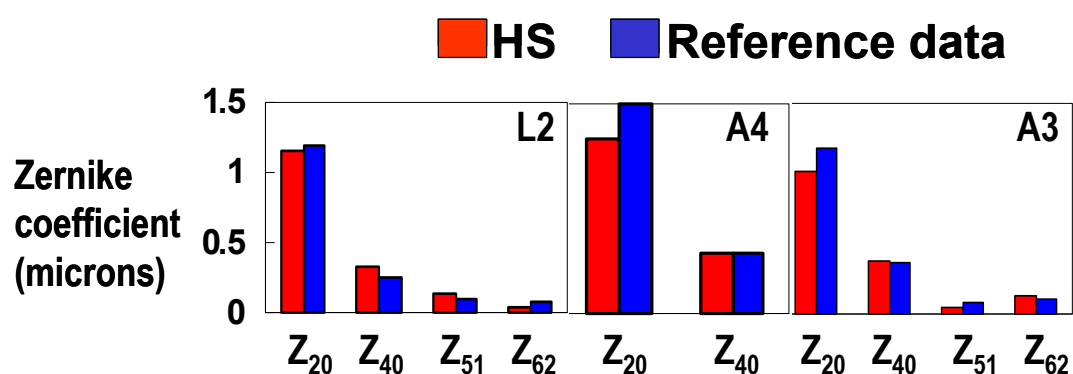


Figure 2.9 Comparison of high order aberrations from our Hartmann-Shack aberrometer and nominal data for a PMMA artificial eye (provided by C.Campbell)

2.2. Measurement of biometric parameters

In addition to ocular aberrations, the measurement of other biometric parameters was essential to assess the ocular dimensions and power during natural development or following treatment in experimental animal models (under awake conditions). We implemented techniques to measure axial length and corneal radius of curvature, as well as refractive error in animal models.

2.2.1. Refractive error

In this thesis we present measurements of refractive error from two different techniques: retinoscopy and based on aberrometry when retinoscopy was not possible (in chick refractive surgery and mouse models).

2.2.1.1. Streak Retinoscopy

Retinoscopy is an objective technique to evaluate spherical and cylindrical refractive error. It consists of neutralizing the movement of pupil reflex with trial lenses while sweeping the scope across the pupil. If the streak appears to be moving against the direction of the scope, minus lenses are required, and the opposite when the reflection moves with the scope. If there is no apparent motion, neutrality has been reached. The procedure can be repeated on any meridian to obtain astigmatism. This clinical technique had been widely used in chicks before (Yinon et al. 1980).

In this thesis we performed retinoscopy measurements under natural viewing conditions (no anaesthesia, no cycloplegia, nor



Figure 2.10 The author performing a chick retinoscopy measurement

lid-retractors). Figure 2.10 shows a chick retinoscopy measurement in the laboratory.

2.2.1.2. Spherical equivalent from aberrometry

Refraction was obtained in some experiments as the spherical equivalent from a wave aberration measurement, added to the defocus compensated by the Badal system (see section 2.1.1.2). The spherical equivalent of the wave aberration is defined as the quadratic surface which best represents the wave aberration map, obtained by minimizing the sum of squared deviations between the wave aberration and the quadratic surface. The least square solution is given by the second order Zernike coefficients and can be converted to sphere using equation 2.1, and cylinder at 0° and 45° with equations 2.2 and 2.3, respectively (Thibos et al. 2002).

$$J_0 = \frac{-Z_{22}2\sqrt{6} + Z_{42}6\sqrt{10} - \dots}{r^2} \quad \text{Eq. (2.2)}$$

$$J_{45} = \frac{-Z_{2-2}2\sqrt{6} + Z_{4-2}6\sqrt{10} - \dots}{r^2} \quad \text{Eq. (2.3)}$$

2.2.2. Axial length: Biometry

To evaluate eye length is important to assess ocular growth due to natural development in control eyes and treatment-induced elongation in treated eyes. We measured axial length in awake chicks with a standard ultrasound biometry (for measurements in humans) adapted to chick eye's dimension, using a technique

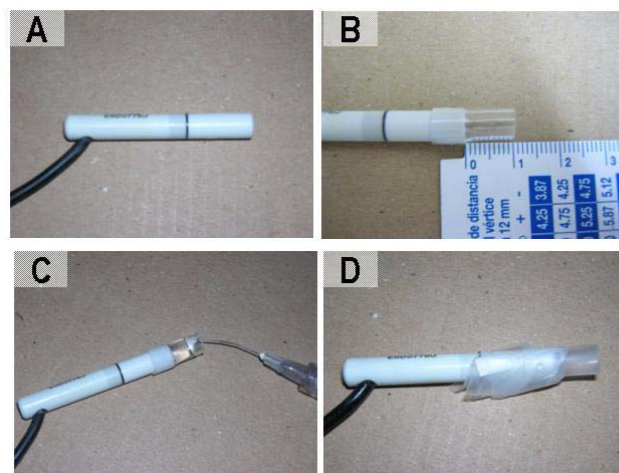


Figure 2.11 Biometer probe adapted. A. Normal probe. B. Plastic tube extension. C. Filling the tube with water. D. Covered with paraffin film.

proposed by Schaeffel et al (Schaeffel and Howland 1991). We used an Allergan Humphrey ultrasound biometer (Mod. 826) with a custom-adapted probe. A 10-mm plastic tube was attached to the probe, filled it with water and covered with paraffin film, as described in the literature (Schaeffel and Howland 1991), and illustrated in Figure 2.11. This technique requires topical anaesthesia due to the contact between the probe and the cornea. Figure 2.12 shows the author of this thesis performing an ultrasound biometry measurement on a chick and a typical result on the display of the commercial instrument. In normal clinical measurements two peaks are obtained, indicating two interfaces: probe-cornea and vitreous-retina. The distance between these peaks is the axial length. In the instrument with the adapted probe and additional peak is obtained, resulting from the tube extension - original probe interface. We subtracted the tube extension length from axial length indicated by the biometer to obtain axial length in small animal eyes. For each measurement the isolated tube length was measured, by capturing a tube measurement with the tube immersed in a water recipient.

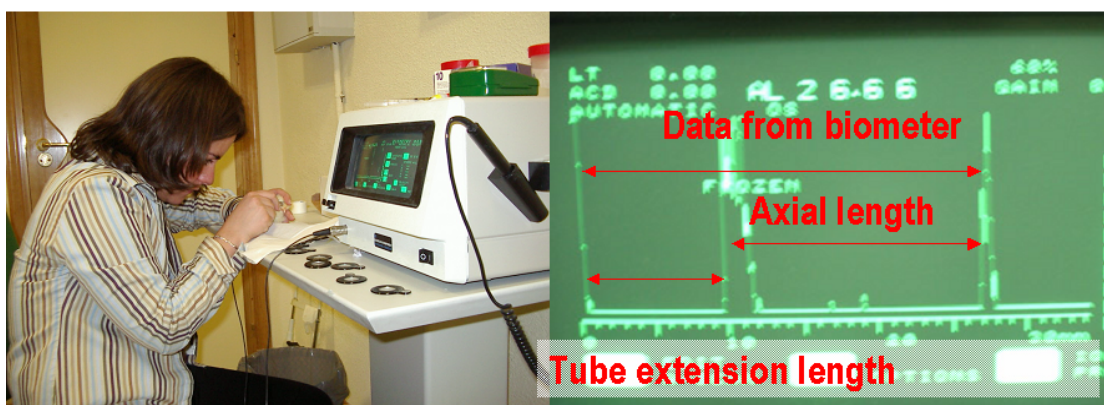


Figure 2.12 Picture of a biometric measurement on a chick and an image of the ultrasound screen.

2.2.3. Corneal radius: Keratometry

For this thesis we also implemented a custom-built infrared (IR) photokeratometer to measure corneal curvature in the chick eye. This method has been applied in animal models previously, and it is described by Schaeffel and Howland (Schaeffel et al. 1986; Schaeffel and Howland 1987). Our keratometer consists of a ring of eight Infrared (IR) LEDs placed around a

circumference of 80 mm diameter and an 8-bit CCD camera (Toshiba Teli America, 1360 x 1023 pixels, Irving, California, USA) provided with a 105 mm focal length camera lens (Rodenstock) and extension tubes (70 mm). A schematic dia gram of the system is depicted in Figure 2.13. The image capture was controlled by the computer using a program written in Visual

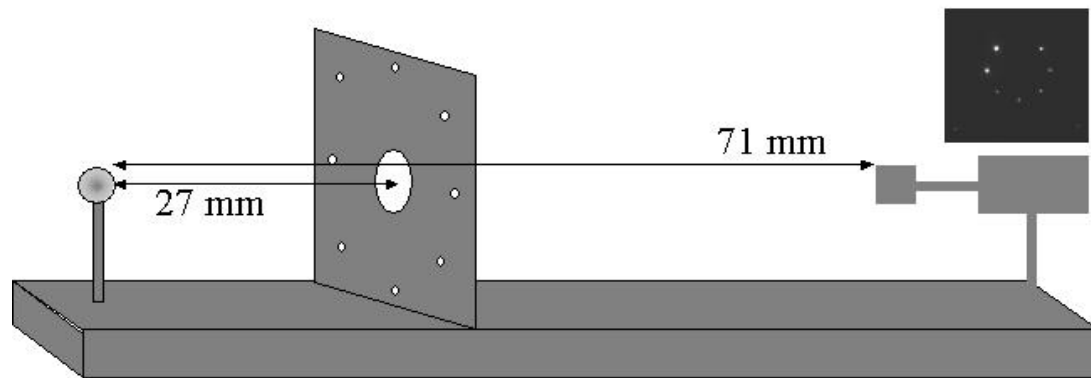


Figure 2.13 A schematic diagram of the implemented keratometer

Basic (Microsoft Corporation, Redmond, Washington). Figure 2.14 shows a screen capture of the software. The pupillary images were processed using routines written in Matlab (Mathworks, Nattick MA). The Purkinje images of the LEDs were detected, and their positions were automatically estimated using a centroiding algorithm. The system was calibrated using a set of calibrated steel spheres, and the calibrated curves were used to convert from the ring diameter on the image (average radial distance between LED image locations) to corneal radius of curvature. Figure 2.15 (A) shows a typical image from a steel sphere and (B) the calibration curve which relates radius of the LEDs circle image with the nominal sphere radius. The diameter of the LED ring on the image was computed, using a scale of 0.019 mm/pixel. The conversion factor, obtained from a linear regression to the data of Figure 2.15 (B) was: 1 mm (ring diameter) / 3.9 mm (corneal radius of curvature).

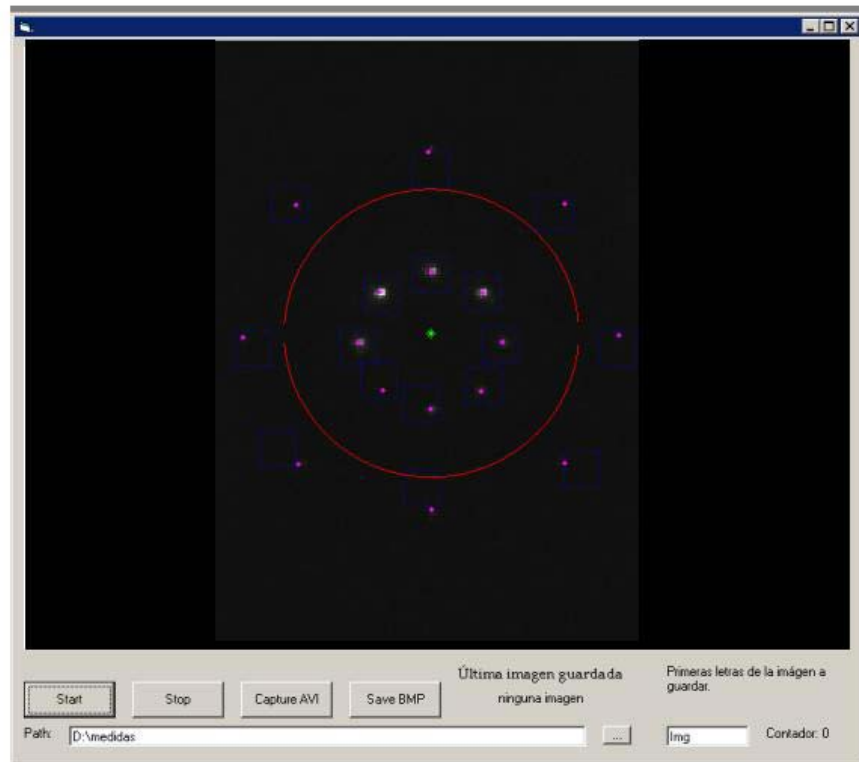


Figure 2.14 An example of a keratometric image from as captured by the custom keratometer software.

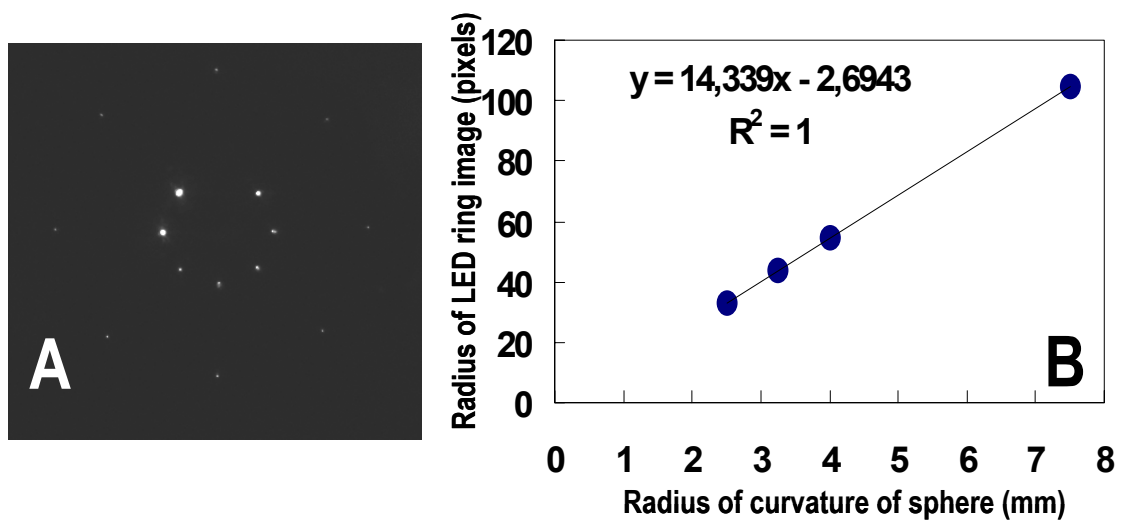


Figure 2.15 A. image from a calibrated steel sphere. B. Calibration curve (radius of the LEDs circle image vs. nominal sphere radius).

Chapter 3: Longitudinal changes of optical aberrations in normal and form-deprived myopic chick eyes

Resumen capítulo 3:

Cambios longitudinales de las aberraciones ópticas in ojos de pollo miopes y emétopes.

Realizamos medidas de refracción (con retinoscopía), longitud axial (con biometría por ultrasonidos) y aberraciones oculares (con un aberrómetro Hartmann-Shack de construcción propia) en 7 pollos “White-Leghorn” despiertos tratados con oclusión monolateral por difusores durante dos semanas. El tratamiento comenzó el primer día después del nacimiento y las medidas se realizaron en varios días hasta el día 13 de vida. Los ojos no ocluidos experimentaron un proceso normal de emetropización, es decir, los valores de hipermetropía disminuyeron a un ritmo de 0.2 ± 0.09 D/día y la longitud axial aumentó 0.05 ± 0.03 mm/día, mientras los ojos ocluidos desarrollaron miopía axial (1.50 ± 0.2 D/día y 0.12 ± 0.02 mm/día). Las diferencias entre ojos de los promedios de refracción y longitud axial para el día 13 fueron 17.43 D y 0.86 mm respectivamente. Las aberraciones de alto orden monocromáticas disminuyeron con la edad en ambos ojos. El promedio de la RMS (Raíz cuadrática media) para pupilas de 1.5 mm de diámetro disminuyó de 0.11 ± 0.03 micras en el día 0 hasta 0.06 ± 0.03 micras en el día 13 en los ojos ocluidos y de 0.12 ± 0.05 micras hasta 0.03 ± 0.01 micras en ojos sin ocluir. La calidad óptica en términos de MTF (Función de transferencia de modulación) también muestra una mejora con la edad. A partir del día 8 los ojos miopes tienden a mostrar valores significativamente mayores de aberraciones oculares y, por tanto, peor calidad óptica con corrección óptimo de desenfoque que los ojos emétopes. La degradación impuesta por las aberraciones es pequeña comparada con la impuesta por el desenfoque y el difusor. Esos resultados sugieren un mecanismo de disminución de las aberraciones durante el desarrollo que no está guiado por estímulos visuales. Los ojos miopes presentan una calidad óptica peor que los ojos control, sugiriendo que los cambios geométricos debidos al excesivo alargamiento del globo ocular también afectan a la calidad óptica de las distintas estructuras oculares.

This chapter is based on the article by García de la Cera et al. “Longitudinal changes of optical aberrations in normal and form-deprived myopic chick eyes”, *Vision Research* (2006) 46, 579-589.

The contribution of Elena García de la Cera to the study was to develop the methodology to measure ocular aberrations, to perform all calibrations, and data processing routines, the performance of the experimental measurements on chicks (ocular aberrations, retinoscopy and ultrasound biometry) and data analysis and interpretation.

Coauthors of the study are: Guadalupe Rodríguez and Susana Marcos.

3.1. Abstract

We performed measurements of refraction (with retinoscopy), axial length (with ultrasound biometry) and ocular aberrations (with a custom-built Hartmann-Shack aberrometer) on seven awake White-Leghorn chicks occluded monolaterally with diffusers for two weeks. Treatment started on the first day after hatching (day 0) and measurements were conducted on several days between day 0 and 13. Non-occluded eyes experienced normal emmetropization (decreasing hyperopia at 0.2 ± 0.09 D/day and increasing axial length at 0.05 ± 0.03 mm/day), while occluded eyes developed axial myopia (1.50 ± 0.2 D/day and 0.12 ± 0.02 mm/day). Interocular differences in refraction and axial length by day 13 were on average 17.43 D and 0.86 mm, respectively. Monochromatic high order aberrations decreased with age in both eyes. Average RMS (for 1.5 mm pupil diameter) decreased from 0.11 ± 0.03 at day-0 to 0.06 ± 0.03 microns (day-13) in occluded eyes, and from 0.12 ± 0.05 to 0.03 ± 0.01 microns in non-occluded eyes. MTF-based optical quality metrics also show an improvement with age. However, while this improvement occurs in both eyes, after day 8 myopic eyes tend to show significantly higher amounts of aberrations (and consequently worse best-corrected optical quality) than normal eyes. The degradation imposed by aberrations is small compared to that imposed by defocus and the diffuser. These results suggest a decrease of aberrations during development which does not seem to be visually guided. Myopic eyes showed slightly worse optical quality than normal eyes, suggesting that the geometrical changes resulting from excessive ocular axial growth also affect the optical quality of the ocular components.

3.2. Introduction

There is compelling evidence, mostly from animal models, that the absence of a normal visual experience in the early stages of development compromises emmetropization, i.e. the normal ocular growth aiming at matching axial length of the eye to its optical power and achieving focused images on the retina (Wallman 1993; Wildsoet 1997; Smith 1998). It is well established that visual form deprivation, as well as other ways of altering the visual environment, produces axial elongation and myopia in a variety of species. The chick has been an extensively used animal model, myopia development has been achieved with lid closure (Yinon 1984), deprivation of form vision by placing opaque or translucent goggles in front of the eye (Hayes et al. 1986; Wallman and Adams 1987; Troilo and Wallman 1991), or restricting the contrast and spatial frequencies of the visual environment (Schmid and Wildsoet 1997). With the previous methods the eye growth control system runs open-loop with no possible feedback. Myopia has also been achieved by placing negative lenses in front of the animal's eye. In this case, the eye adjusts its growth to compensate for the imposed defocus (Schaeffel et al. 1988; Kee et al. 2001). It has also been observed that when normal vision is restored, even for short periods of time, the myopia tends to regress (Troilo and Wallman 1991). While many studies have been performed on chicks, the impact of visual experience on normal eye growth has also been demonstrated in primates (Weisel and Raviola 1977; Troilo et al. 2000). Also, pathology-related form deprivation in human infants (by eyelid closure, congenital cataracts or corneal opacities) has been associated to the development of myopia.

The investigation of possible relationships between optical aberrations and myopia seems suggestive, in particular since the causes of myopia are not well understood. Several studies have investigated potential correlation between high order aberrations and myopia (Liang et al. 1994; He et al. 1998; Moreno-Barriuso et al. 2001; Atchison et al. 1995; Paquin et al. 2002). However although some of these studies show a co-variability, a cause-effect relationship

cannot be inferred. Some results suggest that the constant degradation of the image quality produced by increased aberrations could disrupt the emmetropization process (Buehren et al. 2003). Also, results from clinical trials have shown that rigid contact lenses reduced the progression of myopia in children and adolescent subjects, compared to controls wearing soft contact lenses or spectacles (Perrigin et al. 1990; Khoo et al. 1999). Interestingly, aberration measurements on rigid gas permeable (RGP) contact lens wearers with and without the contact lens on have shown the capability of RGP contact lenses to correct for significant amounts of high order aberrations (Dorransoro et al. 2003). While those results are suggestive, there is no definite proof that aberrations could be a cause of myopia nor that cancelling aberrations could be a potential way of reducing excessive ocular growth. On the other hand, it has been argued that the presence of aberrations may provide cues to determine the sign of defocus, since interactions between high order aberrations and defocus (and as a consequence retinal image quality) change with the sign of defocus, and that these effects may be important in the emmetropization process (Wilson et al. 2002). Alternatively, the ocular enlargement of myopic eyes (and therefore different geometrical properties of the ocular components) could be the reason for the increased amount of aberrations found in myopic eyes. The question is whether the increased optical aberrations in myopic eyes is a cause or a consequence of myopia.

Unlike studies in animal models, to test cause-effect relationships in humans is complicated, due to the time cost of longitudinal studies and impossibility of intervening the ocular optical properties in infants. While chicks have been widely used as animal models of myopia, their optical quality has not been studied experimentally in much detail. In most studies, modelling and conclusions assume diffraction-limited optics. Coletta and co-workers (Coletta et al. 2003) reported optical quality (in terms of modulation transfer function) of normal and myopic chick eyes using a double-pass method. To our knowledge, two studies have attempted to measure monochromatic aberrations in younger chicks using Hartmann-Shack aberrometers (Liang et al. 1994; Liang and Williams 1997). The study from the University of Waterloo was published

(Kisilak et al. 2006) several months after our own study (García de la Cera et al. 2006).

In this chapter we present longitudinal measurements of refraction, axial length and monochromatic aberrations in occluded eyes and normal chick eyes during the first two weeks of development. The aims of the study presented in this chapter are to investigate:

- 1) longitudinal changes of aberrations during normal emmetropization;
- 2) the effect of myopia development on ocular aberrations;
- 3) possible effects of natural aberrations on myopia development;
- 4) the differences in optical quality in myopic and emmetropic eyes;
- 5) longitudinal changes of aberrations in myopic eyes.

Unlike myopia caused by lens treatment (where the lens+elongated eye tends to form an optically good system), form deprived eyes are subject to the continuous degradation produced by the diffuser. If we find that this treatment resulting in myopia also produces increased amounts of high order aberrations, we will favor the hypothesis that aberrations are a consequence, rather than a cause of myopia. In such a model, the enlargement of the eye (and subsequent modification of structural properties of the ocular components) would be the reason for the larger aberrations found in myopic eyes.

3.3. Methods

3.3.1. Subjects and experimental protocols.

Ten White-Leghorn chicks were used in this experiment. All experimental protocols were approved by the Institutional Review Boards and followed the tenets of Helsinki. Seven chicks were monocularly treated and measured periodically. Another three, two untreated and one treated, were measured only on the last day, as control subjects (to discard possible interferences from the repeated measurements). All chicks were labelled with color wires attached around their feet. Chicks were reared under fluorescent lighting (12h/12h

light/dark cycle conditions) in a cage inside a controlled heated room (24-28 °C). They were allowed to eat and drink ad libitum. Adequate measures were taken to minimize pain or discomfort.

The seven non-control chicks were initially measured in their first day after hatching. This day was named “day 0”. Days of age are therefore estimated adding one day to the measurement day. Immediately after the measurements, the right eye of each chick was occluded, and the non-occluded eye (left eye) was used as a reference. Occluders consisted of translucent diffusers which were manufactured with a sheet of plastic, moulded to obtain hemispherical translucent goggles (Frank Schaeffel, Personal communication). The occluders were attached with velcro rings glued to the feathers around the eye. They were only removed during measurements on days 0, 1, 4, 6, 8, 11 & 13. On these days we obtained measurements of refractive error, axial length and monochromatic aberrations in both eyes. An experimental session, including the three types of measurements, lasted typically five minutes per eye. All measurements were performed with the animals awake and under natural viewing conditions.

3.3.2. Refraction and ultrasound biometry

Refraction was measured using streak retinoscopy with trial lenses in the horizontal meridian. Chicks were awake and unanaesthetized. We did not use cycloplegia nor lid-retractors.

An adapted ultrasound biometer (Allergan Humphrey Mod. 826) was used for axial length measurements. The probe was adapted to the chick eye's dimensions using a 10-mm tube filled in with water and covered with paraffin film (Schaeffel and Howland 1991), as described in section 2.2.2. Measurements were conducted under topical anaesthesia, a drop of lidocaine 1%. Five data were obtained per condition.

3.3.3. Shack-Hartmann aberrometry

Aberrations were measured with a custom-built compact Hartmann-Shack (HS) wavefront sensor, which we built specifically to measure ocular aberrations in animal models (described in Section 2.1.1. of this thesis). The entire system is mounted on an x-y translational stage. The chick sits on an elevating platform mounted in front of the system, which was moved to ensure correct centration and focusing of animal's pupil. The animal usually stayed quiet during the measurement, allowing us to capture several images per eye (See Figure 3.1A). The number of spots captured per image was related to the pupil size. We estimated pupil diameter as the distance between the two most separated spots in a HS image. We found that pupil increased with age, from (treated/untreated eyes) on day 0 to 2.3/2.9 mm on day 13, on average. Figure 3.1 (B,C & D) shows three typical examples of HS images from chick eyes.

Zernike coefficients were obtained by modal fitting of the lateral deviations to derivatives Zernike polynomial expansion up to the 5th order. We obtained a maximum of 20 images per condition and selected the best five. Presence of artifact reflections, limited number of spots or low intensity were used as rejection criteria. Data were processed for the maximum pupil diameter

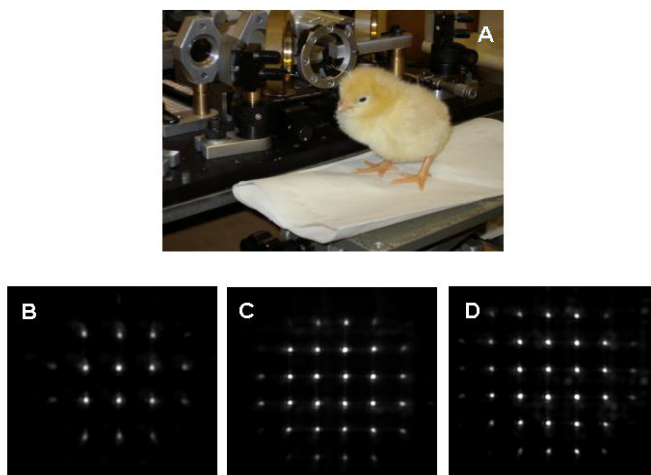


Figure 3.1 (A) Chick during an experiment session, photographed in front of the Hartmann Shack system. (B-D) Examples of Hartmann-Shack images on chick eyes (Chick #5): (A) day 0: before occlusion, (B) day 13: treated eye, and (C) day 13: untreated eye.

(ranging from 1.5 to 3.26 mm). However, for comparative purposes across eyes and days, the minimum pupil diameter of 1.5 mm was used. The optical quality of the eye was assessed in terms of individual Zernike terms or orders and root-mean-square wavefront error (RMS). Modulation Transfer Functions (MTF) and Point Spread Functions (PSFs) were also obtained from the wave aberrations. Strehl ratio was also used as an optical quality metric.

3.3.4. Statistical analysis

We used univariate ANOVA to test the changes with time and global differences between treated and non-treated eyes. Unpaired t-test was used to test differences between treated and untreated eyes on individual days.

3.4. Results

3.4.1. Ultrasound biometry and refraction

Figure 3.2 (A) shows axial length as a function of age in both eyes of the monolaterally treated chicks. Data from all chicks are shown, with squares representing non occluded eyes and the circles representing the corresponding occluded contralateral eye. While both eyes elongate during the first weeks of life ($p < 0.0001$; univariate ANOVA), the occluded eyes grow at a faster rate, and are significantly longer than the non occluded eyes ($p < 0.0001$; univariate ANOVA). The mean growth rate is 0.05 mm/day in non-occluded eyes and 0.12 mm/day in occluded eyes. Axial length increased from 7.2 ± 0.4 mm in non-occluded eyes and 7.1 ± 0.1 mm in occluded-eyes on average on day 0 (prior to treatment) to 7.9 ± 0.2 mm in non-occluded eyes and 8.8 ± 0.3 mm in occluded eyes on day 13. Control measurements on eyes that were left untreated or monolaterally occluded, but only measured on day 13 (to ensure that measurements did not interfere with normal emmetropization or the treatment) revealed similar results: 0.2 ± 0.3 mm interocular axial length difference in two chicks without any treatment, whereas 1.5 ± 0.1 mm interocular axial length

difference between the occluded and non occluded eyes of a non occluded chick.

Figure 3.2 (B) shows refraction as a function of age in both eyes of the monolaterally occluded chick eyes. Each color represents a chick (squares are non occluded eyes and circles are occluded eyes). According to refraction, all eyes were hyperopic on day 0 prior to treatment (OD: $+4.5 \pm 1.2$ D; OS: $+4.1 \pm 1.6$ D) but differences between eyes are statistically significant ($p < 0.0001$; univariate ANOVA) from day 1 ($p = 0.01$; unpaired t-test). Refraction tends gradually toward less hyperopic (non occluded eyes) or more myopic values (occluded eyes). Refraction changes at a rate of 0.21 D/day in the non occluded eye and 1.53 D/day in the occluded eye. By day 13, the non occluded eyes

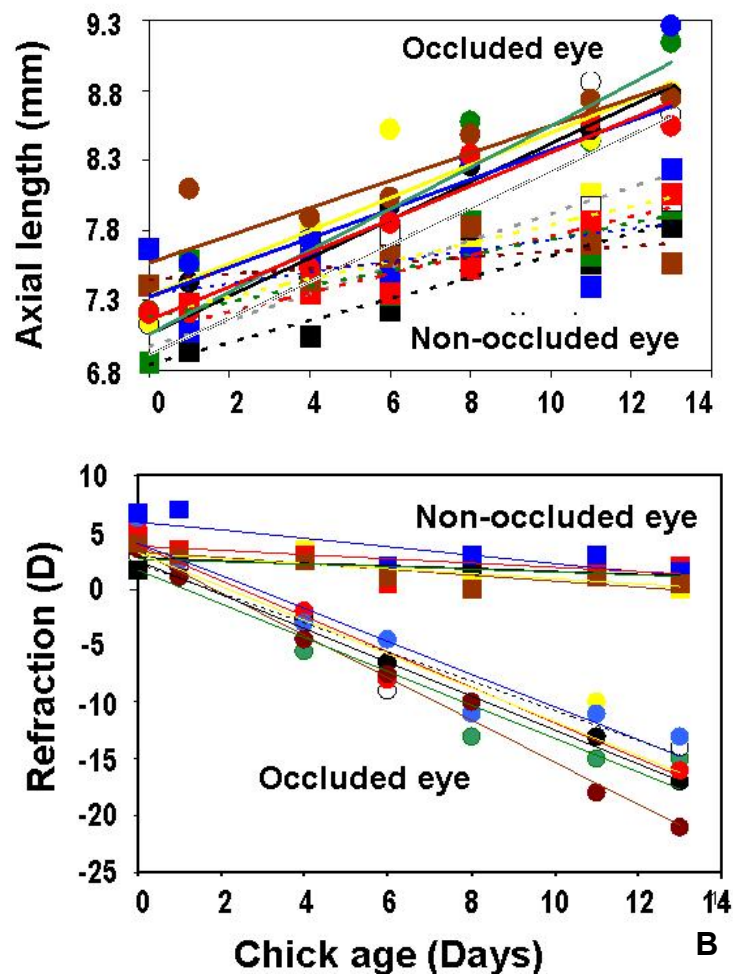


Figure 3.2 (A) Axial length as a function of age. (B) Refraction as a function of age. Each colour corresponds to a different chick. Squares symbols and dotted lines correspond to non-occluded eyes and circle symbols and solid lines correspond to occluded eyes.

show an average refraction of $+0.9 \pm 0.7$ D while occluded eyes show an average refraction of -16 ± 3 D. As we found for axial length, the non occluded chicks show the same trends in refraction as the chicks that were measured repeatedly throughout the study: Untreated non occluded chicks showed 0.5 D and 1.50 D difference between eyes respectively, while monolaterally occluded control chicks showed an interocular difference of 17 D.

3.4.2. Optical aberrations.

Figure 3.3 shows wave aberration patterns for days 0, 8 and 13 on chicks # 1 and # 7 corresponding to the eyes labelled in yellow and green respectively in Figure 3.2. Data are for 3rd and higher order aberrations and 1.5-mm pupil diameters. In both occluded and non occluded eyes, aberrations decrease with age and non-occluded eyes show lower amounts of aberrations than the occluded eyes. These trends are common in all eyes. Figure 3.4 shows longitudinal mean changes of 3rd and higher order RMS (A), 3rd order RMS only

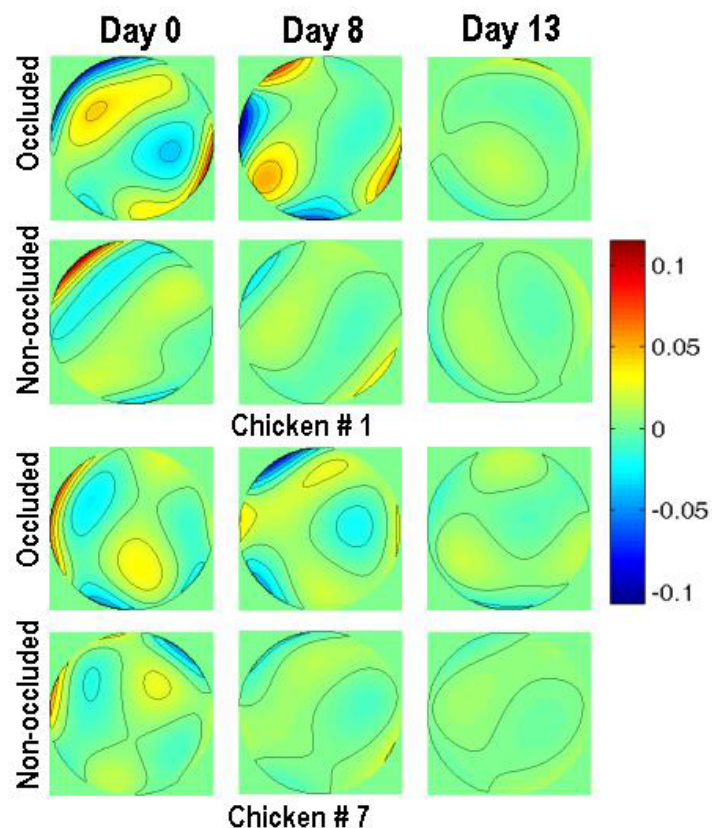


Figure 3.3 Wave aberration patterns for chick # 1 (represented in yellow in Figure 2) and # 7 (green) on days 0, 8 and 13. Data are for 3rd and higher order aberrations and 1.5mm.

and spherical aberration (B & C). For comparison, all RMSs have been computed for the same pupil diameter (1.5 mm). RMS decreases gradually and significantly with age ($p < 0.0001$; univariate ANOVA), and this happens in both non-occluded and occluded eyes, with differences being statistically significant between both groups ($p = 0.01$). Prior to occlusion (day 0), RMS is similar in both eyes ($p = 0.8$) but RMS is significantly higher in the occluded eyes on days 8 ($p = 0.005$; unpaired t-test), 11 ($p = 0.001$) and 13 ($p = 0.03$). From days 8 to 13, both eyes follow an approximately parallel decrease in RMS, with occluded eyes showing higher RMS values in all cases. We found larger intersubject variability in younger (days 0-4) than older chicks (days 6-13) with 0.05 microns vs. 0.02 microns average standard deviations across individuals, respectively. Measurements are also noisier in younger than older chicks: 0.2 and 0.08-microns standard deviations respectively for repeated measurements. Third and higher order RMS decreased from $0.12 \pm 0.05 / 0.11 \pm 0.03$ microns at day 0 to $0.03 \pm 0.01 / 0.06 \pm 0.03$ microns at day 13 for non occluded/occluded eyes. Third order RMS decreased from $0.09 \pm 0.04 / 0.08 \pm 0.02$ microns to $0.02 \pm 0.01 / 0.04 \pm 0.02$ microns.

Average changes of spherical aberration with age are shown in Figure 3.4 (in terms of RMS in C and 4th order spherical aberration Zernike coefficient in D). In the first 4 days the tendency is irregular in both non-occluded and occluded eyes, and tends to stabilize after day 6. Older non occluded eyes show spherical aberration very close to 0, while occluded eyes show slightly negative spherical aberration. On day 13, spherical aberration is practically 0 in both groups: -0.001 ± 0.006 and $+0.002 \pm 0.009$ microns in non occluded and occluded eyes respectively. Differences with age are not statistically significant ($p = 0.4$; univariate ANOVA), nor the differences between treated and non-treated eyes ($p = 0.1$).

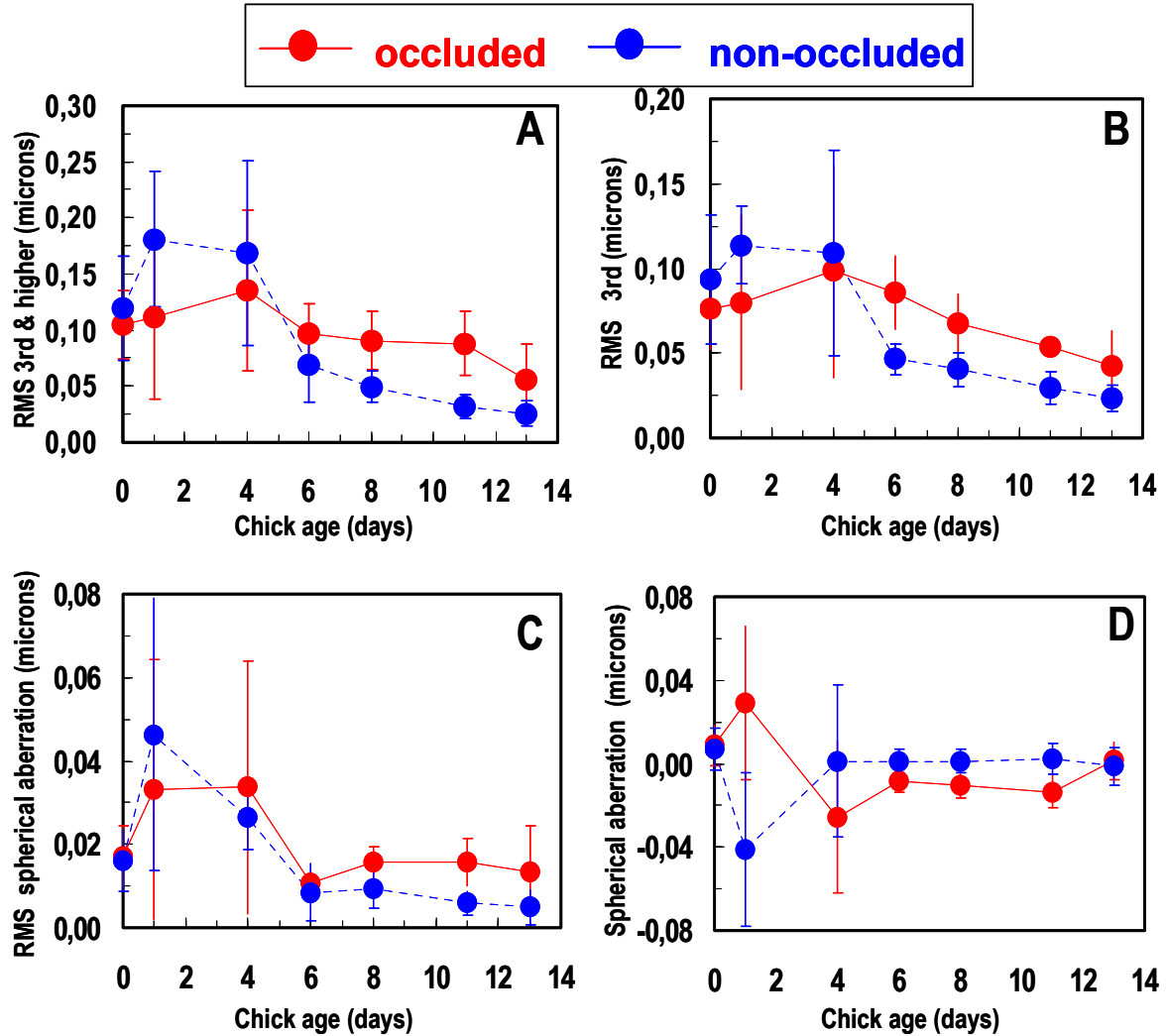


Figure 3.4. Mean 3rd and higher order RMS (A), 3rd order RMS (B), spherical aberration RMS (C), and 4th order spherical aberration Zernike coefficient (D) as a function of age, averaged across all chicks. Pupil diameter: 1.5mm. Blue circles and dotted lines correspond to non-occluded eyes and red circles and solid lines correspond to occluded eyes. Error bars stand for standard deviations.

3.4.3. Modulation transfer function.

Figure 3.5 shows mean MTFs (radial profile), for non occluded and occluded eyes, for several days throughout the experiment. The MTF for an ideal eye without aberrations is also shown for comparison. All data are for 1.5 mm pupil diameters. Prior to treatment, both eyes show similar optical quality in terms of Strehl ratio ($p=0.8$; unpaired t-test). Changes in Strehl ratio with age are significant ($p<0.0001$; univariate ANOVA) as well as the global differences between non occluded and occluded eye ($p<0.0001$; univariate ANOVA). On days 8 and 11 Strehl ratios are significantly better in the non occluded than in

the occluded eye ($p=0.006$ and $p=0.05$, respectively; unpaired t-test). As expected from the RMS values, optical quality improves from day 0 to day 13, gradually approaching the ideal MTF. Differences are reduced on day 13 ($p=0.06$), with the non occluded eyes being practically diffraction-limited at the end of the experiment. The MTF in non-occluded eyes is higher than in occluded eyes in all chicks except one on day 6, in all chicks on day 8 and 11

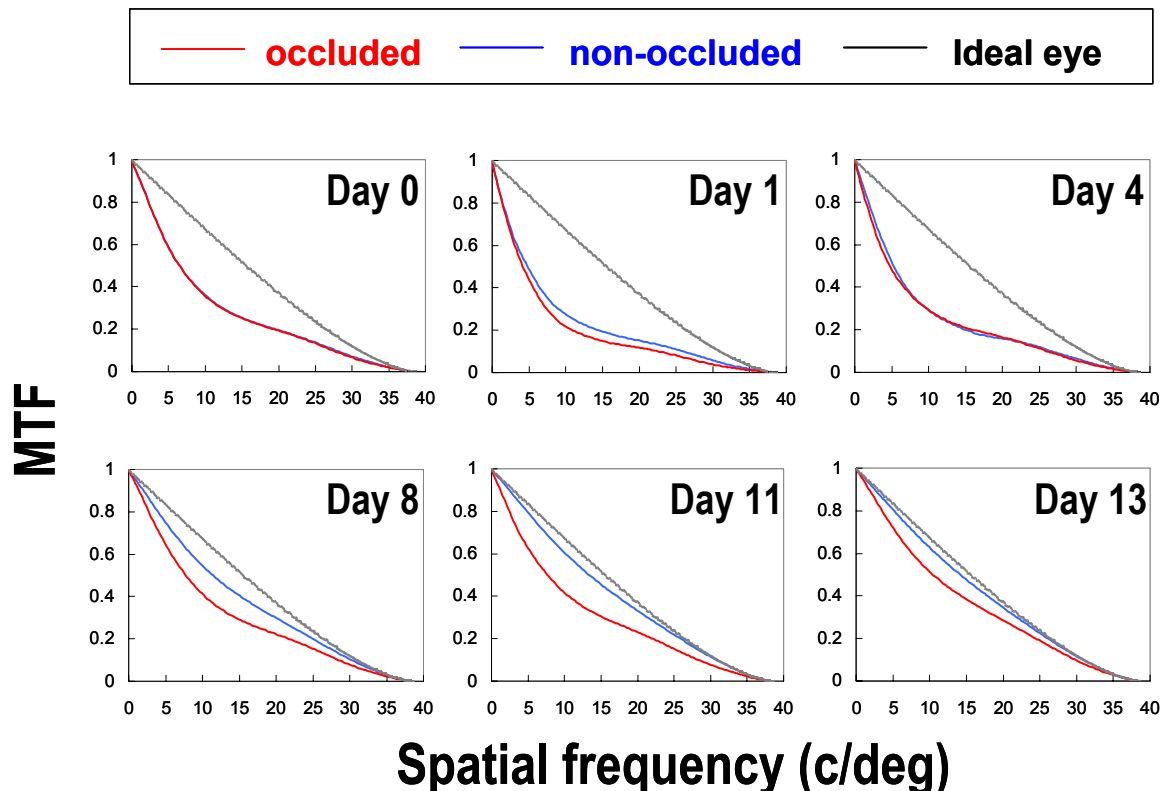


Figure 3.5 Mean MTFs (radial profile) averaged across all chicks, for non occluded (blue line) and occluded (red line) eyes on different days of the experiment (days 0, 1, 4, 8, 11, 13). Pupil diameter: 1.5 mm. The MTF of an ideal diffraction-limited eye of the same diameter is shown for comparison (black line).

and in all but two chicks on day 13. Figure 3.6 represents MTF ratios (non occluded/occluded eye) for all chicks for day 8. Values are greater than 1 for all spatial frequencies and subjects, indicating better optical quality in non-occluded eyes. MTF ratios (averaged across spatial frequencies) range between 1.08 for chick #5 and 2.02 for chick #1. Differences between the non-occluded and occluded eye tends to increase with spatial frequency and in some cases peak at mid spatial frequencies. Figure 3.7 shows modulation transfer as function of age for two different spatial frequencies, 1.5 c/deg and 7 c/deg, which seem to be relevant for the chick's visual system (Troilo and

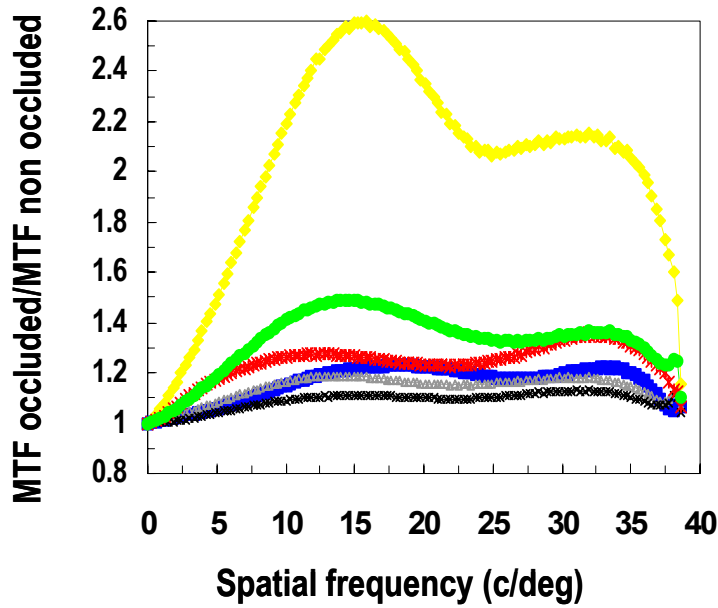


Figure 3.6 MTF ratios non-occluded/occluded eye for all chicks on day 8. MTF ratios (averaged across spatial frequencies). All data are for pupil diameter of 1.5 mm. Each color corresponds to a different chick.

Wallman 1991). After day 4, the occluded eye tends to show lower modulation than the non-occluded eye for 1.5 c/deg, but differences are in general not significant. However, for 7 c/deg differences are globally significant ($p=0.01$; univariate ANOVA). Figure 3.8 represents mean Strehl ratio (as a global image

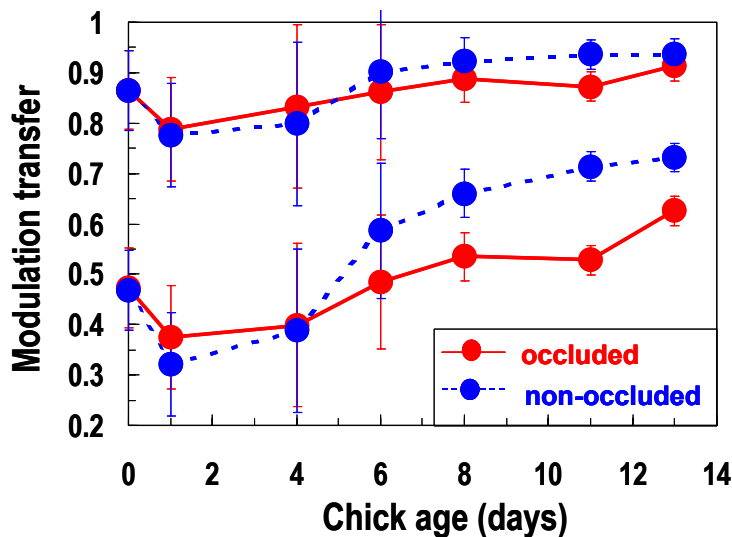


Figure 3.7 Mean modulation transfer as function of age (averaged across all chicks) for two different spatial frequencies, 1.5 c/deg and 7 c/deg. Blue circles correspond to non-occluded eyes and red symbols correspond to occluded eyes. Error bars stand for standard deviations.

quality metric) as a function of age, showing the consistent improvement of optical quality with age in both eyes, and significantly better optical quality in the non-occluded compared to the occluded eye ($p=0.02$ on day 13). Strehl ratio increases from 0.57 ± 0.10 on day 0 to 0.95 ± 0.05 on day 13 in non-occluded eyes, and from 0.56 ± 0.14 to 0.79 ± 0.15 for the occluded eyes. Interestingly, by the end of the experiment the optical quality is very close to diffraction limited (according to the Rayleigh criterion) for 1.5 mm pupils.

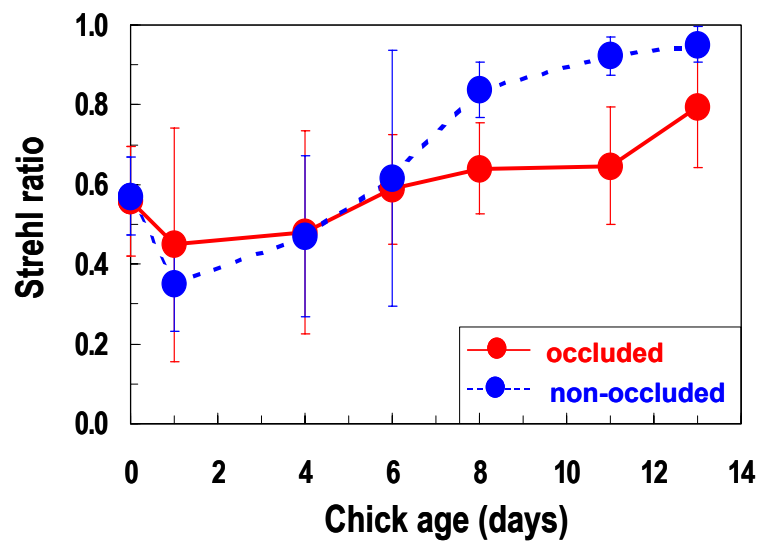


Figure 3.8 Mean Strehl ratio as a function of age. Blue circles and dotted lines correspond to non-occluded eyes and red circles and solid lines correspond to occluded eyes. Error bars stand for standard deviations

3.5. Discussion

3.5.1. Comparison with previous studies in experimental models

Our method of myopia induction in chicks by depriving forms has been widely used and studied. Normal eyes in our study developed as reported in the literature (starting moderately hyperopic, with a progressive tendency toward emmetropia). Our refraction and axial length changes in occluded eyes are consistent with results from previous studies in White Leghorn chicks, although for similar treatment periods our average myopia outcomes were slightly lower. A previous study (Guggenheim et al. 2002) found in a similar experiment with restricted vision in one eye and normal vision in the contralateral eye, interocular differences of 1.4 ± 0.4 mm in axial length and -26.4 ± 7 D in refraction, after 2 weeks of treatment. Our results on day 13 showed interocular differences of 0.9 ± 0.4 mm and -17 ± 3 D respectively. Another study (Schmid and Wildsoet 1997) using constant form deprivation with diffusers reported interocular differences of 0.49 ± 0.10 mm and 0.82 ± 0.20 mm in axial length, and -12 ± 3 D and -19 ± 6 D in refraction, on days 5 and 10 respectively. We obtained interocular differences of 0.5 ± 0.5 mm and 0.80 ± 0.3 mm in axial length and -10 ± 2 D and -14.8 ± 3 D in refraction, on days 6 and 11 respectively. While the outcomes are similar, we obtained slightly lower values of myopia induction. One reason for the differences between studies could have been the amount of diffusion produced by the occluder, since correlations between the amount of myopia induced and the density of the diffuser material have been demonstrated (Bartmann and Schaeffel 1994). Another potential factor contributing to lower myopia outcomes could have been the fact that we took out the occluders for brief time periods while we were taking the measurements, and given that additional measurements (Hartmann-Shack aberrations) required longer measurement times, chicks may have been exposed to longer periods of “normal viewing” than in previous studies. It has been shown (Schmid and Wildsoet 1997) that, if the treatment is interrupted with 20 minutes of “visual stimulation” each day, form-deprivation myopia is significantly reduced. However our control chick (monolaterally treated, but not

measured during intermediate days) developed an interocular refraction difference of 17 D, similar to the average refraction on day 13 that we found on the occluded eyes that participated in all measurements. Differences cannot be attributed to the fact that all chicks in our experiment were males since it has been shown (Guggenheim et al. 2002) that there is no sex-related difference in refraction data following form-deprivation, and if anything, slightly higher elongation (~ 0.2 mm) in males than females in three strains of chickens, included White Leghorn (Kisilak et al. 2002; Thibos et al. 2002; Campbell et al. 2003).

A previous study (Coletta et al. 2003) measured the modulation transfer function (MTF) using a double pass technique in older chickens' eyes, both normal and myopic after different treatments. Aberrometry allows individual assessment of individual Zernike terms, as well as estimates of point spread functions (PSF) and modulation transfer function for any pupil size and defocus, while the double-pass technique only allows measurement of MTF for the pupil size and focus correction of the measurement. Thibos and colleagues (Thibos et al. 2002) measured higher-order optical aberrations in normal chicks during the first week of life with a HS aberrometer. When normalized by pupil area, the equivalent defocus of all the Zernike modes decreased slightly with age, a tendency in agreement with our finding of the increasing optical quality with age (in our case for a constant pupil diameter). However, they concluded that the optical quality during the first week of life in the chick eye is significantly worse than in human adult eyes, while we found good optical quality in chicks (for 1.5 mm pupils), and close to diffraction-limit by day 13 in non treated eyes. Coletta et al. (Coletta et al. 2003) found relatively good optical quality in chick eyes, although worse than in human eyes. However, their data are for older chicks (from 3 to 6 weeks old) and larger pupils (4.50-mm mean pupil diameter) than in Thibos' or the study presented in this chapter. In any case, our results support Coletta et al.'s conclusions that optical quality is not limiting spatial resolution in chicks, since the MTF's cut-off frequencies are well above reported chicks spatial acuity: 1.5 c/deg from behavioral studies (Over and Moore 1981) or up to 8.6 c/deg from optokinetic nystagmus responses (Schmid and Wildsoet 1998).

Campbell and colleagues (Campbell et al. 2003) also found an improvement with age of the optical quality of young normal chicks, for 1.6-mm pupils. All reports show trends of decreased optical quality in myopic eyes, regardless the method of myopia induction. Coletta et al. (2003) found that myopic eyes had poorer optical quality than normal chicks. Unlike our study, where we induced myopia with diffusers, Campbell et al. induced myopia in chicks with -15 D lenses. They found that average optical quality (for 1.6-mm pupils) did not change between days 0 and 7, unlike control eyes that experienced a decrease in the amount of aberrations. For higher order aberrations alone, goggled eyes had significantly worse optical quality at day 7 than controls. While we also found significantly less aberrations in control eyes than in treated eyes, we found that higher order aberrations decrease in both normal and treated eyes. However, it should be noted that in our experiment, the most significant differences occur after day 8, and trends are observed when extending the experiment for at least five more days.

Similar tendencies were found recently in mammal models (Ramamirtham et al. 2004). These authors found that manipulation of visual experience with diffusers or spectacle lenses in young Rhesus monkeys resulted in greater amounts of ocular aberrations, with no significant differences in the magnitude or pattern of higher order aberrations between the control and treated groups before treatment and significant RMS differences ($0.09 \mu\text{m}$) by the end of the treatment period.

3.5.2. *An emmetropization of the optical aberrations?*

We found that aberrations tend to decrease during development in chicks. This was also found by Thibos et al. (Thibos et al. 2002) and Campbell et al. (Campbell et al. 2003) in normal chick eyes. While working with chicks allows longitudinal measurements, some cross-sectional measurements in the literature are suggestive that a similar tendency is found in humans. Human results reported by Brunette et al. (Brunette et al. 2003) showed that optical aberrations decrease during development. These authors measured optical aberrations in subjects ranging from 5.7 to 82.3 years and found that the

average optical quality in early childhood was significantly worse than in the advanced age, with aberrations decreasing during childhood and adolescence. It is well known that the optical aberrations of the crystalline lens (showing negative spherical aberration) partially compensate corneal aberrations (showing positive spherical aberration) in the normal young human eye, and that this compensation gets disrupted later in age (Calver et al. 1999; Guirao and Artal 1999; Mclellan et al. 2001). Brunette et al.'s cross-sectional data, as well as the mentioned longitudinal data in chicks, may suggest that the optimal performance found in young adults is reached after an optimization process that takes place during development. Other authors (Wang and Candy 2005), however found that the optical quality was as good in infants (5-7 weeks) as in young adults (younger than 40 years), with no significant difference in the levels of 3rd order monochromatic aberrations, and only a higher tendency in infants to show negative spherical aberration with adults eyes tending to show positive spherical aberration.

Aberration balance between optical components, and even more a potential improvement of the optical quality of the eye during development, may lead to consider an active process for the development of optical components. If an active visually guided process tunes the eye length to the power of the optical component, one may think of a similar system adjusting the optical and geometrical properties of the optical components to reduce high order aberrations and produce optimal image quality. Our results do not support such a system, or at least this process being visually guided. We found that the improvement of the optical quality with age occurs even in the eye occluded with diffusers, subject to dramatic image quality degradation. While a lens treatment may have provided a different approach to answering this question, excluding any visual feedback with the diffusers suggests that the tuning of optical aberrations of ocular components is likely the result of a pre-programmed process or just geometrical scaling but it does not seem to rely on visual experience to occur, at least to a great extent. These findings are in good agreement with a scaling model recently proposed by Howland (Howland 2005). This model, based on reported data of corneal curvature increase in White Leghorn chicks during the first week of life, shows that aberrations measured in

a growing eye at a constant pupil size decrease with time. A more elaborate model, including geometrical properties of the cornea and crystalline lens of the developing myopic and normal eye would be necessary to assess if scaling accounts for all decrease in aberrations and to explain the differences between both eyes. This question will be further addressed in Chapter 6, using more complex computer eye models.

3.5.3. *Optical aberrations and emmetropization*

We found higher amounts of optical aberrations in myopic eyes than in the normal control eyes after six days of treatment. While the differences are significant, the amount of blur produced by aberrations is minimal compared to the optical degradation produced by the diffuser or the developed refractive error. By day 13 even myopic eyes are close to diffraction-limited. These experiments shed light on possible relationships between aberrations and myopia development. There are several cross-sectional studies in humans reporting optical aberrations as a function of refractive error (Collins et al. 1995; Carkeet et al. 2002; Marcos et al. 2002; Paquin et al. 2002; Cheng et al. 2003; Llorente et al. 2004). Most studies found higher amounts of aberrations as myopia increased (Atchison et al. 1995; Coletta et al. 2003). Several studies only found a significant correlation for high myopes, and third order aberrations, but not spherical aberration (Marcos et al. 2002). One study (Carkeet et al. 2002) did not find correlations between refractive error and high order aberrations (for myopic Singaporean children, < 3 D), and another study (Cheng et al. 2003) on 200 normal human eyes failed to find correlations between high order aberrations and refractive errors (from +5.00 to -10.00). In the study presented in this chapter, in chicks interocular statistically significant differences in the amount of higher order aberrations only appear for amounts of myopia beyond -7.3 D. The fact that increased amounts of aberrations are found in higher myopes may lead to the hypothesis that aberrations may be a cause for myopia. Suggestive evidence of this hypothesis has been presented in the Introduction. Longitudinal measurements allow to shed light into the question whether higher aberrations are a cause or an effect of myopia development. Our experiment clearly favors the hypothesis that aberrations are a

consequence of the structural changes occurring in the excessively elongated eye: 1) We did not find that eyes with higher amounts of aberrations at birth emmetropized less efficiently; 2) The retinal image degradation imposed by diffusers induces myopia in the treated eyes. Unlike a potential treatment with lenses, where eye/lens system can project good optical quality images on the retina, a treatment with diffusers allows no visual feedback. Treated eyes turned out to be more aberrated most likely as a result of the treatment, but it is unlikely that the increased aberrations may have played any role at all in the development of myopia. 3) While aberrations are significantly higher in myopic eyes than in the normal eyes, the retinal image degradation induced is negligible compared to the degradation imposed by the diffuser and the induced defocus. While in the present experiment aberrations result from the myopia development, the next chapters test the hypothesis in the reversed direction (aberrations as a potential cause for myopia development).

**Chapter 4: Emmetropization and optical aberrations in
a myopic corneal refractive surgery chick model**

Resumen capítulo 4:**Emetropización y aberraciones ópticas en un modelo de cirugía refractiva corneal en pollos.**

En este capítulo estudiamos el potencial de la cirugía láser refractiva corneal para inducir miopía (alargamiento axial del ojo) y las potenciales interacciones entre las aberraciones (inherente a la propia cirugía) y el desarrollo de la miopía en pollos (*Gallus domesticus*). Para ello diez pollos “White Leghorn” fueron tratados con PRK (Queratometría fotorefractiva) de forma monolateral el día posterior a su nacimiento. La cirugía fue programada para generar un cambio de -9.9 D, es decir hipermetropizando el ojo. La longitud axial se midió mediante biometría de ultrasonidos, el radio de curvatura de la cornea se midió con un video-queratómetro desarrollado para este experimento y el error esférico y aberraciones de alto orden fueron medidos con un Hartmann Shack de desarrollo propio. Todas las medidas tras la cirugía se hicieron en los días 9, 12, 14 y 16 de edad de los pollos. A las dos semanas de la cirugía no se aprecian diferencias significativas en los radios corneales entre ojo tratado y control. Tras el tratamiento con PRK el astigmatismo aumentó de media en un factor 2.6 y las aberraciones de tercer orden y superior en un factor 4.3 con respecto al ojo control. Ambos ojos, tratado y control, son prácticamente emétopes tras el tratamiento. Además los ojos tratados no presentan mayor longitud axial que la encontrada en los ojos control. La escasa efectividad de la cirugía refractiva para obtener reducciones significativas de la potencia de la cornea puede ser debido a las propiedades biomecánicas del ojo del pollo. Las aberraciones de alto orden medidas inducían una importante disminución del contraste (de un factor 1.7 a 4.5 ciclos/grado) en la MTF. Sin embargo, la baja calidad de imagen no parece producir una suficiente deprivación de contraste como para generar un error refractivo miope, ni alargamiento axial del ojo en ojos operados con cirugía refractiva corneal. Tras estudiar los datos de ojos normales y tratados se pudo concluir que el aumento de las aberraciones oculares impuestas no parecen ser un factor de riesgo para el desarrollo de la miopía.

This chapter is based on the article by García de la Cera et al. “Emmetropization and optical aberrations in a myopic corneal refractive surgery chick model”, *Vision Research*, 47, 2465-2472 (2007), doi:10.1016/j.visres.2007.06.005.

The contribution of Elena García de la Cera to the study was to develop the methodology to measure ocular aberrations in chicks (optical set-up, calibrations, automatic control, data processing routines), as well as the development of routines to measure corneal radius of curvature in chicks. She also performed the experimental measurements on chicks (control and post-refractive surgery) and participated in the data analysis and interpretation.

Coauthors of the study are: Guadalupe Rodríguez, Alberto de Castro, Jesús Merayo and Susana Marcos.

4.1. Abstract

We studied the potential of myopic corneal refractive laser surgery to induce myopia (axial elongation) and potential interactions between aberrations (generally resulting from the procedure) and myopia development in chicks (*Gallus domesticus*). Ten white Leghorn chicks were monolaterally treated one day post-hatching with photorefractive keratectomy (PRK), with a nominal dioptric change of -9.9 D (imposed hyperopia). Axial length was measured using an adapted ultrasonic biometer; corneal radius of curvature was measured using a custom-built videokeratometer and spherical error and high order aberrations were measured using custom-built Hartmann-Shack aberrometer post-operatively on days 9, 12, 14 & 16 after hatching. Two-weeks after surgery, there were no significant differences in corneal radius of curvature between treated and control eyes. Astigmatism increased on average by a factor of 2.6 and 3rd and higher order aberrations by a factor of 4.3 after PRK. Both treated and control eyes were close to emmetropia, and no axial elongation was found in the treated eyes. The inability of the refractive procedure to achieve significant reductions in the corneal power could be attributed to the biomechanical properties of the chick cornea. High order aberrations induced significant contrast decrease (by a factor of 1.7 at 4.5 c/deg). However, reduced image quality neither produced myopic refractive error nor axial elongation in the treated eyes. Both normal and treated eyes emmetropized, indicating that increased amounts of aberrations do not appear to be a risk factor for myopia.

4.2. Introduction

The quality of visual experience in early stages of post-natal development is critical for proper eye growth and normal emmetropization. In the study presented in Chapter 3 we measured optical aberrations in eyes where myopia had been achieved by severe retinal image quality degradation with diffusers (with no feedback loop) and found that increased aberrations were a cause rather than a consequence of myopia development. Also, a recent study showed that chick eyes that had undergone ciliary nerve section showed larger amounts of higher-order aberrations but did not become myopic, implying that retinal image degradation imposed by certain amounts of aberrations do not necessarily affect the emmetropization process (Tian and Wildsoet 2006). On the other hand, Campbell et al. (Kisilak et al. 2006) found that increased aberrations immediately preceded myopia development in chicks treated with negative lenses, suggesting some role of ocular aberrations in emmetropization.

An increasingly popular technique to correct refractive errors in humans is corneal refractive surgery. Corneal power is changed using excimer laser, reshaping the anterior surface of the cornea by laser ablation of corneal tissue. Corneal photorefractive keratectomy (PRK) has been shown to produce reliable refractive results in humans, with efficacies of 90%, and stability (changes in spherical equivalent less than 1 D, 6 and 12 months after surgery) of 85.8% (Tuunanen and Tervo 1998). The potential use of corneal refractive surgery to produce a permanent change in corneal power seems attractive as an alternative to current methods used to impose experimental refractive errors in laboratory animals and to study mechanisms of refractive error development. PRK has been used to alter emmetropization in the rabbit (Bryant et al. 1999) and infant Rhesus Monkeys (Zhong et al. 2004). In both cases, the axial length changed to compensate for the induced defocus. In this chapter, we will evaluate the feasibility of a refractive surgery myopia model in chicks. In addition, we will evaluate the optical outcomes of the refractive surgery model in

chick, by measuring the effective change in corneal curvature, refraction and optical aberrations. A refractive surgery model in adult chickens had been previously used to test the effect of refractive surgery on corneal transparency (Merayo-Llodes et al. 2001).

Several studies, primarily in human patients, have shown that while laser refractive surgery is in general successful at correcting defocus and astigmatism, high order aberrations are generally induced (Moreno-Barriuso et al. 2001) and these affect the quality of the retinal image (Marcos 2001). If, as found in human patients, corneal refractive surgery induces significant amounts of high order aberrations, a refractive surgery model could be used as a model of permanently imposed abnormally high aberrations. Retinal image degradation caused by high order aberrations may be particularly relevant in the chick eye, which (unlike other species (see Chapter 5) (García de la Cera et al. 2006) shows naturally very low amounts of high order aberrations (see Chapter 3) (García de la Cera et al. 2006) allowing the study of potential interactions between aberrations and myopia development. If corneal power is altered (by flattening the anterior cornea) and high order aberrations are induced in the laser treatment, but axial elongation still occurs to compensate for the imposed defocus, we will conclude that the presence of aberrations does not interfere with normal emmetropization.

In this chapter we present post-operative measurements of refraction, axial length, corneal radius of curvature and monochromatic aberrations in chick eyes treated with myopic corneal refractive surgery and their contralateral, untreated eyes during. The aims of the study were to investigate:

- 1) The potential of a chick myopia model using corneal refractive surgery to impose hyperopic defocus;
- 2) The changes in corneal curvature, refractive error and ocular aberrations produced by refractive surgery;
- 3) effects of increased aberrations in the emmetropization process;

If corneal surgery produces a hyperopic defocus in chicks, this technique could be an alternative way for developing chick models of myopia. Also, while the chick has been used as an experimental model of refractive surgery, the optical changes induced by the treatment (other than corneal transparency) have never been evaluated. Finally, the experiments presented in the previous chapter showed that increased aberrations resulted as a consequence on induced myopia. The experiments of the present chapter will aim at testing the hypothesis in the reversed direction, i.e. whether artificially induced aberrations may result in myopia development.

4.3. Methods

4.3.1. Subjects and experimental protocols

Ten White-Leghorn chicks were monocularly treated (OD) with myopic corneal refractive surgery with excimer laser (PRK) one-day post hatching (Day 0), while the left eye was not treated and was used as control. All experimental protocols followed the ARVO Statement for the Use of Animals in Ophthalmic and Vision Research and had been approved by the Institutional Review Boards. Chicks were labeled for identification with color wires attached around their feet. Chicks were reared under fluorescent lighting (12h/12h light/dark cycle conditions) in a cage inside a controlled heated room (24-28 °C). They were allowed to eat and drink *ad libitum*. Adequate measures were taken to minimize pain or discomfort. Axial length was measured in all chicks on their first day after hatching (Day 0) and prior to surgery. Post-operative measurements were done on both eyes on days 9, 12, 14 and 16. Measurements were not done immediately following surgery since corneal re-epithelization and wound healing processes, as well as increased tear secretion, would have prevented from obtaining reliable results. Measurements consisted of Hartmann-Shack aberrometry and keratometry in five chicks and ultrasound biometry in all chicks. Measurements were done with the animals awake and under natural viewing conditions.

4.3.2. Refractive surgery

Refractive surgery was performed using an excimer laser SVS Apex Plus™ (Summit Technology) (see Figure 4.1). Chicks underwent refractive surgery under total and topical anesthesia (0.02 ml Ketamine, 0.1 g/ml). Prior to laser treatment, the corneal epithelium was removed mechanically, and then laser treatment was applied on Bowman's layer (178 pulses). Finally the cornea was irrigated with buffered saline solution (BSS). The nominal myopia correction programmed into the laser system was -9.9 D, with an optical zone of 3.5 mm and a nominal corneal tissue depth ablation of 45 microns. Pachymetry measurements on 8 newborn chick eyes (used in trial surgeries) showed a pre-operative corneal thickness of 190 ± 6 microns. Computer simulations using theoretical ablation profiles (based on Munnerlyn or the parabolic approximation of the Munnerlyn equation (Cano et al. 2004)) predicted similar refractive outcomes using chick corneal dimensions than human corneal dimensions. All surgeries were uneventful and all chicks had recovered (i.e. they opened the eyes normally and exhibited no signs of photosensitivity) 8 days after surgery.



Figure 4.1. Photograph of the excimer laser (left) and a chick refractive surgery (right) used to perform surgery on chicks.

4.3.3. Hartmann-Shack aberrometry and refraction

Aberrations were measured using the custom-built Hartmann-Shack (HS) aberrometer described in section 2.1.1. Measurements of the refractive state with streak retinoscopy were attempted in treated eyes, but the bad quality of the reflections (showing scissor-type images) prevented us from obtaining reliable results. The HS aberrometry data were repetitive and consistent, and the spherical error was obtained from 2nd order polynomials. The animal were placed on an elevated platform in front of the system, which was mounted on an x-y translational stage, allowing correct centering and focusing of the pupil. The eye pupil was continuously monitored and aligned to the optical axis of the instrument. The animal fixated the illumination spot during a few seconds, allowing obtaining 5-10 Hartmann-Shack images per eye. Typically, HS image frames contained 17-21 spots in the pupillary zone. Pupil diameters were 2.7 ± 0.3 mm on average. The best H-S images were selected for processing and computing the centroids of the retinal spots, following a procedure described in detail in methods chapter. Estimating the wave aberrations were done using modal fitting (up to 5th order Zernike expansion) of the ray deviations. We obtained defocus, astigmatism, and RMS high order aberrations from Zernike coefficients for the maximum pupil size, and also scaled down to 2-mm pupils for comparative purposes. Point spread functions and modulations transfer functions were computed from the wave aberrations assuming a pupil with homogeneous transmittance.

4.3.4. Keratometry

Measurements of the corneal radius of curvature were obtained using a custom-built infrared (IR) photokeratometer, implemented specifically for this study and described in section 2.2.3. The chick was held in front of the camera, at a distance of 27 mm from the LED ring and 71 mm from the CCD. Sequences of images were captured when the pupil appeared in focus and the image of LED-ring was well aligned with the pupil center. Images were processed according to the description of section 2.2.3. Differences in corneal curvature across 4 meridians (45, 90, 135, and 180 deg) allowed estimation of corneal astigmatism

4.3.5. Ultrasound biometry

Axial length was obtained by an adapted ultrasound biometer (Allergan Humphrey Mod. 826), described in 2.2.2. The axial length for each eye was specified as the average of at least five measurements.

4.3.6. Statistical analysis

Agreement of repeated measurements was tested using confidence intervals (CI), with confidence levels of 95%. Statistical differences between control and treated eyes were tested using paired-t test, with significance levels of $p < 0.05$. Significance of linear correlations was tested using Pearson's coefficient of correlation, with significance levels of $p < 0.05$.

4.4. Results

4.4.1. Refractive error

Refractive error and astigmatism were obtained from the defocus Zernike term for 2 mm pupil diameter. Figure 4.2 shows the average spherical refractive errors and astigmatism in treated and control eyes on 4 different days, starting 8 days after surgery. Both eyes were close to emmetropia, and although spherical refractive error tended to decrease slightly with age (-0.03 D/day and in control eye and -0.07 D/day) these changes were not statistically significant. There were no statistically significant differences in refractive error (paired t-test) between the treated and control eyes in any of the days. Individually, we only found significant differences in chick #1, day 14 ($p=0.0014$), chick #3, day 16 ($p=0.0176$) and chick #4, day 12 ($p=0.0243$). The changes and amounts in refractive state were consistent with previous data in the literature, and surprisingly, these were not modified by refractive surgery. Measurements tended to be slightly noisier in the treated eyes than in the control eyes, with average standard deviations for repeated measurements of 0.99 D and 0.57 D, respectively. The 95% confidence interval (CI) for repeated measurements was ± 0.97 D and ± 0.57 D respectively. Inter-subject variability was also larger in treated eyes than in the control eyes (0.98 D in treated eye and 0.66 D in control eyes), and 95% CI were ± 1.26 and ± 0.62 respectively. Astigmatism was almost constant throughout the measurement period. Treated eyes showed higher values of astigmatism (2.6 ± 0.5 D) on average than the control eyes (1.0 ± 0.2 D), and these differences were statistically significant in all days ($p=0.0013$).

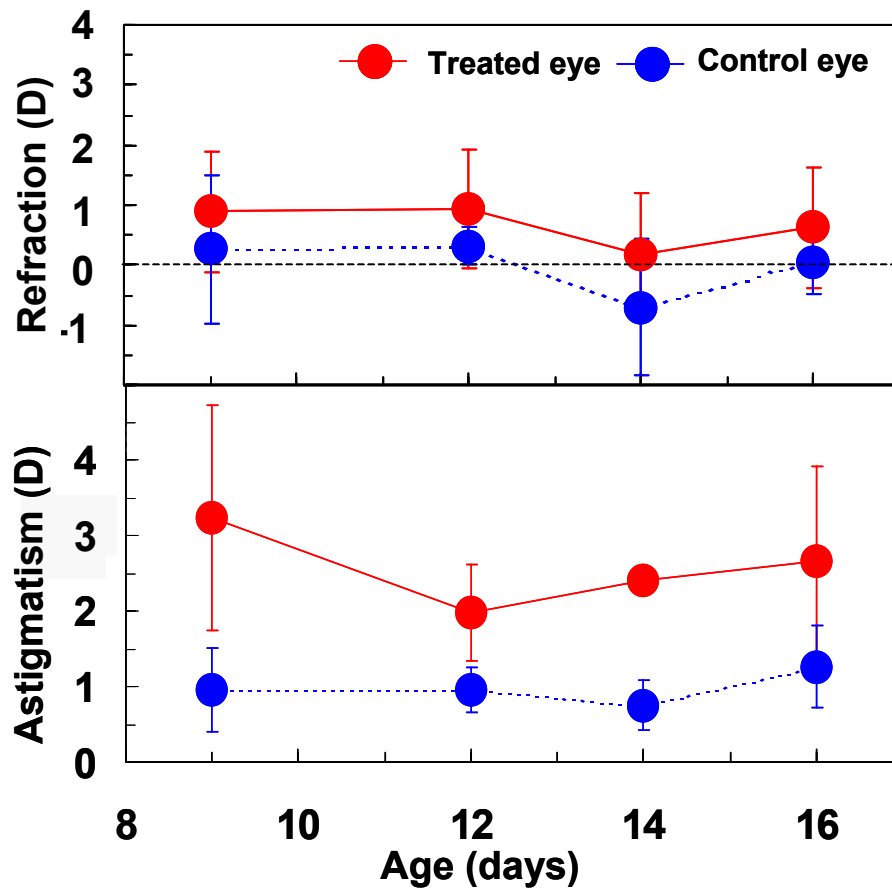


Figure 4.2: Spherical error and astigmatism obtained from defocus and astigmatism Zernike terms during the experiment period (from 8 to 15) days post-operatively. Red circles correspond to eyes treated with refractive surgery, and blue circles to untreated contralateral eyes. Error bars represent \pm standard deviations.

4.4.2. Optical aberrations

Figure 4.3 shows examples of wave aberrations for 3rd and higher order in the treated and control eye of the same chick, on day 16 and their corresponding PSFs for 2-mm pupils. The higher number of contour lines in the wave aberration map and larger PSF in the treated eye were indicative of larger optical degradation.

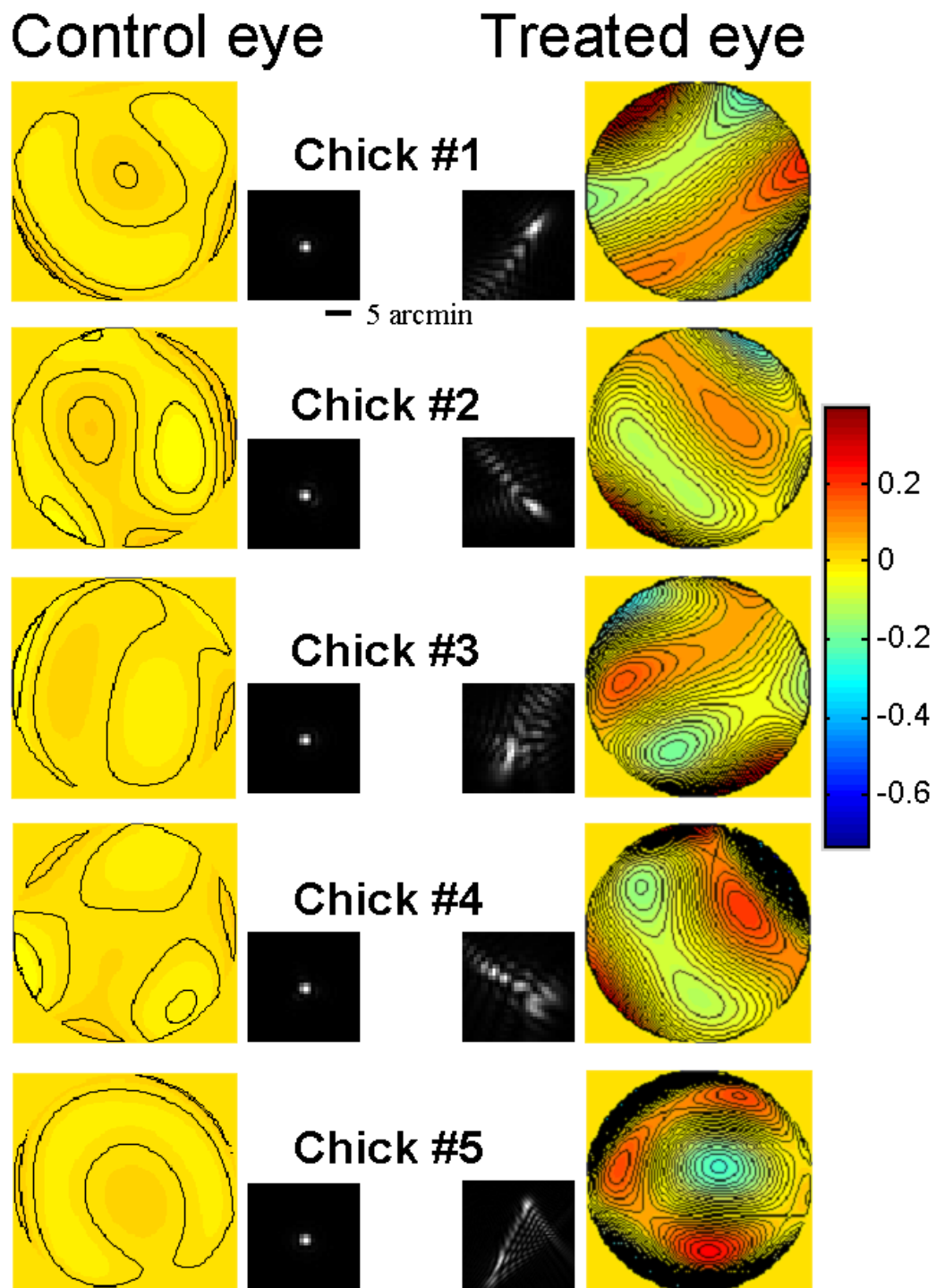


Figure 4.3: Examples of wave aberration maps from all chicks (treated and untreated eye) for 3rd and higher order Zernike coefficients at day 16 and their corresponding PSF for 3rd and higher order aberrations. Data are for 2-mm pupil diameters. Map contour lines are plotted in 0.01 μm steps.

Figure 4.4 shows average 3rd and higher order (A), 3rd order aberrations (B) and spherical aberrations (Z_{40} term) (C) in treated and control eyes on 4 different days, starting 8 days after surgery. Third and higher order root-mean-square wave front error (RMS) was higher in the surgical eyes (4.3 times larger,

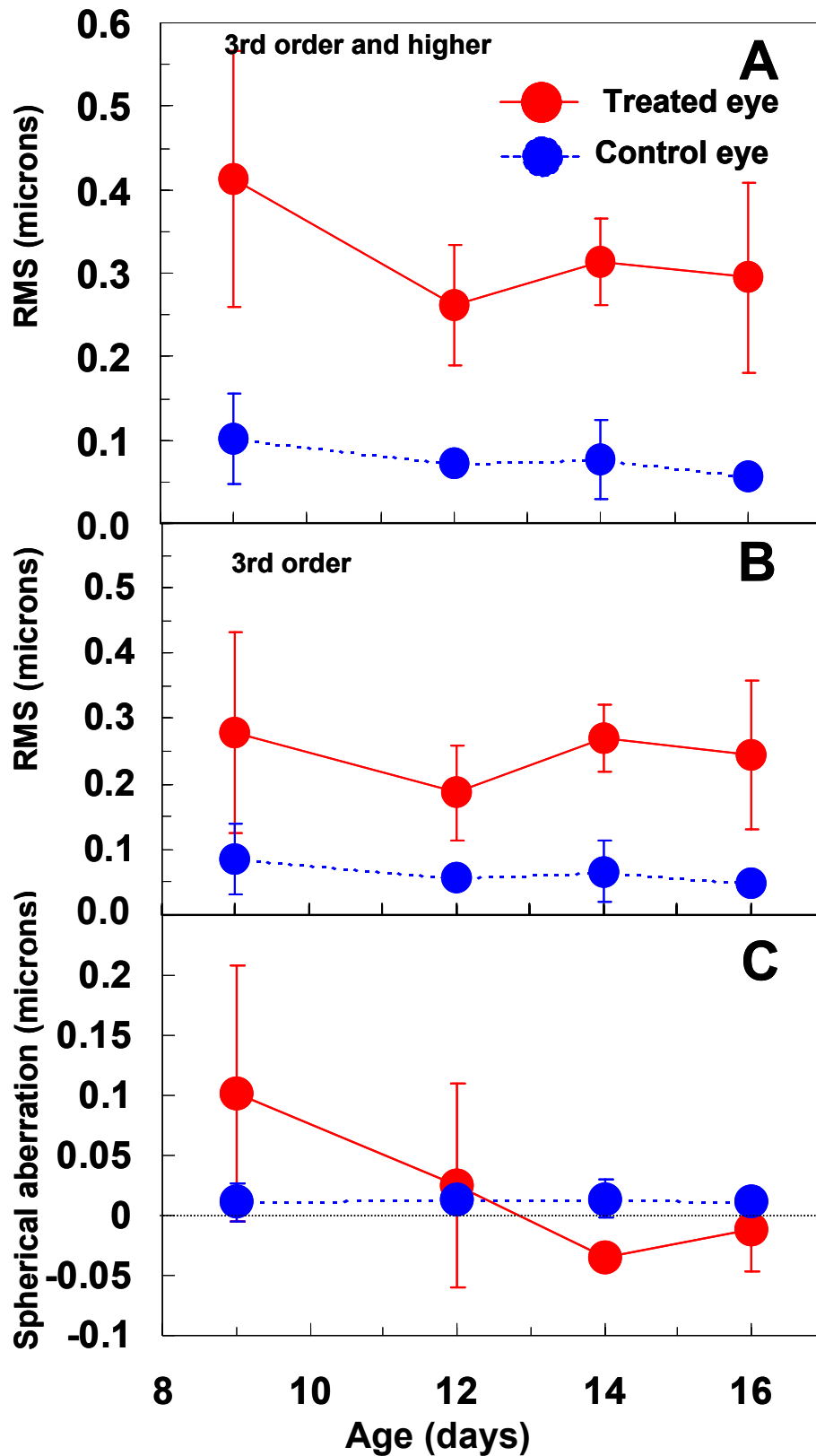


Figure 4.4: A. Mean 3rd and higher order RMS B. 3rd order RMS C. spherical aberration Zernike coefficient (Z_{40}) for days #9,#12,#14 and #16 for treated (red circles) and untreated (blue circles) eyes. Error bars represent \pm standard deviations. Data are for 2-mm pupil diameters.

on average) than the control eyes, and the differences were highly statistically significant in all days ($p < 0.001$, paired t-test). The increase in RMS was primarily driven by 3rd order aberrations. There were no significant changes in aberrations with time during the studied period. In the control eyes, spherical aberration was not significantly different from zero ($p = 0.56$), it presented very little inter subject variability and it remains unchanged across days. In the treated eyes, spherical aberration showed larger inter-subject variability, and tended to decrease with time from positive values to negative values in the studied period, although the differences between treated and control eyes were only significant on day 14. The increase of high order aberrations in the treated eyes resulted in significantly lower modulation transfer functions (MTFs). Figure 4.5 shows MTFs (averaged across eyes) on day 16, for 3rd and higher order in both the treated and control eyes, for 2 mm pupil diameters. Contrast was reduced with surgery at all spatial frequencies. For example, for 4.5 c/deg and 10 c/deg modulation transfer (from 3rd & higher order aberrations) was 1.7 and 2.6 times higher in control than treated eyes.

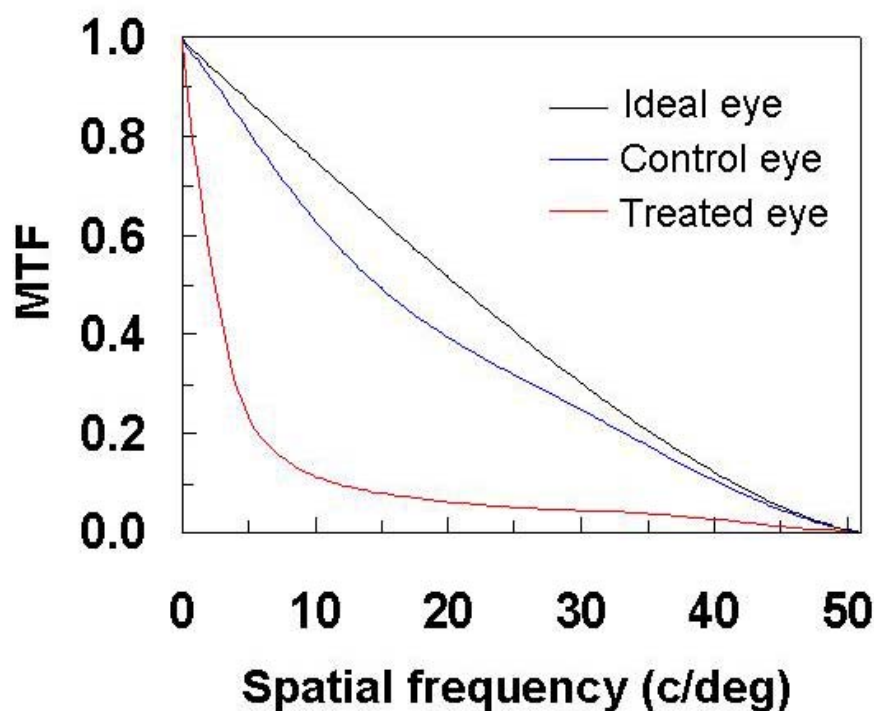


Figure 4.5. Mean MTFs (radial profile) for treated (circles) and untreated (cross) chick eyes, for 3rd and higher order aberrations and 2 mm pupil diameter. For comparison the theoretical MTF of a diffraction-limited eye is also represented (680 nm).

Figure 4.6 shows average corneal radius of curvature in treated and control eyes on 4 different days. In the control eyes corneal radius of curvature increases slightly and the correlation with time was significant (at a rate of 0.023 mm/day, -0.84 D/day, $p=0.02$), while longitudinal changes in the treated eye were less systematic and the increase was not statistically significant. There were no statistically significant differences in corneal radius of curvature (paired t-test) between the treated and control eyes in any of the days. The mean values of corneal radius (3.15 ± 0.09 mm, or 120 ± 4 D, in treated eye and 3.10 ± 0.07 mm, or 122 ± 3 D, in the control eyes) were consistent with previous data on normal eyes in the literature, and surprisingly, these did not appear to have been modified by refractive surgery 8 days after the procedure. Average standard deviations for repeated measurements were similar in treated eyes than in control eyes (0.10 mm, averaging across days and chicks). The 95% CI for repeated measurements was ± 0.08 mm in treated eyes and ± 0.04 mm in

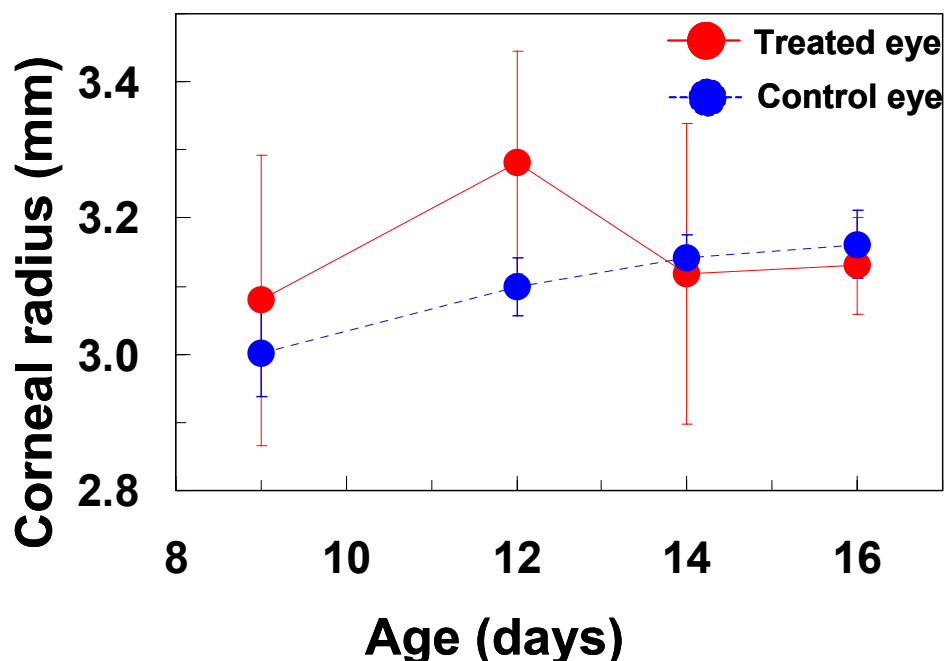


Figure 4.6. Average corneal radius of curvature throughout the experiment period (8 to 15 days post-operatively). Red circles correspond to eyes treated with refractive surgery, and blue circles to untreated contralateral eyes. Error bars represent \pm standard deviations.

control eyes, averaging across days and chicks. Intersubject variability was larger in treated eyes (standard deviation: ± 0.18 mm, 95% CI= ± 0.09 mm, averaging across days) than in control eyes (Standard deviation: ± 0.04 mm,

95% CI= ± 0.07 mm). Consistent with the HS measurements of total astigmatism, differences in radii of curvature between the steepest and flattest meridian were higher for the treated eyes (0.28 ± 0.13 mm, averaging across eyes and days) than for control eyes (0.08 ± 0.06 mm), although the differences were not statistically significant.

4.4.4. Axial length

Figure 4.7 shows axial length in treated and control eyes on 4 different days. Axial length increased significantly with age from Day 0 (measured just before treatment, not shown in the graph, 7.39 ± 0.09 mm in the treated eyes and 7.35 ± 0.03 mm in the control eyes) and Day 16 (7.8 ± 0.6 mm in the treated eyes and 8.16 ± 0.16 mm in the control eyes). Differences in axial length between treated and control eyes were not statistically significant (paired t-test) in any of the days. The mean values of axial length were consistent with previous data on normal eyes in the literature, and again were not altered by the treatment. Inter-subject variability was slightly higher in treated eyes (0.11 mm, average across eyes and days) than in control eyes (0.08 mm) and 95% CI were ± 0.14 mm and ± 0.17 mm respectively.

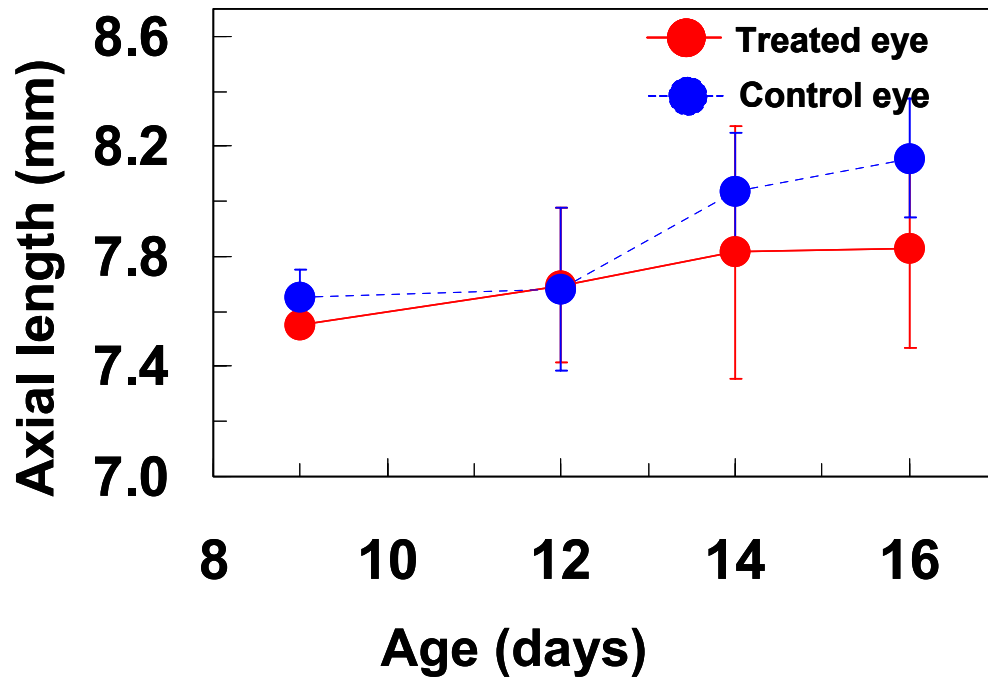


Figure 4.7. Axial length throughout the experiment period (from 8 to 15 days post-operatively). Red circles correspond to eyes treated with refractive surgery, and blue circles to untreated contralateral eyes. Error bars represent \pm standard deviations.

4.5. Discussion

We have applied corneal refractive surgery to new born chicks. We did not find that refractive surgery was an efficient way to induce axial elongation: 1) corneal curvature in eyes treated with myopic PRK was not significantly different to control eyes 8 days after treatment; 2) treated eyes exhibited significantly higher amounts of high order aberrations, but the reduction in retinal contrast did not interfere with the emmetropization process.

Chicks have been extensively shown to respond to form deprivation and lens treatments by altering axial ocular growth (Hayes et al. 1986; Wallman and Adams 1987; Troilo and Wallman 1991). In the study presented in Chapter 3 using the same chick strain, from the same hatchery as that used in the present study, and similar time course for treatment and measurements, we found interocular differences between eyes treated with frosted occluders and control contralateral eyes of -17 ± 3 D for refraction and of treatment and axial length of 0.81 ± 0.3 mm by day 13. Numerous studies have shown that functional hyperopia induced by negative lenses induces axial growth that tends to compensate for the induced defocus, at least partially (Schaeffel et al. 1988; Wildsoet and Wallman 1995; Diether and Schaeffel 1997; Priolo et al. 2000; Choh et al. 2006; Schippert and Schaeffel 2006). Some studies found consistently lower amounts of myopia than the power imposed by the negative lens, while others found even larger amounts of myopia that produced by form deprivation when high power lenses were used. For example, Diether and Schaeffel (1997) achieved -3.82 ± 2.48 D using -7.5 D lenses; Schaeffel, Glasser et al. (1988) found similar myopia (-1.5 D) for treatments with either -4 D or -8 D, while Wildsoet and Wallman (1995) achieved -8.6 D after treatment with -15 D lenses and Priolo and Sivak (2000) achieved -12.8 ± 0.7 D with -10 D lenses in eyes treated one day after hatching. Differences in the effectiveness of the treatment can be affected by the large amplitude of accommodation in chicks (in the experiments performed under natural conditions) and the start day of the treatment (the younger, the more effective).

We attempted to impose hyperopic defocus in chicks (as in negative lens experiments) directly on the cornea, using PRK. Previous studies showed induction of refractive errors in experimental models in infant rhesus monkeys and young rabbits. The hyperopic defocus imposed by treating infant monkey eyes with 3 D myopic PRK, produced consistent hyperopic shifts, corneal flattening and compensatory axial elongation (Zhong et al. 2004). Results from a study in which rabbits (5 and 10 weeks of age) monocularly treated with 5-6 D myopic PRK showed also initially refractive changes which tended to be compensated by increased rate in axial length in the treated eyes (Bryant et al. 1999). In addition to the regression from induced refractive errors in the young group, at the end of the observation period no significant differences were observed in the corneal curvatures between the treated and the control eyes. Surprisingly, hyperopic errors were found in the treated eyes, along with increased axial lengths and similar corneal curvature than in control eyes.

In the present study in chicks, one week after surgery, the refractive treatment with PRK surgery with a nominal negative correction of -9.9 D, did not produce a significant change in corneal curvature. In addition it did not produce increased axial elongations previously obtained as it would have resulted from treatment with a negative lens with the same amount of correction. And it not produce statistically significant anisometropia. Measurements immediately after surgery would have allowed us to assess whether surgery produced the expected corneal curvature and refractive changes which were then cancelled out by regression during the following days. Unfortunately, tear secretion and epithelial changes prevent those measurements to be reliable (even if they were conducted under anesthesia). In this study we did not attempt to measure corneal transparency or scattering following surgery (although transparency measurements in vitro had been performed in this model (del Val et al. 2001)). If haze increased during wound healing, this certainly was not sufficient to induce form deprivation myopia. Refraction, axial length and corneal radius of curvature in the control eyes in this study were similar to previous studies. For example, refraction and axial length of untreated 13-day old chick eyes from the study of the previous

chapter on the same chick strain (0.9 ± 0.7 D and 7.9 ± 0.2 mm) (García de la Cera et al. 2006) were similar to those found here despite the differences in the refraction measurement techniques (retinoscopy in the previous study, and Hartmann-Shack here). Published corneal radius of curvature of untreated 2-week old chicks (3.18 ± 0.03 mm) (Li et al. 2000) were similar to these of our study. While some corneal flattening was observed in the treated eyes during the first days of the observation period, the change in corneal power was consistently below the accommodation ability of chicks and in most cases not statistically significantly different from the corneal curvature of the control eyes. If the treatment was effective in reshaping the cornea at all, regression in less than two weeks following surgery may have cancelled the nominally imposed corneal curvature. This effect, also described in a PRK rabbit model, may have occurred more rapidly in chicks for several reasons: 1) the treatment was applied earlier –one day after hatching–, and regression had been associated with earlier treatment (5 versus 10 weeks in the rabbit experiment); 2) chick corneas exhibit higher elasticity than mammalian corneas (Troilo and Wallman 1987; Glasser et al. 1994). It has been proved that under normal physiological conditions, a pressure-mediated mechanism would be able to alter corneal curvature in chicks by about only 3 D (Glasser et al. 1994). However it is likely that the changes in intraocular pressure and decreased corneal thickness following PRK (Schipper et al. 1995) play a major role in increasing corneal curvature and cause regression.

While we have found that, unlike other species, PRK was not effective in changing corneal power of chicks, and therefore as an alternative to spectacle-rearing procedures, high order aberrations were systematically induced by the procedure. As a result, modulation transfer functions in treated eyes were significantly lower than in control eyes. Unlike in human eyes (Marcos et al. 2001; Moreno-Barriuso et al. 2001), spherical aberration did not increase significantly with the procedure (although longitudinal variations were found), perhaps as a result of regression mechanisms similar to defocus. Astigmatism was significantly higher in treated than control eyes (see Figure 4.2). Other asymmetric aberrations such as coma increased significantly, producing increased blur in the retinal images (see Figure 4.2) and consistently decreased

contrast (see Figure 4.5) in the treated eyes with respect to control eyes. Bartman and Schaeffel (Bartmann and Schaeffel 1994) found 9 D of induced myopia in chicks wearing diffusers that caused a 4-time decrease in the modulation transfer at 4.5 c/deg. For the same frequency, in this experiment, high order aberrations decreased modulation transfer functions by 2. When astigmatism was considered, the MTF decreased from 0.69 (normal eyes) to 0.21 (treated eyes) for this spatial frequency. Previous studies in chicks had shown that induced astigmatism actually resulted in low but significant hyperopic (and not myopic) refractive error (Mc Lean & Wallman 2003). In infant monkeys it has been shown that induced astigmatism produces both hyperopic and myopic refractive errors (Kee CS, Hung LF et al., 2004). Thus, presence of laser induced astigmatism could prevent myopia development in the treated eye. We did not find that the contrast degradation produced by high order aberrations induced neither refractive changes nor significant changes in axial length. This was consistent with recent findings in chicks that had undergone ciliary nerve section (Tian and Wildsoet 2006). The treated chicks showed higher amounts of higher-order aberrations but they did not become myopic. For the same pupil size (2-mm) we found slightly lower HOA aberration values than Tian et al. (Tian and Wildsoet 2006) for the control eyes and of the same order of magnitude for the treated eyes (0.53 D vs. 2-3 D using the equivalent defocus power metric (Cheng et al. 2004)). On the other hand, this was in contrast with studies suggesting that increased aberrations may precede myopia development (Kisilak et al. 2006). Along with differences in magnitude which may set a threshold for image blur below which the emmetropization process was not affected, the nature of the image degradation induced by diffusers (scattering) may be different from that induced by aberrations. We found that the predominant induced aberrations were non-rotationally symmetric. It could be that this type of aberrations (as previously found for astigmatism, Mc Lean and Wallman 2003) may not necessarily trigger myopia development. Future research on the potential involvement of specific high order aberrations (i.e. spherical aberration) in myopia development could be addressed by using phase-plates or customized contact lenses with a better a priori control on the magnitude and type of aberration induced.

Chapter 5: Optical aberrations in the mouse eye

Resumen capítulo 5:

Aberraciones ópticas en ojos de ratón.

El ojo de ratón es un modelo muy utilizado para el estudio de enfermedades retinianas y presenta potencial para convertirse en un modelo de miopía.

Para el estudio de enfermedades de la retina es importante mejorar la obtención de imágenes del fondo de ojo en vivo. Por otro lado, modelos experimentales de miopía se basan en la manipulación de la experiencia visual. En ambos casos el conocimiento de la calidad óptica del ojo, y en particular de la calidad de imagen retiniana, afectados por las aberraciones intrínsecas al ojo es esencial. En este trabajo medimos las aberraciones oculares en el ratón. Se estudiaron doce ojos de seis ratones C57BL/6 de cuatro semanas de edad. Las medidas fueron realizadas en animales despiertos, sin anestésicos, excepto uno, medido bajo anestesia para estudios comparativos. Las aberraciones de onda se ajustaron a quinto orden en una expansión en Polinomios de Zernike. El equivalente esférico y el astigmatismo se obtuvieron a partir de los términos de segundo orden. La función de transferencia de modulación (MTF) se estimó a partir del mejor foco y en función del foco para calcular la profundidad de foco. Todas las estimaciones fueron realizadas para pupilas de 1.5 mm. Los datos de refracción obtenidos a partir de las medidas del Hartmann-Shack fueron consistentemente hipermétropes (media \pm desviación estándar, 10.12 ± 1.4 D) y se encontró astigmatismo significativo en varios ojos, en promedio 3.64 ± 3.70 D. La aberración esférica era positiva en todos los ojos (0.15 ± 0.07 μm) y la RMS de los términos de coma era alta (0.10 ± 0.03 μm) comparada con la RMS de otros términos de Zernike. La MTF estimada a partir de las aberraciones de onda mostraba una modulación de 0.4 a 2 ciclos/grado en el mejor foco (y 0.15 teniendo en cuenta el desenfoque medido). Para esa frecuencia espacial la profundidad de foco estimada usando el criterio de

Raleigh era de 6 D. Los valores de aberraciones en el ratón anestesiado fueron mayores que en el mismo ojo del animal sin anestesiarse. Los desenfoques hipermetrópicos encontrados en el ojo del ratón en este estudio son consistentes con los datos publicados sobre ratones medidos con retinoscopia. La óptica del ojo del ratón está lejos de ser limitada por difracción con pupilas de 1.5 mm y tiene valores importantes de aberración esférica y coma. De todos modos, las MTFs estimadas a partir de la aberración de onda son mayores que las publicadas con técnicas de doble paso, resultando en una menor profundidad de foco estimada. A pesar de que las aberraciones imponen una degradación importante en la calidad de imagen retiniana, su magnitud no excede valores corregidos típicamente por las técnicas de óptica adaptativa que se podrían utilizar para visualizar el fondo de ojo. Por otro lado, las aberraciones no parecen ser el factor limitante en la resolución espacial del ratón. A pesar de que la óptica del ojo del ratón es mucho más degradada que la de otros modelos experimentales de miopía, su elevada tolerancia al desenfoque no parece estar determinada totalmente por las aberraciones oculares.

This chapter is based on the article by García de la Cera et al. "Optical aberrations in the mouse eye", *Vision Research* (2006) 46, 2546-2553.

The contribution of Elena García de la Cera to the study was to develop the methodology to measure ocular aberrations in mice (optical set-up, calibrations, automatic control, data processing routines), with the adaptations required to the instrument. She also performed the experimental measurements on mice and participated in the data analysis and interpretation.

Coauthors of the study are: Guadalupe Rodríguez, Frank Schaeffel, Christine Schmucker and Susana Marcos.

5.1. Abstract

The mouse eye is a widely used model for retinal disease and has potential to become a model for myopia. Studies of retinal disease will benefit from imaging the fundus in vivo. Experimental models of myopia often rely on manipulation of the visual experience. In both cases, knowledge of the optical quality of the eye, and in particular, the retinal image quality degradation imposed by the ocular aberrations is essential. In this study we measured the ocular aberrations in the wildtype mouse. Twelve eyes from six four-week old black C57BL/6 wildtype mice were studied. Measurements were done on awake animals, one being also measured under anaesthesia for comparative purposes. Wave aberrations were fit to up to 5th order Zernike polynomials. Spherical equivalent and astigmatism were obtained from the 2nd order Zernike terms. Modulation Transfer Functions (MTF) were estimated for the best-focus, and through-focus, to estimate depth-of-focus. All reported data were for 1.5-mm pupils. Hartmann-Shack refractions were consistently hyperopic (10.12 ± 1.4 D, mean and standard deviation) and astigmatism was present in many of the eyes (3.64 ± 3.70 D, on average). Spherical aberration was positive in all eyes (0.15 ± 0.07 μm) and coma terms RMS were significantly compared to other Zernike terms (0.10 ± 0.03 μm). MTFs estimated from wave aberrations show a modulation of 0.4 at 1 c/deg, for best focus (and 0.15 without cancelling the measured defocus). For that spatial frequency, depth-of-focus estimated from through-focus modulation data using the Raleigh criterion was 6 D. Aberrations in the eye of one anaesthetized mouse eye were higher than in the same eye of the awake animal. Hyperopic refractions in the mouse eye are consistent with previous retinoscopic data. The optics of the mouse eye is far from being diffraction limited at 1.5-mm pupil, with significant amounts of spherical aberration and coma. However, estimates of MTFs from wave aberrations are higher than previously reported using a double-pass technique, resulting in smaller depth-of-field predictions. Despite the large degradation imposed by the aberrations they are lower than the amounts of aberrations typically corrected by available correction techniques (i.e adaptive optics). On the other hand

aberrations do not seem to be the limiting factor in the mouse spatial resolution. While the mouse optics are much more degraded than in other experimental models of myopia, its tolerance to large amounts of defocus does not seem to be determined entirely by the ocular aberrations.

5.2. Introduction

The mouse is the most widely used animal model for human diseases, including inherited vision disorders. Its genome has been almost completely sequenced and there are many transgenic models available. For example, mouse models of retinal degeneration have been investigated for many years in the hope of understanding the causes of photoreceptor cell death (Chang et al. 2002). There are also knockout mouse models for cataracts (Hegde et al. 2003), glaucoma (Lindsey and Weinreb 2005), and diabetic retinopathy (Kern and Engerman 1996). Also, there are recent efforts to develop a mouse myopia model by visual deprivation (Beuerman et al. 2003; Schaeffel et al. 2004).

Electrophysiological (Porciatti et al. 1999) and behavioral studies (Gianfranceschi et al. 1999; Prusky et al. 2004; Schmucker et al. 2005) indicate that the visual spatial resolution in the wild type mouse is poor, and the debate is open whether the optics of the eye match the coarse resolution of the neural mosaic (Artal et al. 1998). Knowledge of the retinal image quality in the mouse is important for various reasons. First, it will help to clarify the limits of spatial vision in the mouse. Second, the measurement of the aberrations of the mouse eye and their potential correction by means of adaptive optics (Roorda and Williams 2001) or phase-plates (Burns et al. 2002) will open the possibility of applying new *in vivo* retinal imaging methods. *In vivo* observations of critical retinal features in mice with retinal degenerations, glaucoma or diabetic retinopathy will allow a better understanding of the pathogenesis, and longitudinal measurements of associated changes and effects of drug therapies, not possible in the cross-sectional data provided by histology (Marcos et al. 2004; Ritter et al. 2005; Schmucker et al. 2005). However, the current correction technology, and the resolution of the fundus images will be limited by the actual amounts of aberrations present in these eyes. Finally, most frequent myopia models rely on the ability of the ocular growth mechanisms to respond to visual

experience. However, optical aberrations determine to a great extent the depth-of-focus of the eye (Marcos et al. 1999; Marcos et al. 2005), and the effects of defocus on retinal image quality will be drastically different whether the eye is diffraction-limited or highly aberrated.

Despite the need for a clearer understanding on the degradation imposed by the optics of the mouse on the retinal image, there are very limited studies that have attempted to assess it, and none, to our knowledge has measured the optical aberrations in the mouse. The very few studies available suggest that the optics of the rodent eye is highly degraded (Artal et al. 1998). Hughes & Wassle (Hughes and Wassle 1979) reported drastic drop in the contrast of grating targets projected on rat retinas and observed by indirect retinoscopy. Schmucker et.al. (Schmucker and Schaeffel 2004) reported photoretinoscopic reflexes consistent with high amounts of aberrations. A recent report (Irving et al. 2005) shows very distorted Hartman-Shack images and consequently high amounts of aberrations in the awake rat eye. To our knowledge the only published study on the objective retinal image quality of the rodent eye (six 3-month Long Evans rats and three C57BL/6J mice of the same age) was that of Artal et al., using a double-pass system (Artal et al. 1998). Animals were fully anaesthetized. By recording through focus double-pass aerial images of a point source they found very little optical quality change (less than 10%) across 24 D, with a slight tendency of optical quality to increase with hyperopic corrections (although they failed at finding a “best focus”). Large depth-of-focus in the rat eye (± 10 D) had been predicted by Green and coworkers (Green et al. 1980). Remtulla and Hallett (Remtulla and Hallett 1985), based on eye size and photoreceptor diameters predicted a depth-of-focus of ± 56 D in adult mice, or ± 11 D once differences between behavioural and ganglion cell acuity were taken into account. Other studies report ± 10 D from whole-body optomotor responses (Schmucker et al. 2005). Hyperopic defocus has also been reported using streak retinoscopy and IR photoretinoscopy in mice, with refractive states ranging from +15.0 D in adult Balb/CJ mice (Beuerman et al. 2003), +13.5 D in 30-day-old C57BL/6J mice (Tejedor and de la Villa 2003), or +7.0 D in 70-day-old mice by Schmucker et

al. (Schmucker and Schaeffel 2004). These hyperopic refractions do not match however those estimated by visual evoked potentials (Mutti et al. 1997), the potential difference being attributed to relatively large distance between the photoreceptor plane layer and the retinal layer where the retinoscopic reflection potentially takes place.

The only experimental modulation transfer functions (MTFs) available in the rodent eye (mostly rat's and one example for one mouse) are those from Artal et al.'s study (Artal et al. 1998) on anaesthetized animals. This study reports modulations of less than 0.1 for the mouse and 1 for the rat at 1 c/deg, for 1-mm pupils. In the double-pass method MTFs are estimated from the intensity distributions of the aerial images of a point source reflected by the retina, and therefore highly dependent on retinal scattering. It is questionable however whether this veiling pedestal affecting the double-pass aerial image truly represents the actual point spread function of the ocular optics. Provided that the ocular media are clear, and intraocular scattering is not a major source of retinal image degradation, MTFs obtained from wave aberrations will account for the actual contrast losses caused by the ocular optics in the mouse, unaffected by retinal scattering. In addition, the measurement of individual aberrations in the mouse eye will allow us to better understand the sources of optical degradation. A previous study (Artal et al. 1998) attempted to predict aberrations in the rat eye using a simple eye model and biometric data provided by Hughes (Hughes 1979). Those simulations found significant amounts of spherical aberrations due to the highly curved surfaces of small eyes. However the predicted MTFs were higher than the experimental MTFs that let the authors to conclude that other unknown high order aberrations were also present. Currently, new biometric data in the mouse are available using new technology (Lin et al. 2004; Schmucker and Schaeffel 2004). Predictions based on eye models could be revisited in the light of those newly reported biometric data and the ocular aberrations reported here and it will be addressed in this thesis in Chapter 6. Finally, measurements of the wave aberrations will allow us to obtain the refractive state of mice, from the defocus term in the polynomial expansion describing the wave aberration function, and also to estimate the depth-of-

focus, by computing through-focus optical quality as the defocus term is computationally changed in the wave aberration function.

In this chapter we present measurements of ocular aberrations (low and higher order) in the wild type mouse. The aims of the study were to investigate:

- 1) Ocular aberrations and retinal image quality in the mouse eye
- 2) The optical depth-of-focus in the mouse eye
- 3) Relationships between ocular aberrations and refractive error in the mouse eye

This experiment could reveal if ocular aberrations in mice have any effect in ocular development and their consequences in the potential of mouse as myopia model.

5.3. Methods

5.3.1. Subjects

Black C57BL/6 wildtype mice were obtained from Charles River, Barcelona, Spain and kept in the animal facilities of the Instituto de Oftalmobiología Aplicada, Universidad de Valladolid, Spain, housed in standard mouse cages under 12 hours light/dark cycle. All experimental protocols were approved by the Institutional Review Boards, and met the ARVO resolution for care and use of laboratory animals. Six four week old females were used in this study.

5.3.2. Hartmann-Shack aberrometer

Ocular aberrations were measured with a Hartmann-Shack aberrometer built at the Instituto de Optica (Consejo Superior de Investigaciones Cientificas), Madrid, Spain, described in Section 2.1.1. The particularly low quality of the Hartmann-Shack spots from mouse eyes prevented to use the more standard processing algorithms developed previously. Therefore new routines for HS spot detection, and centroiding algorithms were written in Matlab (Mathworks, Natick MA) and specifically developed for the present study. Zernike coefficients were obtained by modal fitting of the lateral deviations to the derivatives of the Zernike polynomial expansion up to the 5th order.

5.3.3. Experimental protocols

Mice were measured in the Hartmann-Shack system under awake and normal viewing conditions, i.e. without anaesthesia nor with cyclopegia. The animals were restrained by holding their tails while they were sitting on an elevated platform mounted in front of the system, which allowed centration and focusing of the animal's pupil. Figure 5.1 The pupil image channel

provided continuous pupil monitoring and let us controlling Purkinje images from the IR ring during measurements. We made sure that the Purkinje images remained within the pupil, as used this as an indication that fixation was not too eccentric. Additional centration could be achieved by moving the x-y stage that translates the entire Hartmann-Shack system. After some adaptation to the task, the mice became cooperative and did not move during the measurement, allowing us to capture several (5- 10) images per eye. The same procedure was repeated for left and right eyes.



Figure 5.1. Mouse previous to measurements. Animal was placing in a platform in front of the Harman-Shack system near to IR ring LEDs.

For comparative purposes, mouse labelled as # 2 was also measured under anaesthesia . Mouse # 2 were anaesthetized with an subcutaneous injection of a mixture of 1.2ml 10% ketamine hydrochloride and 0.8 ml 2% xylazine hydrochloride, dissolved in 8.0 ml sterile saline. In those measurements eyelids were held open and the cornea was moistened with eye drops (Viscofresh 0.5% ,Allergan).

5.3.4. Data analysis

Typical Hartmann-Shack images contained about 12 spots. In general, images from the same eye were very similar, suggesting a good fixation by the animal. Data were processed for the maximum pupil diameter (ranging from 1.63 to 2.17mm). For comparative purposes, across eyes the minimum pupil diameter of 1.5mm was used. Reported data for each eye are averaged

of at least 5 individual measurements. The optical quality of the eye was assessed in terms of individual Zernike coefficients and the root-mean-square wavefront error (RMS) of the different terms or orders. Modulation Transfer Functions (MTF) and Point Spread Functions (PSFs) were also obtained from the wave aberrations. The volume under the MTF and the modulation at 2 c/deg were also used as an optical quality metric. Through-focus estimates of these metrics were used to compute depth-of-focus.

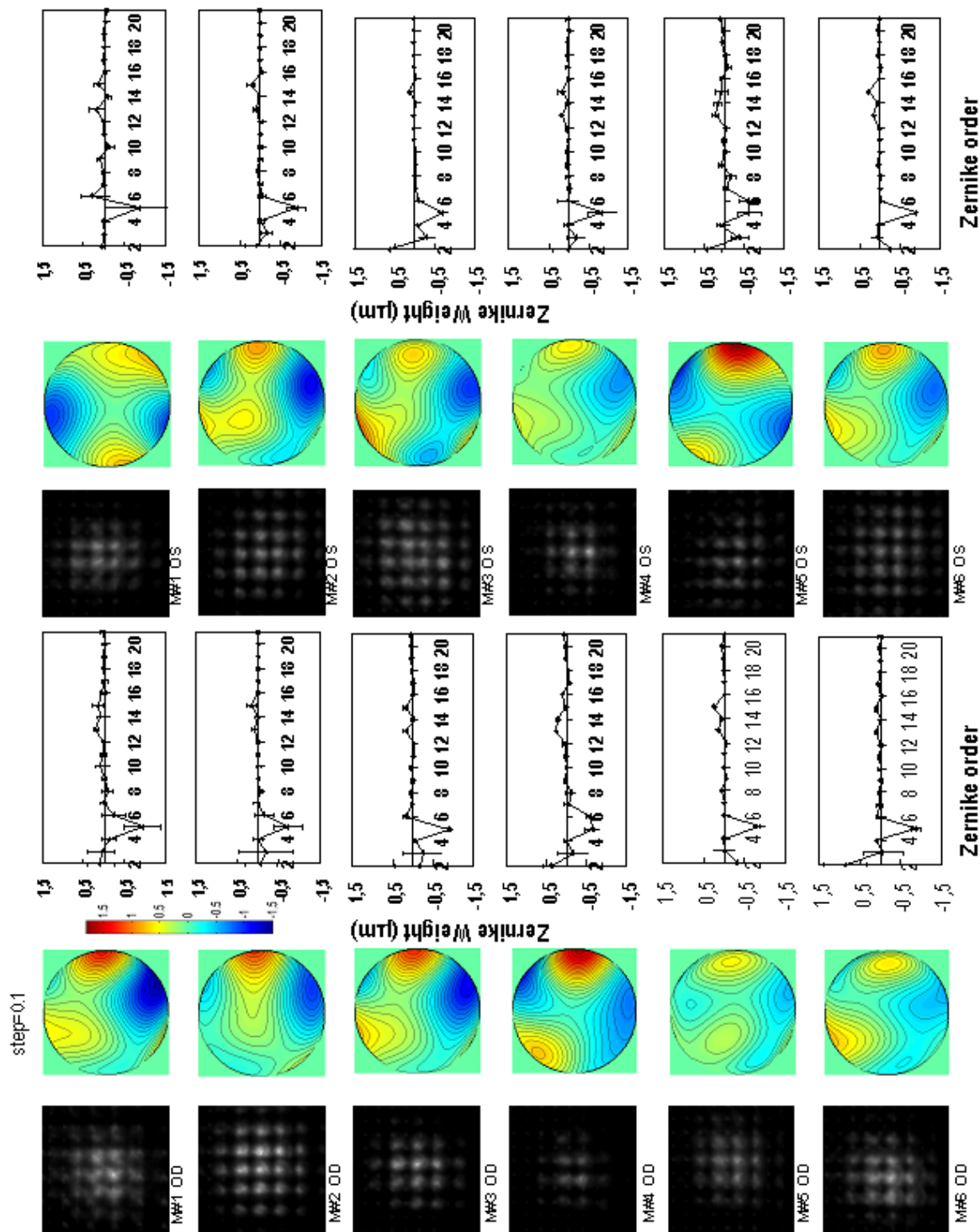


Figure 5.2. Examples of Hartmann-Shack images on awake mouse eyes (scale: 3.4 mm x 3.4 mm), and corresponding wave aberration maps and mean Zernike coefficients. Wave aberration maps are for 3rd and higher order aberrations, and contour lines are plotted in 0.1 μ m steps. Zernike coefficients are ordered following the OSA convention, and the error bars stand for standard deviations. Data are for 1.5-mm pupil diameters

5.4. Results

5.4.1. Hartmann-Shack images and wave aberrations

Figure 5.2 shows the Hartmann-Shack raw data (left), clearly more degraded than those typically found in human eyes (Liang and Williams 1997), chicks (Chapter 3) (García de la Cera et al. 2006), rhesus monkeys (Vilupuru et al. 2004) or cats (Huxlin et al. 2004). The corresponding wave aberrations (center), for 3rd and higher order aberrations (for 1.5 mm pupils) show prevalence of positive spherical aberration in most of the animals, as well as significant amounts of other high order aberrations, even for these small pupil sizes. Zernike coefficients are also shown (right) in all eyes (average across measurements in each eye, and the corresponding standard deviation), following the Optical Society of America notation (Thibos et al. 2000).

5.4.2. Refractive state

Zernike coefficient Z_2^0 , corresponding to the defocus term (with negative sign, consistent with hyperopic defocus), is the largest in all eyes, as shown in Figure 5.2. Figure 5.3 shows the average spherical equivalent found

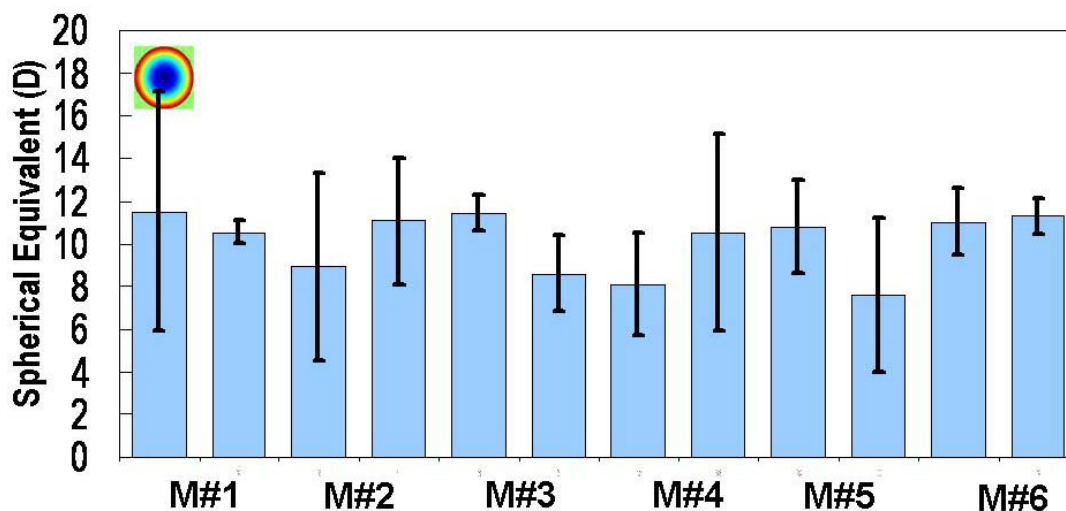


Figure 5.3. Spherical equivalent for all mice. red bars correspond to right eyes and blue bars to left eyes. Error bars stand for standard deviations across measurements.

for each eye, computed from the defocus term of the Zernike polynomial expansion, for a wavelength of 678 nm. The spherical equivalent is consistently hyperopic in all eyes, $+10.12 \pm 1.41$ D (average \pm standard deviation). Intersubject variability is of the order of the average interocular differences (1.97 D) and smaller than the average measurement variability (2.61 D). Astigmatism was computed from Zernike terms Z_2^1 and Z_2^{-1} and found to be on average 3.64 ± 3.70 D. Taking the measured astigmatism into account, pure spherical error resulted in 8.30 ± 3.00 D. We did not find a preference for the horizontal or vertical meridian to be the least hyperopic. The astigmatism axis tended to be mirror symmetric across left and right eyes. Astigmatism axis values are clustered around 37 ± 4 deg and -37 ± 9 deg (or 127 ± 9 deg in the positive cylinder convention) in all eyes except one (#4, left eye).

5.4.3. High order aberrations

Figure 5.4 shows root mean square wavefront errors (RMS) for different terms and all eyes, for 1.5-mm pupils. Average third and higher order aberration RMS is 0.32 ± 0.08 microns. Spherical aberration accounts for a significant proportion of the high order aberrations (0.15 ± 0.06 microns), equivalent to a blur of 1.85 D. However third order aberrations alone (RMS=

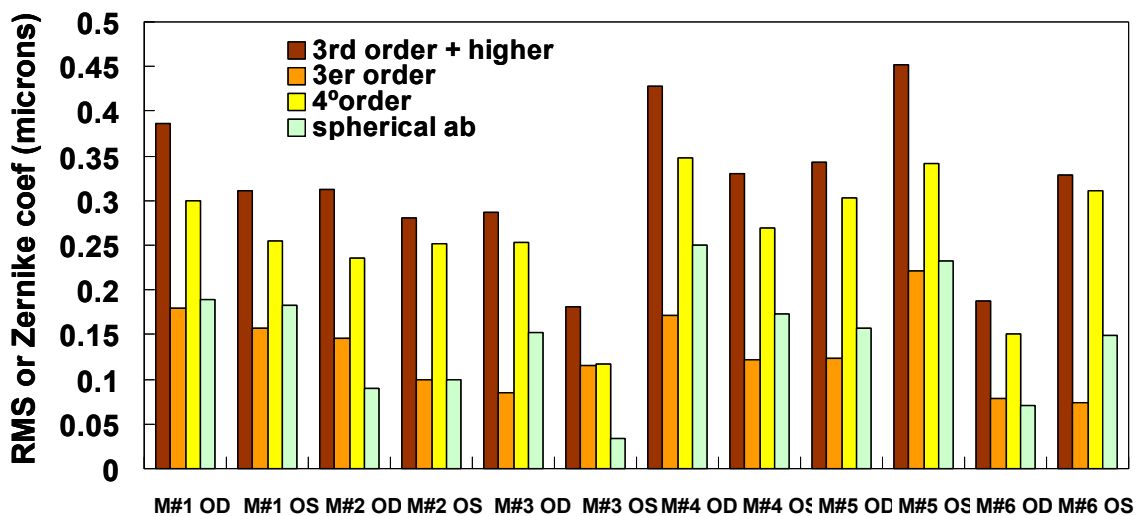


Figure 5.4. Mean 3rd and higher order RMS (black bars), 3rd order RMS (light grey) bars, 4th order RMS (dark grey bars), spherical aberration Zernike coefficient (white bars) and 5th order RMS (dotted bars). Error bars represent intersubject variability and stand for standard deviations across eyes. Data are for 1.5-mm pupil diameters.

0.13 ± 0.04 microns represent also a major source of degradation, particularly coma (RMS= 0.10 ± 0.03 microns). While other non-spherical 4th order terms are important (compare dark gray and dotted bars in Figure 5.4), 5th order terms are not very different from zero (0.09 ± 0.04 microns). High order aberration intersubject variability is low and comparable with variability of repeated measurements on the same eye (0.07 microns, on average).

5.4.4. Modulation Transfer Functions

Figure 5.5 shows average radial-profile MTFs across all eyes obtained from wave aberrations, for 1.5 mm pupils and for the illumination wavelength (678 nm). Average best-focus MTF (i.e. correcting for hyperopic defocus) is shown in black line, and average non-corrected MTF (i.e. with all low and higher order aberrations) is shown in dotted blue line. For proper comparison of MTFs, it should be noted that the mouse eye has a particularly low numerical aperture (NA= 0.5). MTFs for 1.5 mm pupils in another small eye (chick eye, NA= 2.6) from Chapter 3 and the average human eye MTFs for 6.5-mm pupil diameter (NA= 3.4) are also shown for comparison, along with the diffraction-limited MTF for 1.5mm pupils. As a reference, the diffraction-

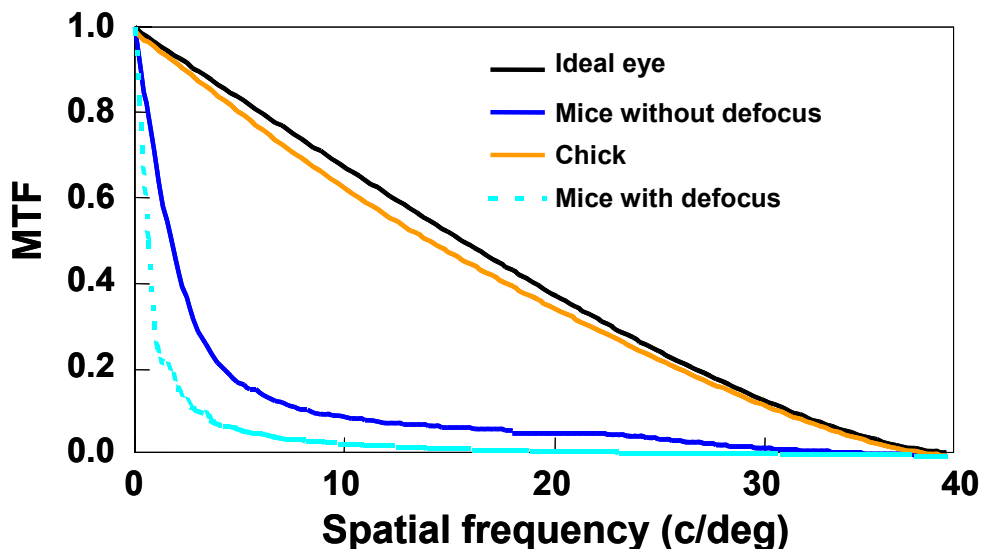


Figure 5.5. Mean MTFs (radial profile) averaged across all mouse eyes for best focus (solid dark blue line), and uncorrected defocus (dotted light blue line) for 1.5 mm pupil diameter. For comparison average MTF for 4-week old chicks (n= 5) for 1.5 mm-pupils (yellow line) from wave aberrations measured with the same Hartmann-Shack system (Chapter 3 and García de la Cera et al. 2006) and the theoretical MTF of a diffraction-limited eye for 1.5-mm pupil is also represented.

limited MTF with the same amount of defocus as found in the mouse eye has also been included. Both the human and chick eyes are nearly diffraction-limited for this pupil size. In the mouse, while defocus imposes additional optical degradation, major losses in contrast are produced by high order aberrations.

5.4.5. Depth-of-focus

Through-focus image quality estimated by computationally changing the defocus term (at 1 D steps) in the wave aberration, for 1.5-mm pupils, is represented in Figure 5.6. Modulation transfer for 2 c/deg (same spatial frequency used by Artal et al. 1998 for the rat eye) was used as an image quality metric. The curves in Figure 5.6 are referred to zero defocus, i.e. compensating the spherical equivalent given by the defocus term in each eye. However, in most eyes, the highest optical quality does not correspond to that correction, as typically found in the presence of high order aberrations (Guirao and Williams 2003). We found best-optical quality to be shifted on

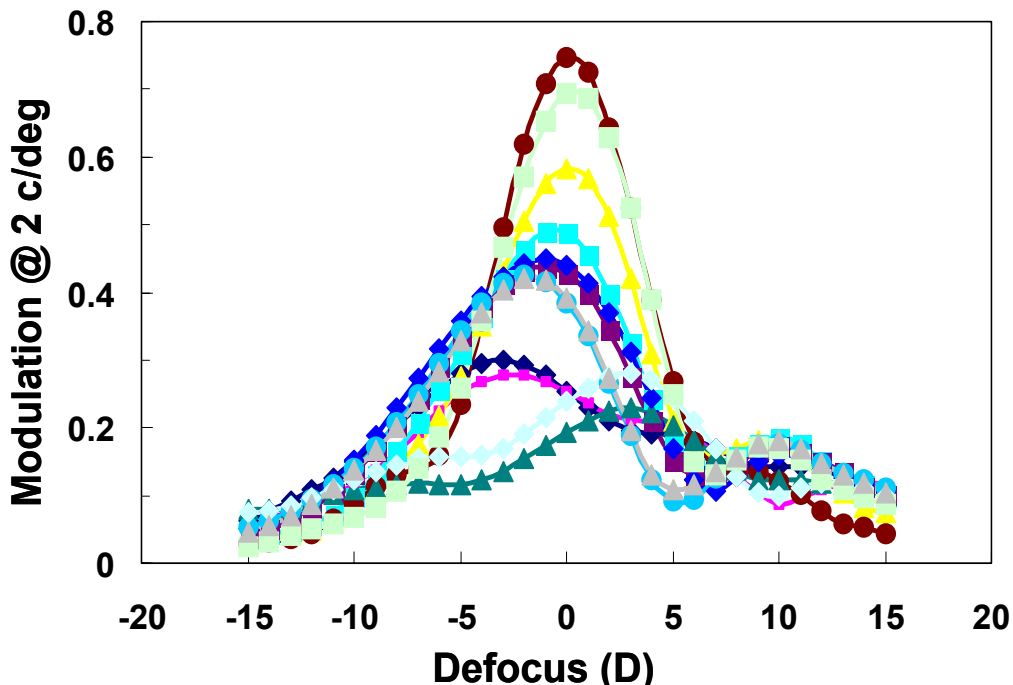


Figure 5.6. Through-focus modulation transfer at 2 c/deg, estimated from radial profile MTFs. Each colour corresponds to a different mouse eye. A positive defocus sign is indicative of positive defocus at the retinal plane (and therefore required myopic correction) and viceversa for negative defocus.

average 0.42 D toward less hyperopic values. Depth-of-focus was estimated using the Raileigh criterion, i.e. as the defocus range for which optical quality was at least 80% of the value at best focus (Marcos et al. 1999) and ranges from 7.9 to +4.5 D. The volume under the MTF was used as another metric to obtain the depth-of-focus, and values ranging from 11 to 1.7 D were found using this metric. We found that depth-of-focus was highly correlated with the amount of individual 4th order spherical aberration present in each eye ($r=0.726$, $p<0.0001$), as shown in Figure 5.7.

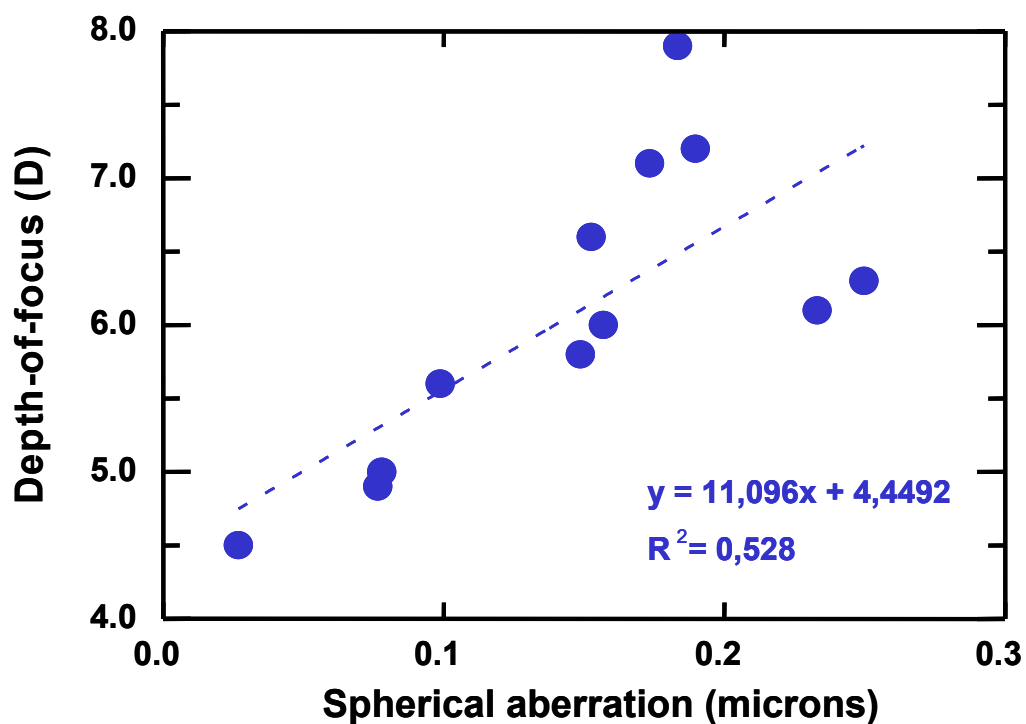


Figure 5. 7. 4th order spherical aberration from Zernike expansion vs. depth-of-focus from through-focus modulation transfer at 2 c/deg using the Raileigh criterion for all eyes. Data are from 1.5 mm pupil diameters.

5.5. Discussion

5.5.1. *The effect of anaesthesia*

While the measurement of the optical quality of the mouse eye under normal viewing conditions is important to get insights on the limits of spatial resolution, and to assess the prospects of the mouse as a myopia animal model, several applications will very likely require the use of anaesthesia to immobilize the animal, for example in vivo retinal imaging. Also, previous measurements of the double-pass MTF in the rodent eye (Artal et al. 1998) were performed under total anaesthesia (Equistesin) (Artal et al. 1998).

We compared measurements with and without anaesthesia on the same eye (right eye of mouse # 2), to assess possible effects of the drug on optical quality. Measurements were attempted on other animals, but rapid opacification of the crystalline lens during anesthesia prevented completion of these measurements. We found larger HS spots in the anaesthetized eye than previous measurements under awake conditions on the same eye. We found higher amounts of aberrations in the anaesthetized eye (RMS for 3rd and higher order was 0.42 microns in the anaesthetized animal vs 0.32 microns in the awake animal; spherical aberration was 0.14 microns vs 0.09 microns; and RMS for 3rd order was 0.32 microns vs 0.15 microns). We also found a lower hyperopic spherical equivalent in the anaesthetized eye (+3.28 D vs +10.12 D).

While these results are only for one eye, they may be indicative of larger optical degradation in anaesthetized mouse eyes, and perhaps a possible cause of the differences in retinoscopic refractions from different authors (Beuerman et al. 2003; Tejedor and de la Villa 2003; Schmucker and Schaeffel 2004). As previously reported other additional complications further deteriorating optical quality under anaesthesia, not accounted for by aberrometric MTFs but very likely decreasing contrast of retinal images are

the corneal dryness and transient cataracts induced by anaesthesia (Calderone et al. 1986).

5.5.2. Comparisons with other studies: refraction, MTF and depth-of-focus

We found hyperopic defocus in the 4-week old mouse eye of $+10.12 \pm 1.41$ D using Hartmann-Shack aberrometry at 680 nm, only slightly higher than those reported by Schmucker & Schaeffel (Schmucker and Schaeffel 2004) for mice of the same age ($+7.0 \pm 2.5$ D) using infrared photoretinoscopy at 880 nm. These results are in contrast to previous studies using streak retinoscopy, reporting larger amounts of hyperopic defocus with eyelid suture (up to $+13.5$ D by (Tejedor and de la Villa 2003)). A control experiment performed by Schmucker & Schaeffel (Schmucker and Schaeffel 2004) demonstrates that chromatic aberration is not the cause for the discrepancy. The fact that the retinal reflection may occur in a retinal layer different from the photoreceptor layer, which is effectively aggravated in eyes with short focal lengths (the so-called “small eye artifact” (Glickstein and Millidot 1970)) and reported differences with refractive errors obtained visually evoked potentials (less hyperopic) leaves the question open of whether the mouse eye is truly hyperopic. Additionally, (Schmucker and Schaeffel 2004) observed ring-shaped intensity distributions of the retinoscopic pupillary images, what led them to suggest that the crystalline lenses might be multifocal, similar to what has been described for fish eyes (Kroger et al. 1999). The spatial sampling resolution of our lenslets (400 microns) is too coarse to draw any conclusion regarding multifocality in the mouse eye.

We have computed MTFs from the measured wave aberrations in the mouse eye, for best focus (i.e. simulating correction of the measured hyperopia) and different amounts of defocus. The average MTF at best focus can be compared with, to our knowledge, the only MTF previously reported, which corresponds to one single mouse eye, using a double-pass technique. While we found generally low MTFs, these are not as severely degraded as the MTF reported by Artal et al. (1998). While that study shows modulations

lower than 0.1 for 2 c/deg for 1-mm, we found modulations close to 0.4 for that spatial frequency (see Figure 5.5), for 1.5 mm pupils. There are several possible reasons for the discrepancy: 1) the previous study performed measurements under anaesthesia, which appears to lower image quality, and presumably increase corneal and intraocular scattering, what the double-pass method is able to capture; 2) double-pass MTFs are likely affected by the presence of retinal scattering, producing halos in the aerial image resulting in a lower MTF; 3) the previous study only reports limited data on a single mouse, even though three animals were used as subjects, and the authors did not mention whether this was due to problems in data processing in the other two animals, or due to other reasons.

On the other hand, the enlarged aerial spots in the Hartmann-Shack images may be suggestive of fine structure in the wave aberration not being resolved by the lenslet array. However, the fact that 5th order aberrations are of much lower magnitude than 3rd or 4th order aberrations indicates that we are probably not overestimating the MTF by not capturing higher order aberrations. The degraded retinal spots may be just indicative of large amounts of retinal scattering.

We have also obtained estimates of optical depth-of-focus, which can be compared with previous predictions and measurements from the literature. As shown by Figure 5.6, the actual depth-of-focus will very much depend on the definition used. We found large depth-of-focus particularly in eyes with larger amounts of spherical aberration. However, our data of optical depth-of-focus are lower than previous predictions and reports using the double-pass method.

5.5.3. *Implications of the results*

Our results confirm previous speculations that higher order aberrations are major sources of optical quality degradation in the mouse eye. Significant amounts of spherical aberrations are consistent with highly curved spherical surfaces, although a complete predictive model should incorporate aspheric surfaces and gradient index distributions in the crystalline lens (and will be shown in Chapter 6). The presence of large amounts of third order aberrations and astigmatism may be due to eccentric fixations with respect to the optical axis. Interestingly, the high repeatability of the measured coma terms and relatively low intersubject variability seems to indicate that mouse use a certain fixation axis or did not make too large eye movements, despite their afoveated retinas.

Even if we found severely degraded optics compared to the diffraction-limit, our MTF estimates for best-correction in the mouse are higher than previously reported using double-pass in one anaesthetized mouse, and even rats. Even with defocus, the modulation at 2 c/deg is 0.2, which indicates that the optics does not impose the limits to spatial vision in the mouse eye. Behavioral and electrophysiological experiments report visual acuities of 0.5-0.6 c/deg (Gianfranceschi et al. 1999; Porciatti et al. 1999). The fact that anaesthetized animals show larger amounts of aberrations than awake animals complicates further their correction for in vivo imaging. Provided that the second order aberrations are corrected by other means, current adaptive optics technology generally provides sufficient stroke to compensate the RMS measured in the anaesthetized animal (0.5 microns). It seems more challenging to generate centroiding algorithms that process the severely degraded Hartmann-Shack in real time (our algorithms are accurate but not time-efficient), and to handle the presence of cataracts and corneal dryness.

The use of the mouse as an animal model for myopia has been challenging. Degrading the optical quality by diffusers (Schaeffel and Burkhardt 2002) or minus-lens power wear (Beuerman et al. 2003) has been shown to change the refractive state in the myopic direction but not all the studies show clear axial elongation. In fact, in one of the studies (Tejedor and de la Villa 2003) the refractive and axial length change did not seem to correspond with each other (Tejedor and de la Villa 2003). Our results show that moderate amounts of imposed spherical defocus (see Figure 5.6) will not alter optical quality significantly, and therefore it is not surprising that mice do not respond to a lens-treatment as easily as other models. However, the measured optical depth-of-focus is lower than estimated from behavioral measurements (Schmucker et al. 2005) suggesting that tolerance to defocus may be ultimately limited by neural sampling. Our results show (see Figure 5.5) that natural aberrations in the eye cause severe decrease in the contrast and spatial resolution of retinal images, even in the absence of defocus (as it would occur if the hyperopic defocus measured using reflectometric techniques was caused by the small eye artefact and the eye was in fact nearly emmetropic). This is very different to what we found in the chick model (Chapter 3) where the optics was almost diffraction-limited both in normal eyes and myopic eyes treated with diffusers (removing the defocus term). While in normal conditions chicks have high contrast retinal images, mice have much poorer retinal images (with, and even without the hyperopic defocus, due to high order ocular aberration). As opposed to what happens in chicks, the high tolerance to defocus and to further degradation by diffusers seems to make eye growth more challenging to respond to changes in visual experience. Other complicating factors (Schmucker and Schaeffel 2004) are the slow ocular growth and a rod-dominated retina.

Chapter 6: Matching ocular biometry to optical aberrations: Chick and mouse computer eye models

Resumen capítulo 6:

Relación de la biometría ocular con las aberraciones ópticas: modelos de ojo de pollo y ratón.

En este capítulo hemos desarrollado un modelo de ojo de pollo (de 0 a 14 días) y un modelo de ojo de ratón de 4 semanas de edad. Estos modelos computacionales están basados en datos biométricos obtenidos de la literatura y en las medidas realizadas en ambos animales en estudios previos, descritos en capítulos anteriores de esta tesis.

Las aberraciones oculares han sido reproducidas utilizando técnicas de trazado de rayos para cada modelo de ojo y comparado posteriormente con las medidas realizadas con aberrometría. Esta comparación ha permitido evaluar la precisión de los datos biométricos en dichos modelos animales y predecir el papel de algunas estructuras oculares, de las que hasta el momento se conoce poco en estos ojos, como la distribución de índice refractivo del cristalino o posibles asfericidades.

En pollos, encontramos que las variaciones de los radios de curvatura corneales, espesor corneal, profundidad de cámara anterior, radios de curvatura y espesor del cristalino, así como la longitud axial, por sí solos no pueden explicar los cambios longitudinales con la edad de la refracción y las aberraciones ópticas medidas experimentalmente. El modelo predice el papel que juega la distribución de gradiente de índice para explicar las magnitudes observadas y los cambios de desenfoque y aberración esférica. Además también demuestra la fiabilidad de los diferentes parámetros oculares obtenidos de la literatura, a veces controvertidos.

Las diferencias de refracción y aberraciones ópticas entre ojos miopes y emmetropes pueden ser explicados por razones principalmente relacionadas con la elongación axial ocular.

En el ratón, la degradación de la óptica del ojo (ver capítulo 5) abre la pregunta sobre el papel que desempeñan las distintas estructuras en la calidad de la imagen retiniana. Los datos biométricos publicados de ratones de 4 semanas de edad (radios de curvatura, espesores...) no explican, al igual que en el pollo, los valores de desenfoque y aberraciones obtenidos experimentalmente. Se hace necesario estudiar por métodos computacionales el posible papel de la distribución del gradiente de índice del cristalino.

This chapter is based on the articles by García de la Cera et al.:

“Matching ocular biometry to optical aberrations (I): Developing normal and myopic chick computer eye model”, in preparation.

“Matching ocular biometry to optical aberrations (II): 4-week old mouse computer eye model”, in preparation.

The contribution of Elena García de la Cera to the study was the literature search and analysis of ocular biometry data, measurement of ocular biometry and optical aberrations in the mouse and chick, development of the computer eye models and data analysis.

Coauthors of the study are Alberto de Castro, Sergio Barbero and Susana Marcos.

6.1. Abstract

In this chapter we have developed a chick eye computer model from 0 to 14 days of age and a 4 week-old mouse eye computer model based on biometric data from the literature and from previous chapters in this thesis. Ocular aberrations have been simulated using ray tracing on these models and compared to the experimental aberrometry measurements presented in this thesis. This comparison has allowed us to evaluate the accuracy of biometric data in these animal models and predict the role of some ocular parameters from which little is known in these eyes (i.e. refractive index distribution or surface asphericities)

In chicks, we found that changes in corneal radii of curvature, corneal thickness, anterior chamber depth, lens radii of curvature and thickness, and axial length alone could not explain the longitudinal changes in refraction and optical aberrations measured in chicks. The model predicts a prominent role of gradient index distribution to explain the observed amounts and changes of defocus and spherical aberration. The model also tests the plausibility of the different ocular biometry data (sometimes controversial) from the literature. Differences in refraction and optical aberrations between normal and myopic eyes can be explained primarily by simple ocular axial elongation

The severely degraded optics in mice eye (see Chapter 5) can be explained by the geometrical structure of the ocular components (radii of curvature, corneal thickness, anterior chamber depth, lens radii of curvature and thickness, and axial length). A model with a homogeneous index of refraction in the lens would predict even larger amounts of aberrations.. A plausible gradient index profile in the lens was assumed, and allowed to reproduce experimental data.

6.2. Introduction

Ocular biometry in animal models of myopia has been widely reported, as it is critical to assess the structural changes of the ocular components during development of the normal eye, or the eye undergoing treatments leading to refractive errors. More recently, aberrometers have been developed that have allowed for the first time the measurement of optical aberrations in animal eyes (chicks (García de la Cera et al. 2006; Kisilak et al. 2006; Tian and Wildsoet 2006; García de la Cera et al. 2007), mice (García de la Cera et al. 2006) - presented in this thesis-, cat (Huxlin et al. 2004) or monkeys (Ramamirtham et al. 2006). Aberrations have been measured both in wild type species and normal eyes, during normal development and during development of refractive errors (imposed by form deprivation or lenses), as presented in this thesis.

The geometrical and structural properties of the ocular components are intrinsically related to the optical quality of the eye. Schematic eye models in the chick (Schaeffel and Howland 1988) , mouse (Remtulla and Hallett 1985), rat (Hughes 1979) or primate (Lapuerta and Schein 1995) eyes have been reported in the literature, similarly to well-known schematic model eyes of the human. However, in most cases, these models have been used to predict paraxial properties of the eye, most frequently refractive errors. Today, customized computer eye models of the human eye, primarily pseudophakic eyes have been shown to predict experimentally measured high order aberrations with a high accuracy (Rosales and Marcos 2007). These model eyes include individual data of corneal topography, lens geometry and misalignments, and the off-axis location of the fovea (Rosales and Marcos 2006). Also, the use of schematic model eyes is important to assess the relative importance of each component to the overall optical quality, and to identify the potential contribution of unknown factors (such as the refractive index of the lens, or asphericities). Also, while previous simulations of optical quality with increasing age have been able to extract suggestive suggestions (such as the geometrical nature of the improvement of optical quality in chicks, for constant pupil sizes), those were

based on very simple models (Howland 2005). Schematic models including all known parameters will provide more extended predictability.

In this chapter we developed computer models of chick and mice eyes to understand the sources of optical degradation in these eyes. We used refraction and ocular biometry data obtained both in this thesis as well as in previous studies in the literature and developed schematic eye models to predict high order ocular aberrations (primarily spherical aberration). The simulated aberrations were compared to measured aberrations (reported in this thesis). We will assess the impact of the change of the ocular components with development and across refractive errors on the optical aberrations, to which extent geometrical and structural properties of the ocular components, and the potential role of not well known properties (gradient index, surface asphericities).

This chapter presents a comprehensive review of ocular parameters of the chick eye of different ages (Section 6.3.1), sometimes controversial across studies. The most plausible data geometrical and structural properties of the cornea, crystalline lens and interocular distances have been identified, to explain the changes in refraction and spherical aberration with age and refractive errors. .

6.2.1. A compilation of chick biometric data

Biometric data have been compiled from various sources. Data include anterior corneal radius and asphericity, corneal thickness, anterior chamber depth, lens radii of curvature, refractive indices, lens thickness and axial length. Table 6.1 (A & B) summarizes the data from the different studies that we have tested in the reported model eyes and used to simulate the optical aberration. Figures 6.1-6.7 show the change of ocular biometry parameters in the chick eye as a function of age, from different studies.

Ocular parameter	Reference	Total number of eyes	Age range (days)	Longitudinal study	Experimental condition	Technic used
Anterior Corneal radius	Gottlieb et al., 1987		0-44	yes	in vivo	keratometry
	Li et al., 2000	10	0-15	yes	in vivo	photokeratometry
	Wallman & Adams, 1987	10	0-17	yes	in vivo	photokeratometry
	Troilo et al. 1987	12	0-30	yes	anaesthetized	keratometry
	Li & Howland, 2003	12	21	no	in vivo	photokeratometry
	García de la Cera et al., 2007	10	0-13	Yes	in vivo	photokeratometry
	Guggenheim et al., 2002	10	28	no	anaesthetized	keratometry
	Troilo & Wallman, 1991	9	14	no	anaesthetized	keratometry
	Troilo & Wallman, 1987		28	no	anaesthetized	keratometry
	Schaeffel & Howland, 1988	156	14-86		in vivo	photokeratometry
Irving et.al, 1996	234	0-14	Yes	in vivo	keratometry	
Corneal asphericity	Schaeffel & Howland, 1987	4	14-42		in vivo	photokeratometry
Corneal thickness	Montiani-Ferrerira, 2004	25	0-450	yes	in vivo	Ultrasonic pachimetry
	Irving et.al, 1996	234	0-14	yes	ex vivo	
	Irving et.al, 1996	52	14		ex vivo	measurements of frozen sections
	Choh & Sivak, 2002 (a)	9	7	no	ex vivo	ultrasound biomicroscopy
n corneal	Sivak & Mandelman, 1982	4		no	ex vivo	refractometry
	Irving et.al, 1996	6	Adults		ex vivo	Abbe-refractometry
Anterior chamber	Gottlieb et al., 1987		0-43	yes	in vivo	A-scan ultrasonography
	Li et al., 2000	10	0-14	yes	in vivo	A-scan ultrasonography
	Wallman et al., 1994	16	12,32	no	in vivo	Ultrasonography
	Zhu et al., 1995	103	14,28	no	anaesthetized	A-scan ultrasonography
	Guggenheim et al., 2002	10	28	no	anaesthetized	A-scan ultrasonography
	Li & Howland, 2003	12	21	no	in vivo	A-scan ultrasonography
	Troilo & Wallman, 1991	9	14	no	anaesthetized	A-scan ultrasonography
	Pickett-Seltner et al., 1988	10	0-15	Yes	ex vivo	measurements of frozen sections
	Schaeffel & Howland, 1988	20	30		ex vivo	measurements of frozen sections
	Irving et.al, 1996	234	0-14	yes	ex vivo	A-scan ultrasonography
	Irving et.al, 1996	52	14		ex vivo	measurements of frozen sections
Choh et al, 2002 (a)	9	7	no	ex vivo	ultrasound biomicroscopy	
n humors	Irving et.al, 1996	6	Adults		ex vivo	Abbe-refractometry

Table 6.1 (A). A compilation of cornea and anterior chamber biometric data used in this work. Empty cells are data that are not indicated by authors. Posterior corneal radius is not show because they are not real measurements but estimations.

Ocular parameter	Reference	Total number of eyes	Age range (days)	Longitudinal study	Experimental condition	Technic used
Anterior lens radius	Irving et.al,1996	52	14		ex vivo	measurements of frozen sections
	Schaeffel & Howland, 1988	20	30		ex vivo	measurements of frozen sections
Lens thickness	Gottlieb et al.,1987		0-45	yes	in vivo	A-scan ultrasonography
	Troilo et al.1987	12	0-29	yes	anaesthetized	A-scan ultrasonography
	Nickla et al.1997	10	1,5	no	anaesthetized	A-scan ultrasonography
	Zhu et al.,1995	103	14,28	no	anaesthetized	A-scan ultrasonography
	Guggenheim et al., 2002	10	28	no	anaesthetized	A-scan ultrasonography
	Priolo et al.,1999	15	0,7	no	ex vivo	Vernier calipers
	Priolo et al.,2000	12	0,7	no	in vivo	Scanning electron microscopy
	Troilo & Wallman, 1991		21			Vernier calipers
	Schaeffel & Howland, 1988	20	30		anaesthetized	Ultrasound
	Irving et.al,1996	234	0-14	yes	ex vivo	A-scan ultrasonography
	Irving et.al,1996	52	14		ex vivo	measurements of frozen sections
	Choh & Sivak,2002 (a)	12	8	no	ex vivo	ultrasound biomicroscopy
n lens	Sivak & Mandelman,1982	4		no	ex vivo	spectometry
	Schaeffel & Howland, 1988	156	14-86	Yes	ex vivo	refractometry
Posterior radius lens	Irving et.al,1996	52	14		ex vivo	measurements of frozen sections
	Wallman & Adams, 1987	10	0-18	yes	in vivo	Purkinje image photography
	Sivak et al,1978		20-55	no	ex vivo	refractometry
n posterior chamber depth	Sivak & Mandelman,1982	2		no	ex vivo	refractometry
Axial length	Pickett-Seltner et al.,1988	10	0-14	Yes	ex vivo	measurements of frozen sections
	Schaeffel & Howland, 1988	38	14-86		ex vivo	photography of transscleral images
	Irving et.al,1996	234	0-14	yes	ex vivo	A-scan ultrasonography
	Irving et.al,1996	52	14		ex vivo	measurements of frozen sections
	Choh & Sivak,2002 (a)	12	7	no	ex vivo	A-scan ultrasonography
	Gottlieb et al.,1987		0-42	yes	in vivo	A-scan ultrasonography/ measurements of frozen sections
	Zhu et al.,1995	103	14,28	no	anaesthetized	A-scan ultrasonography
	Pickett-Seltner et al.,1987	10	0,14	no	ex vivo	Vernier calipers
	García de la Cera et al., 2006	10	0-13	Yes	in vivo	A-scan ultrasonography

Table 6.1 (B). A compilation of lens, posterior chamber depth and axial length biometric data used in this work. Empty cells are data no indicated by authors.

6.2.1.1. Anterior corneal radius

The cornea is the most important refractive surface in the eye, and corneal curvature is an important contributor to the refractive state. Most data in the literature report anterior corneal radius for chicks of 2-weeks (see Figure 6.1) (Gottlieb et al. 1987; Troilo et al. 1987; Wallman and Adams 1987; Troilo and Wallman 1991; Li et al. 2000; Guggenheim et al. 2002; García de la Cera et al. 2007) and 4-weeks of age (Gottlieb et al. 1987; Troilo et al. 1987; Wallman and Adams 1987; Troilo and Wallman 1991; Guggenheim et al. 2002). Fewer studies report data for 1-week old chicks (Wallman and Adams 1987; Choh and Sivak 2005). Irving et al. (Irving et al. 1996) and Schaeffel & Wallman (Schaeffel and Howland 1988) proposed empirical equations for the change of the anterior corneal radius, although not all reported data in the literature match those equations. Irving et al's data differ the most from other studies, as they report that corneal radius of curvature is constant for the first four days and then increases linearly at rate of 0.05mm/day. However, the behavior is probably not well described by a linear fit. In general, the values reported by Irving et al are higher than other data in the literature, especially for older chicks (see Table 6.1). On the other hand, Schaeffel & Howland (1988) model fits accurately the data from most studies, especially in the second week of age (9-16 days in the data from our own lab) and agree with our data in that period, but diverge from several of the reported data in the first week of age (Wallman and Adams 1987; Choh and Sivak 2005).

While most studies only report corneal radius of curvature, there is evidence that the chick cornea may be an aspheric surface. Corneal asphericity on the pupillary area (Schaeffel and Howland 1987) may have a role in the total spherical aberration of the chick eye. We incorporated corneal asphericity in the model, based on Schaeffel & Howland (Schaeffel and Howland 1987) measurements on corneal radius of curvature at two different corneal areas: corneal center and 1.7 mm off-axis, on two 42-days old chicks. However, the results reported in this study on two different

chicks are not conclusive. One chick showed no change of radius of curvature from the center to the periphery, while the other showed a radius of 3.95 mm at the corneal center and 4.08 mm off-axis. Using the definition of a conic surface (Atchison and Smith 2000), these values are consistent with an asphericity of -1.12, which would yield a negative corneal spherical aberration in the cornea (opposite to the human cornea, which is flatter in the center than in the periphery, with an average asphericity of -0.26 , and generally positive spherical aberration) (Atchison and Smith 2000). As we will discuss later, this hyperboloid corneal shape does not appear to be consistent with the measured spherical aberration and plausible structure of the crystalline lens, at least in the range period of 0-14 day-old chicks, and therefore other values of asphericity will be also tested.

Corneal radii have been reported in ametropic chick eyes. High levels of hyperopia are associated with corneal flattening (Irving et al. 1992) and form-deprived myopic eyes with steeper corneas (Gottlieb et al. 1987). In our model we have considered myopic eyes with (1) a simple

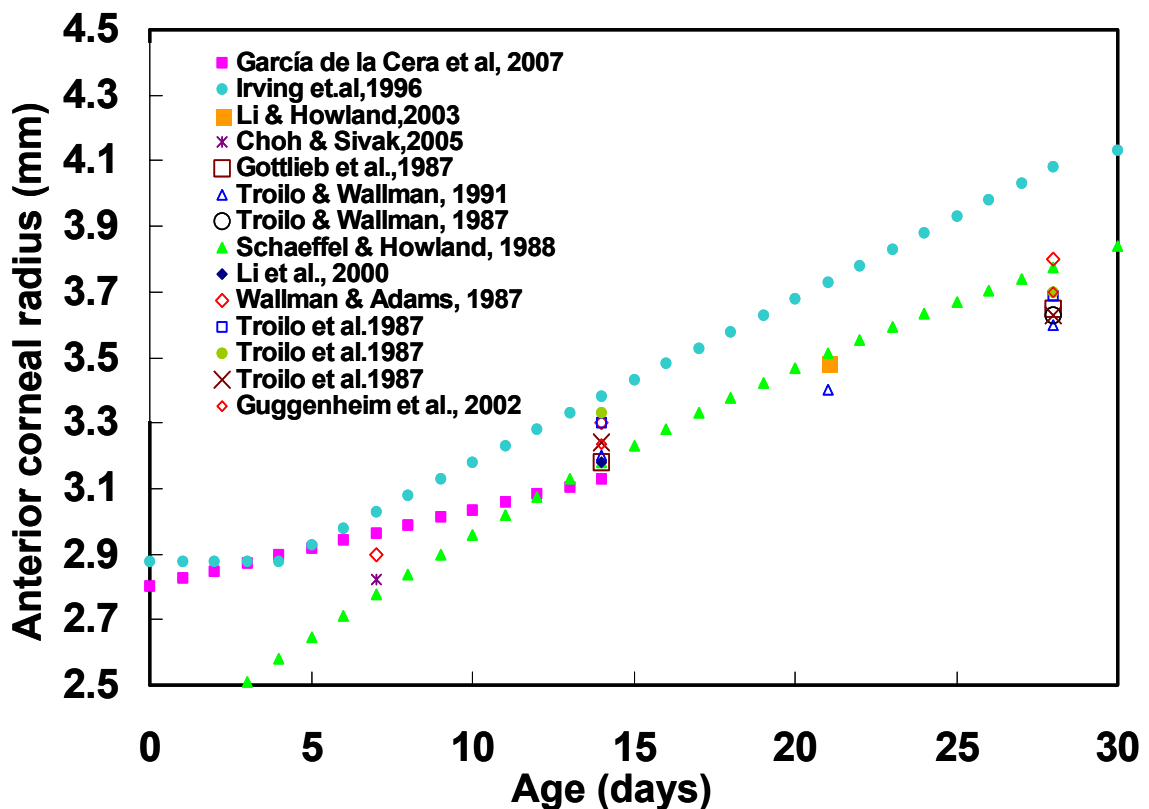


Figure 6.1 Anterior corneal radius reported values from several authors.

elongation of the posterior chamber (2) other ocular changes reported in myopic eyes (Gottlieb et al. 1987; Schaeffel and Howland 1988; Irving et al. 1992).

6.2.1.2. Corneal thickness

Irving et al. (Irving et al. 1996) proposed a constant corneal thickness over the first 14 days of life. On the other hand, Montiani-Ferreira et al. (Montiani-Ferreira et al. 2004) measured variations in the central corneal thickness due to maturation of corneal endothelial cell function until 70 days of age (0.247 mm), when corneal maturity is reached. This study reports a decrease of the central corneal thickness from hatching (0.242 mm) until 12 days of age, when a minimum value was measured (0.238 mm), and then it gradually increased. This trend has also been reported in dogs (Montiani-Ferreira et al. 2003) and human (Portellinha and Belfort 1991). Schaeffel (Schaeffel and Howland 1988) reported similar corneal thickness in 30-day old chicks (0.24 mm) and Hayes et al (Hayes et al. 1986) reported 0.26 mm,

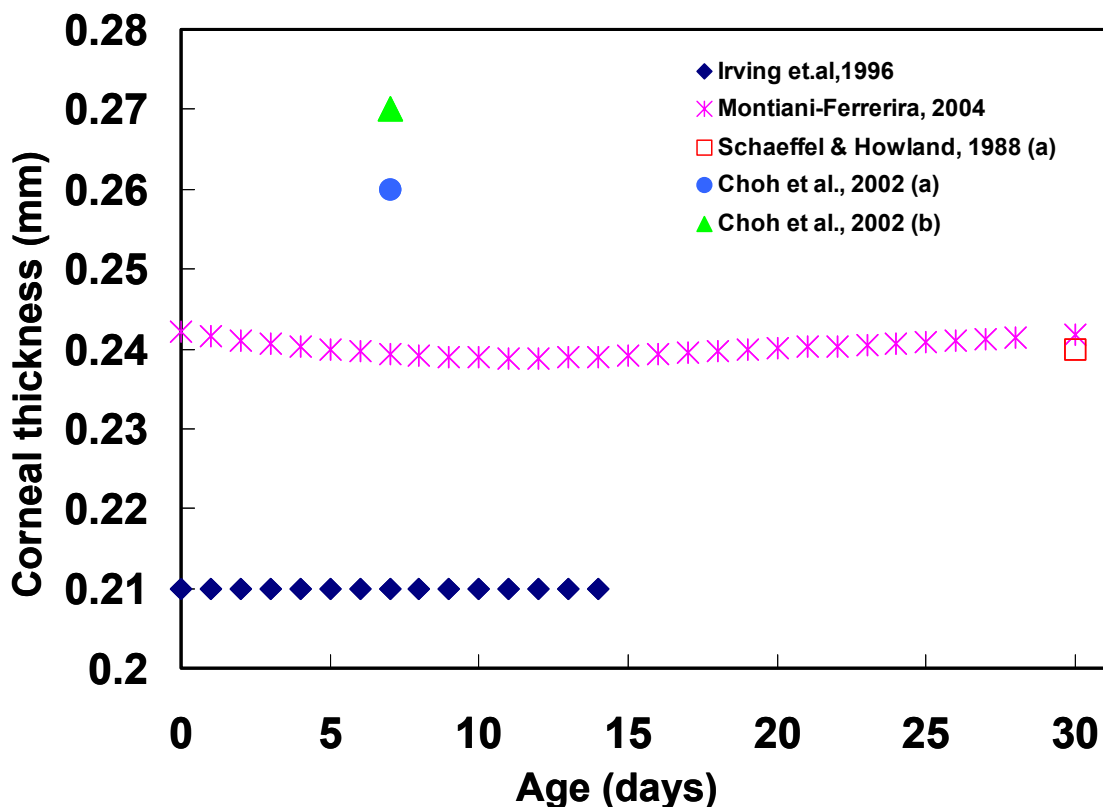


Figure 6.2 Corneal thickness from several authors.

on average for 22 to 55 days old chicks. Choh et. al 2002 (Choh et al. 2002) reported slightly higher values than other studies (0.26 -0.27 mm) in 7-day old chicks. We used the expression proposed by Montiani-Ferreira et al. (Montiani-Ferreira et al. 2004) for the change of corneal thickness with age in the range of ages of our study. Figure 6.2 shows central corneal thickness from several studies and Irving and Howland prediction models.

6.2.1.3. *Posterior corneal radius*

Posterior corneal surface measurements are technically more challenging than the anterior corneal ones, and to our knowledge, only two studies have attempted the estimation of the posterior corneal radius in chicks from refractive index and power measurements in ex vivo corneas. Choh & Sivak (Choh and Sivak 2005) estimated posterior corneal radius of 2.53 mm for 7-day old chicks (lower than anterior corneal radius, 2.82 mm) from Schaeffel & Howland anterior radius predictions (Schaeffel and Howland 1988). Schaeffel & Howland (1988) used the same corneal radius for the anterior and posterior surface (3.84 mm) in their 30-day old chick schematic eye model.

In human there is a correlation between anterior and posterior corneal radius, with the posterior radius of curvature 0.81 times the anterior radius (Atchison and Smith 2000). Since longitudinal data of posterior corneal radius are not available, we assumed similar values and change rate for the anterior and posterior corneal radii, as previously done by Schaeffel & Howland (1988). We tested that slight variations of the corneal posterior surface do not produce significant changes in the total defocus and aberrations of the eye.

6.2.1.4. *Corneal index of refraction*

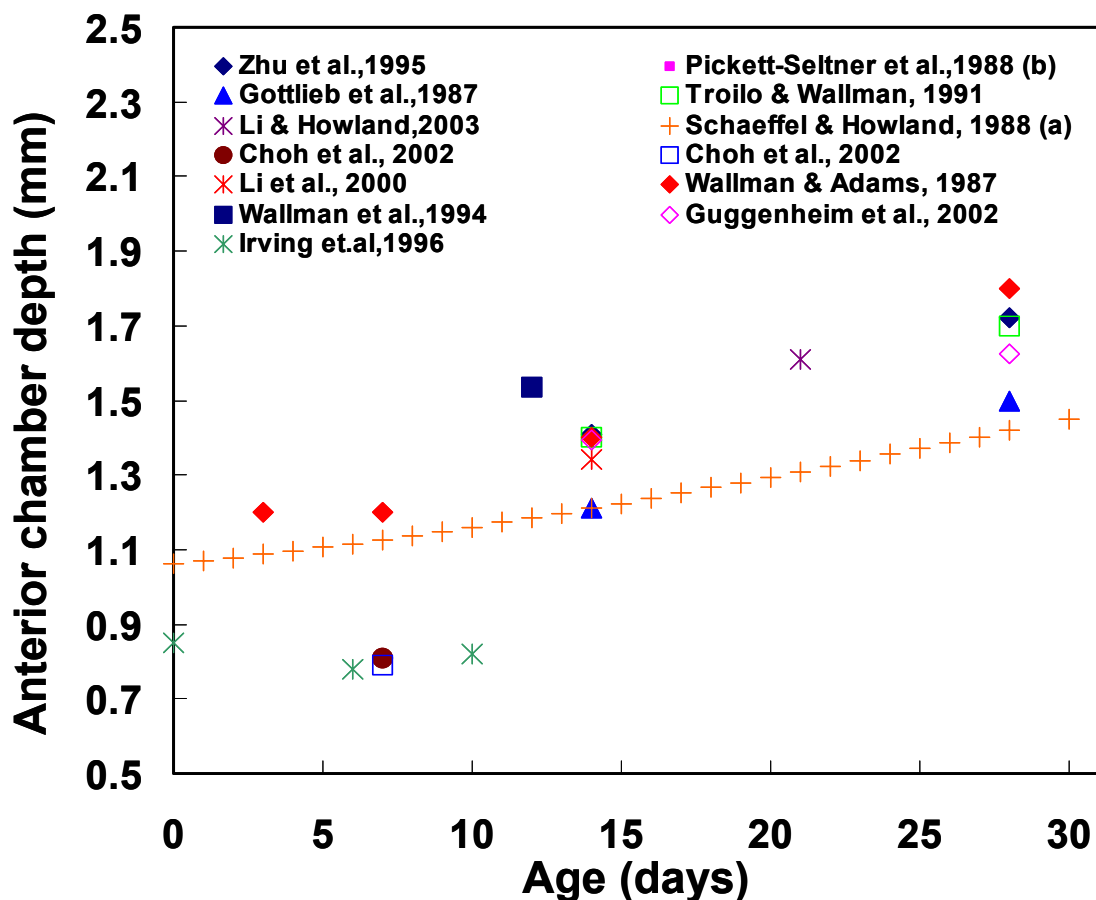
Sivak & Mandelman, 1982 proposed a corneal refractive index of 1.369 and Choh & Sivak (Choh and Sivak 2005) an index of 1.373, similar

than reported by Schaeffel & Howland (1988). These are average data, as the cornea is actually a multilayer structure (Barbero 2006). We used the more recent value from Choh & Sivak (2005). The index of refraction of the chick cornea appears to be lower than the mean index of refraction of the human cornea, 1.376 (Atchison and Smith 2000).

6.2.1.5. Anterior chamber depth

In humans and primates, anterior chamber depth increases during the first years of development (until two years of age in infants, (Curtin 1985) and until at least 1 year in marmosets (Troilo and Judge 1993).

The anterior chamber depth in chicks has been widely reported in the literature (and results are summarized in Figure 6.3). Irving et al. (Irving et al. 1996) showed lower anterior chamber depth values than most authors (although they showed higher axial lengths). Troilo & Wallman's data on 7-



day old chicks appear also above average. We used an empirical expression for the change of anterior chamber depth with age obtained from average results (Schaeffel and Howland 1988). The aqueous index of refraction was measured in vitro by Schaeffel and Howland (1988) by an Abbe refractometer, and it is similar than vitreous chamber $n=1.335$ (Schaeffel and Howland 1988)

Form deprived eyes have deeper anterior chamber depths relative to normal eyes and this increase has been reported to be proportional to total axial length (Gottlieb et al. 1987).

6.2.1.6. *Anterior lens radius*

Lens parameters are not easily accessible, as phakometry techniques used in humans (Mutti et al. 1992; Rosales and Marcos 2006; Rosales and Marcos 2007) do not appear to have been much used in the chick, they have been used however in other animal models such as Rhesus Monkeys. Changes in crystalline lens radii of curvature and lens tilt and decentration during dynamic accommodation in Rhesus Monkeys (Rosales et al. 2008). Other optical properties of the lens, such as a possible gradient refractive index have little been addressed in vitro, and never been measured in vivo. Some studies suggest no or little changes in focal length of the chick crystalline lens (Pickett-Seltner et al. 1988; Sivak et al. 1989) with development, and also with treatments. These authors argue that lens is a “genetically preprogrammed feature” and not easily influenced by environment. However, other authors found changes in lens size and shape from frozen sections, and most models in the literature assume crystalline lens radius of curvature that increase linearly with age, at various rates ranging from 0.11 mm/day from Irving et al. (Irving et al. 1996) to 0.04 mm/day Schaeffel & Wallman (Schaeffel and Howland 1988). Figure 6.4 shows a plot of the anterior lens radius as a function of age from several studies. In the human eye, the lens surfaces have been described using conical surfaces (Dubbelman and Van der Heijde 2004). No data on the asphericity of the chick lens surfaces has been reported.

Several studies have measured the spherical aberration of isolated chick lenses. In lenses from hatchling chicks, spherical aberration varied non-monotonically between positive and negative, with an overall negative spherical aberration predominating (Choh et al. 2002). A study by (Sivak et al. 1989) showed that lens spherical aberration does not increase with development. It should be noted that typically, laser ray tracing techniques used on isolated lenses deliver parallel rays of light (and do not mimic the physiological condition), and therefore the measured spherical aberration cannot be directly compared to that of the cornea. Also, the state of accommodation of isolated human lenses is not necessarily relaxed.

Several studies (Hayes et al. 1986; Pickettseltner et al. 1987) report that there is no change in the chick lens morphology (size, shape, soluble protein content, focal length and transmittance) after induction of myopia.

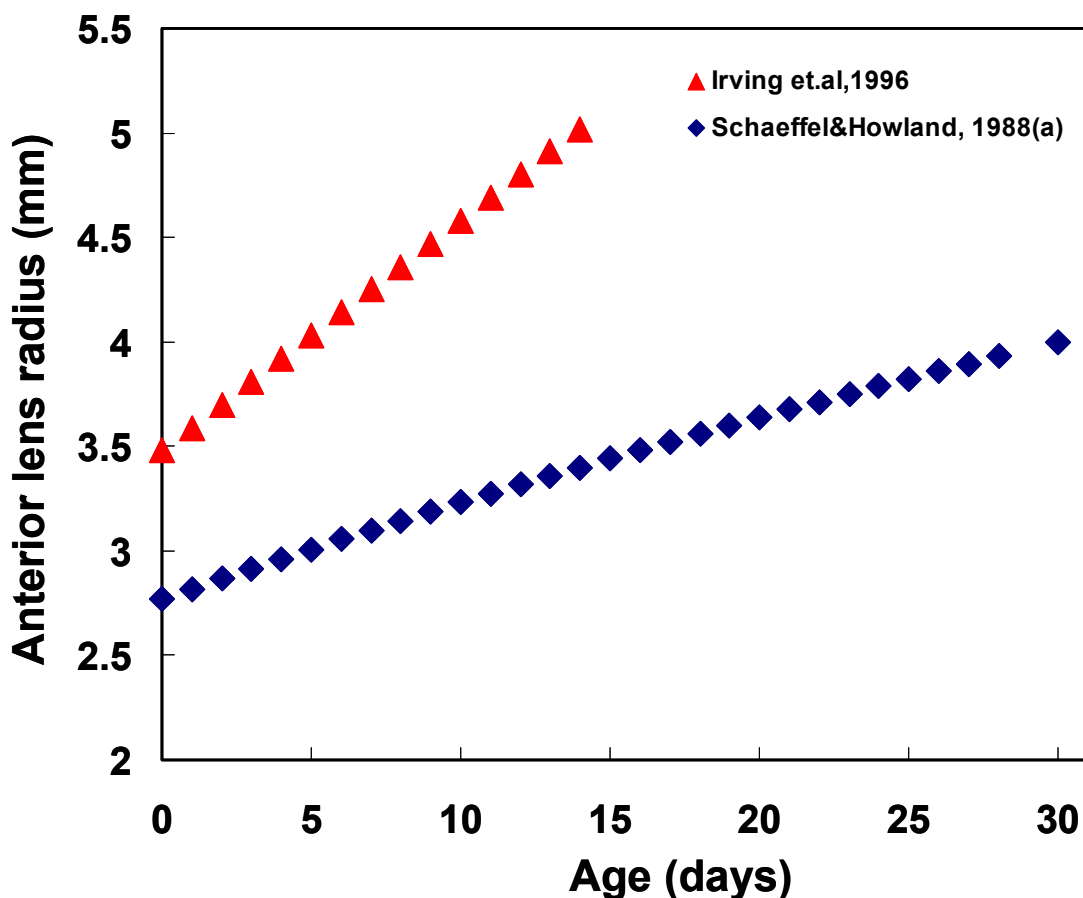


Figure 6.4 Anterior lens radius reported values from several authors.

6.2.1.7. Lens thickness

Figure 6.5 compares measurements of lens thickness as a function age from various studies. Most data, except for those by Irving et al. (Irving et al. 1992) are within close agreement. Lens thickness seems to increase slightly during development. Data from younger chicks appear more variable. The model proposed by Schaeffel and Howland (Schaeffel and Howland 1988) appears to fit most data and was used in our model.

Also, lens thickness in the chick seems to be similar in normal and ametropic eyes. Irving et al. (Irving et al. 1992) observed no differences in lens thickness between control and goggled eyes in myopic or hyperopic chicks induced by goggles from -20 D to +30 D. Gottlieb et al reported the same effect in visually deprived chicks (Gottlieb et al. 1987).

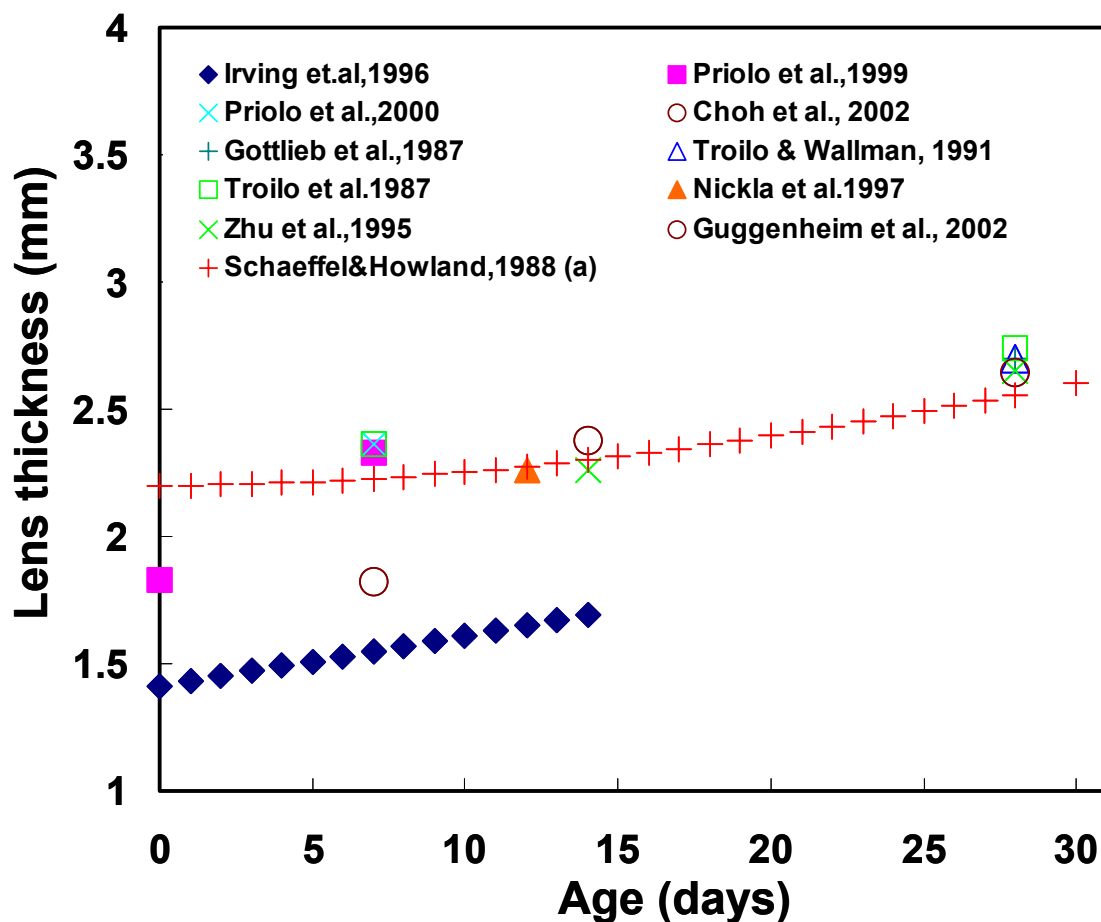


Figure 6.5 Lens thickness reported values from several authors.

6.2.1.8. Lens index refraction of refraction

Very little is known about the refractive index of the lens. Analysis of fiber cell growth in the developing chicken lens (Bassnett and Winzenburger 2003), has led to suggest that the chick lens exhibits a gradient index profile due to the higher concentration of cytoplasmic protein in cells in the center of the lens, and this is likely to change with age, although studies on the potential gradient index profile in the chick lens have never been presented. The Abbe refractometer technique (Sivak and Mandelman 1982), useful for other optical structures index measurements, is not for the complex index gradient from squeezed lens. For an adult chick lens Sivak & Mandelman,1982 (Sivak and Mandelman 1982), estimated an index of 1.3738 in the lens periphery and 1.3947 in the lens core. Schaeffel & Howland assumed an equivalent refractive index of 1.455 to match the observed refractive state. In humans the reported equivalent refractive index of the unaccommodated eye is 1.42 (Atchison and Smith 2000) . We have implemented in our computer chick model both a crystalline lens with a constant refractive index and a parabolic index profile, monotonically decreasing from the center to the periphery according the values reported by Sivak and Mandelmann.

Priolo et al. (Priolo et al. 2000) attributed to changes in the refractive index distribution the differences in the focal length observed in the lens between form-deprived myopic chicks and normal eyes, while the lens shapes appeared unchanged. However, Pickett-Seltner et al. (Pickettseltner et al. 1987) did not observe changes in the lens focal length, light transmittance or protein content in myopic chick eyes with respect to normal eyes.

Index refractive values of all eye components were maintained constant for this period of time. The refractive index of the lens has been described as a gradient function. We used a spherical gradient profile, with spherical symmetry given by equation:

$$n(r) = n_0 \alpha(r-R) + \beta (r-R)^2 \text{ (eq. 6.1)}$$

where R is the half of the lens thickness and α , β are fitting variables (that are varied to match experimental values of spherical aberration). Parabolic gradient index lens functions have been extensively used in human (Blaker 1980); (Nakao et al. 1963) rabbit (Nakao et al. 1968) or cat (Jagger 1990), although higher order quadratic functions have been proposed in the human (Pierscionek and Chan 1989) or fish (Garner et al. 2001). For a review see (Smith 2003).

In our model, we assumed changes with age in the gradient refractive index of the lens, particularly an increase in the index of the periphery, while the core index remains constant, which seems to be anatomically plausible.

6.2.1.9. Posterior lens radius

Measurements of the posterior lens radius of curvature are scarce. The increase of posterior radius with age suggested by (Irving et al. 1996), from 1.97 mm (day 0) to 2.69 mm (day 14) seems higher than the data by

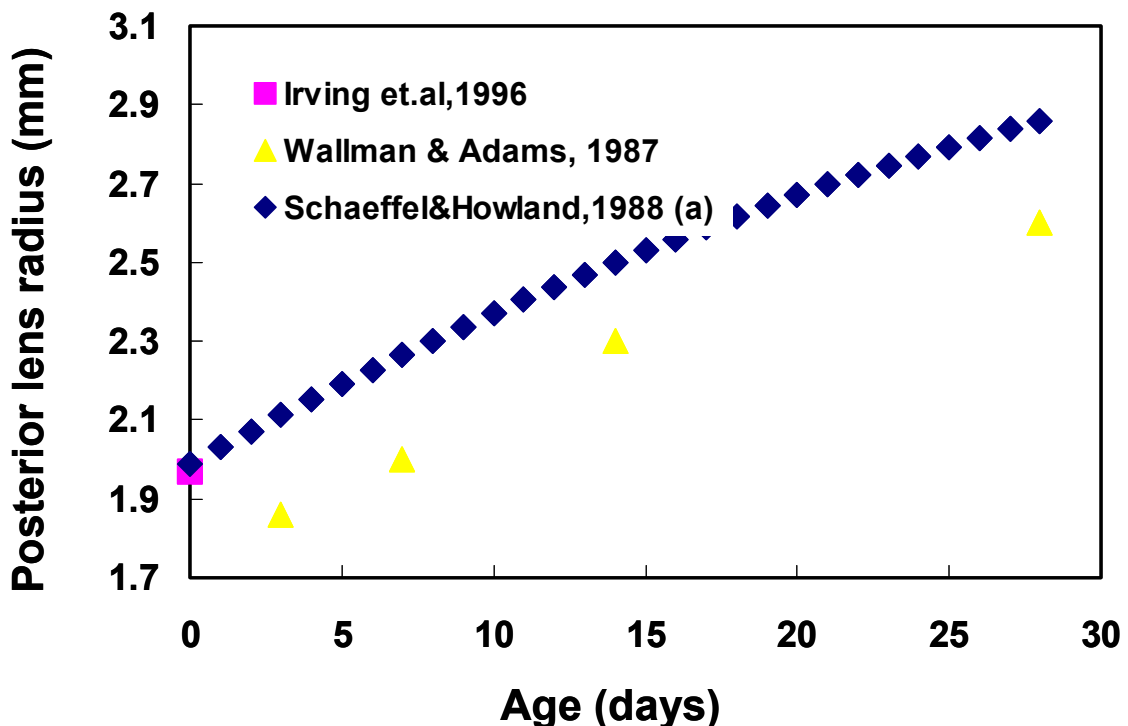


Figure 6.6 Posterior lens radius reported values from several authors.

Wallman & Adams 1987 (Wallman and Adams 1987) or the data used by Schaeffel and Howland, 1988 (Schaeffel and Howland 1988) in their model. Figure 6.6 shows posterior lens radius of curvature from different authors. We choose the values from (Schaeffel and Howland 1988) in our model.

6.2.1.10. Posterior chamber & axial length

Figure 6.7 shows axial length from different studies, including data reported in Chapter 3 of this thesis (which were used in the chick eye computer model) (Gottlieb et al. 1987; Pickettseltner et al. 1987; Pickett-Seltner et al. 1988; Schaeffel et al. 1988; Schaeffel and Howland 1988; Zhu et al. 1995; Irving et al. 1996; Guggenheim et al. 2002; Choh and Sivak 2005; García de la Cera et al. 2006; García de la Cera et al. 2007) . Data are very close although, differences seem to be higher for older chicks. The axial length data measured in this thesis (Chapter 3) agree well with those found in the literature during the first two weeks of age, although these

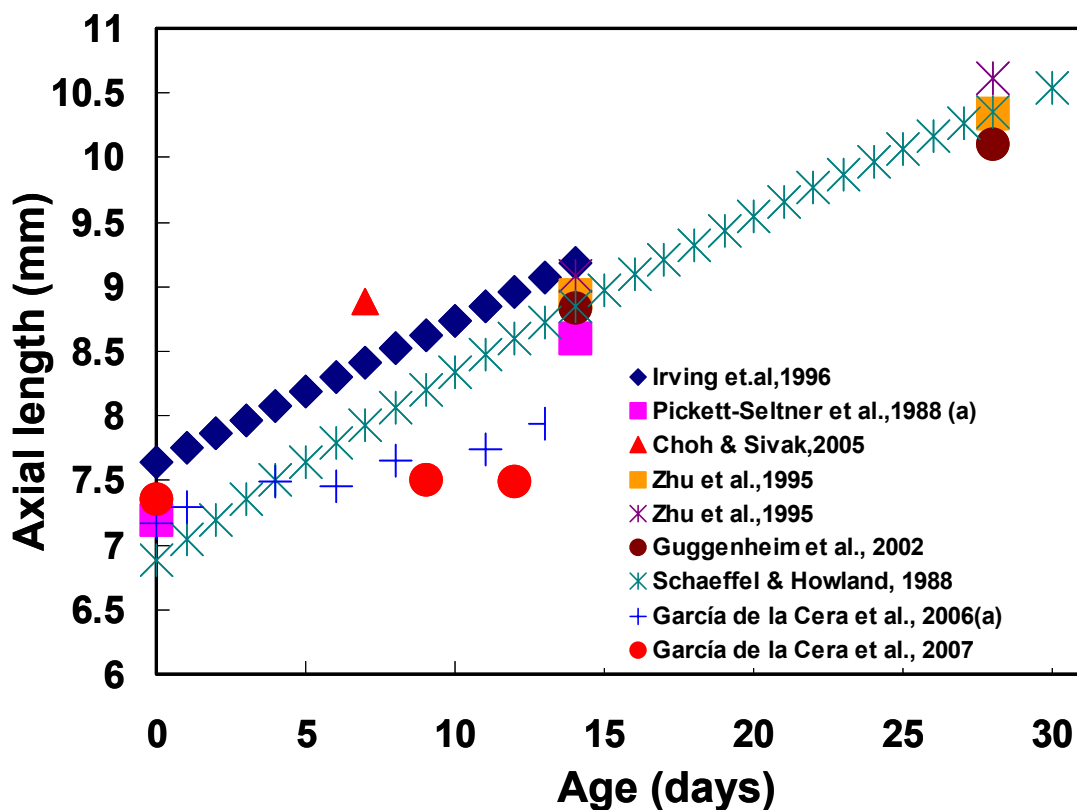


Figure 6.7 Axial length reported values from several authors.

measurements could not be extrapolated with in older chicks. We used data from the lineal regression from our experimental values explained in Chapter 3 for the change in axial length with age.

Posterior chamber depth was estimated as the difference of axial length minus corneal thickness, anterior chamber depth and lens thickness, no constant with age.

To model myopic chick eyes, we used the linear regression of axial length (and posterior chamber depth) of form-deprived eyes to data of Figure 3.2 (A) in Chapter 3. This parameter represents the major difference between the normal and myopic chick eye (Wallman and Adams 1987; Schaeffel and Howland 1991; Kee et al. 2001; Winawer and Wallman 2002).

To our knowledge the only data reported for vitreous chamber refractive index is that of (Sivak and Mandelman 1982), Sivak & Mandelmann (n= 1.3352).

6.2.2. A compilation of mice biometric data

Biometric data have been compiled from various sources. Despite the interest in the mouse as an experimental model of myopia and ocular disease, data are not so extensive as in the chick eye. Data compiled from the different studies are shown in Table 6.2. As in the chick model, we have tested this data in a computer model eye, which has been then used to simulate refractive state and the optical aberrations measured with a Hartmann-Shack aberrometer in a 4 week-year old wild type mice (García de la Cera et al. 2006) (experimental data presented in Chapter 5).

Corneal thickness, anterior chamber depth, lens thickens and posterior chamber depth change with age. The longitudinal changes of these parameters are reported by Schmucker & Schaeffel (Schmucker and Schaeffel 2004) that report a linear increase with age, and we used these expressions for 4-weeks of age.

Schmucker & Schaeffel reported *in vivo* measurements of the anterior corneal radius with a photokeratometric technique and also *ex vivo* measurements from frozen sections. More recent biometric data were obtained by Schmucker & Schaeffel (Schmucker and Schaeffel 2004) using Optical Low Coherence Interferometry) and we used those in our model. There is also some evidences that the mouse cornea may be an aspheric surface (Remtulla and Hallett 1985; Schmucker and Schaeffel 2004).

The lens in the mouse has a higher optical relevance than in other species, as it accounts 56% of the optical pathway in the eye. Radii of the lens were reported by Schmucker & Schaeffel, 2004 (Schmucker and Schaeffel 2004) calculated from photography of frozen sections. The lens was considered as a gradient index structure, spherical model, which follows the expression (eq 6.1).

Schmucker & Schaeffel (Schmucker and Schaeffel 2004) estimated an equivalent refractive index which increases with age. Retmulla & Hallett (Remtulla and Hallett 1985) reported similar value that Schmucker & Schaeffel predictions for adult mice.

Axial length measurements with conventional methods such as A-scan ultrasonography are challenging due to small ocular dimensions. Measurement errors have been reported to be of the same order or greater than axial differences resulting from treatments to induce myopia. Much higher accuracy and reproducibility has been achieved using optical low coherence interferometry. Reported axial length at birth in mice is 1.32 mm of axial length, and achieves 90 % of the total size at 100 days (Schmucker and Schaeffel 2004) (3.15 mm at 4-weeks).

Ocular parameter	Reference	Total number of eyes	Age range (days)	Experimental condition	Technic used	Data measured
Anterior Cornea radius	Schmucker & Schaeffel, 2004	11	35,58,75	anesthetized	Photokeratometry	1,49194 (4 week) *
	Schmucker & Schaeffel, 2004		22-100	ex vivo	Photography from frozen	1,41194 (4 week)
Corneal thickness	Schuliz (2003)	8	4 months	in vivo	OLCR (Optical low coherence reflectometry)	0,106mm (4 month)
	Schmucker & Schaeffel, 2004		4week		OLCI (Optical low coherence reflectometry)	0,085 (4 week)*
	Schmucker & Schaeffel, 2004		4week		Photography from frozen	0,06 (4 week)
	Jester, 2001	8	Adult	in vivo	Confocal microscopy	0,1129 (adult)
	Schmucker & Schaeffel, 2004	3	22-100	ex vivo	Photography from frozen	0,0635 (4 week)
Posterior corneal radius	Schmucker & Schaeffel, 2004		22-100	ex vivo	Photography from frozen	1,4084 (4 week)*
n corneal	Retmulla & Hallet, 1985		20-23 weeks	ex vivo	refractometry / interferometry	1,4015 (4 week)*
Anterior chamber	Schmucker & Schaeffel, 2004		4week		OLCI	0,42 (4 week)*
	Schmucker & Schaeffel, 2004		4week		Photography from frozen	0,266 (4 week)
	Schmucker & Schaeffel, 2004	3	22-100	ex vivo	Photography from frozen	0,2012 (4 week)
n aqueous	Retmulla & Hallet, 1985		20-23 weeks	ex vivo	refractometry / interferometry	1,3336 (Adult)*
Anterior radius lens	Schmucker & Schaeffel, 2004	3	22-100	ex vivo	Photography from frozen	0,9993 (4 week)*
Lens thickness	Schmucker & Schaeffel, 2004	3	22-100	ex vivo	Photography from frozen	1,7729 (4 week)*
n lens	Schmucker & Schaeffel, 2004					1,433 (eff)
	Retmulla & Hallet, 1985		20-23 weeks	ex vivo	refractometry / interferometry	1,659 (eff)
Posterior radius lens	Schmucker & Schaeffel, 2004	3	22-100	ex vivo	Photography from frozen	1,0549 (4 week)*
n post chamb	Retmulla & Hallet, 1985		20-23 weeks	ex vivo	refractometry / interferometry	1,3329 (Adult)*
Axial length	Schmucker & Schaeffel, 2004		4week		OLCI	3,15 (4 week)*
	Schmucker & Schaeffel, 2004		4week		Photography from frozen	3,02 (4 week)
	Schmucker & Schaeffel, 2004	3	22-100	ex vivo	Photography from frozen	2,9031 (4 week)
	Tejedor & de la Villa, 2003	18	30	ex vivo	Photography from frozen	3,264 (30 day)

Table 6.2. A compilation of mice biometric data used in this work. Empty cells are data no indicated by authors.

6.3. Methods

6.3.1. Computer model for the chick eye

Computer eye models were designed in Zemax (Optima Research, Tucson, AZ), using the geometrical parameters and index of refraction of Table 6.3.

Aberrations were simulated using ray tracing in Zemax (using 150 rays across the pupil, for circular 1.5 mm-diameter pupils, and the Zernike coefficients compared to those measured experimentally. Since all surfaces were modeled as rotationally symmetric, only defocus and spherical aberration will be evaluated.

Author	Eye parameter	Age (days)		
		0	7	14
	Corneal radius (mm)	2.6670	2.7800	3.1850
Montiani-Ferrerira (2004)	Corneal thickness (mm)	0.2421	0.2394	0.2390
Choh & Sivak (2005)	n corneal	1.3730		
Schaeffel & Howland (1988,a)	Anterior Chamber Depth (mm)	1.0617	1.1266	1.2105
	n anterior chamber	1.3350		
	Anterior lens radius (mm)	2.7695	3.1000	3.4003
	Lens thickness (mm)	2.2007	2.2269	2.3000
	Posterior lens radius (mm)	1.9876	2.2651	2.5000
	n Lens periphery	1.3710	1.3722	1.3786
Sivak & Mandelmann (1982)	n Lens core	1.3947	1.3947	1.3947
	n posterior chamber	1.3352		
	Posterior chamber depth (mm)	3.6690	3.9700	5.0320

Table 6.3 Data used in chick model for days 0,7 & 14

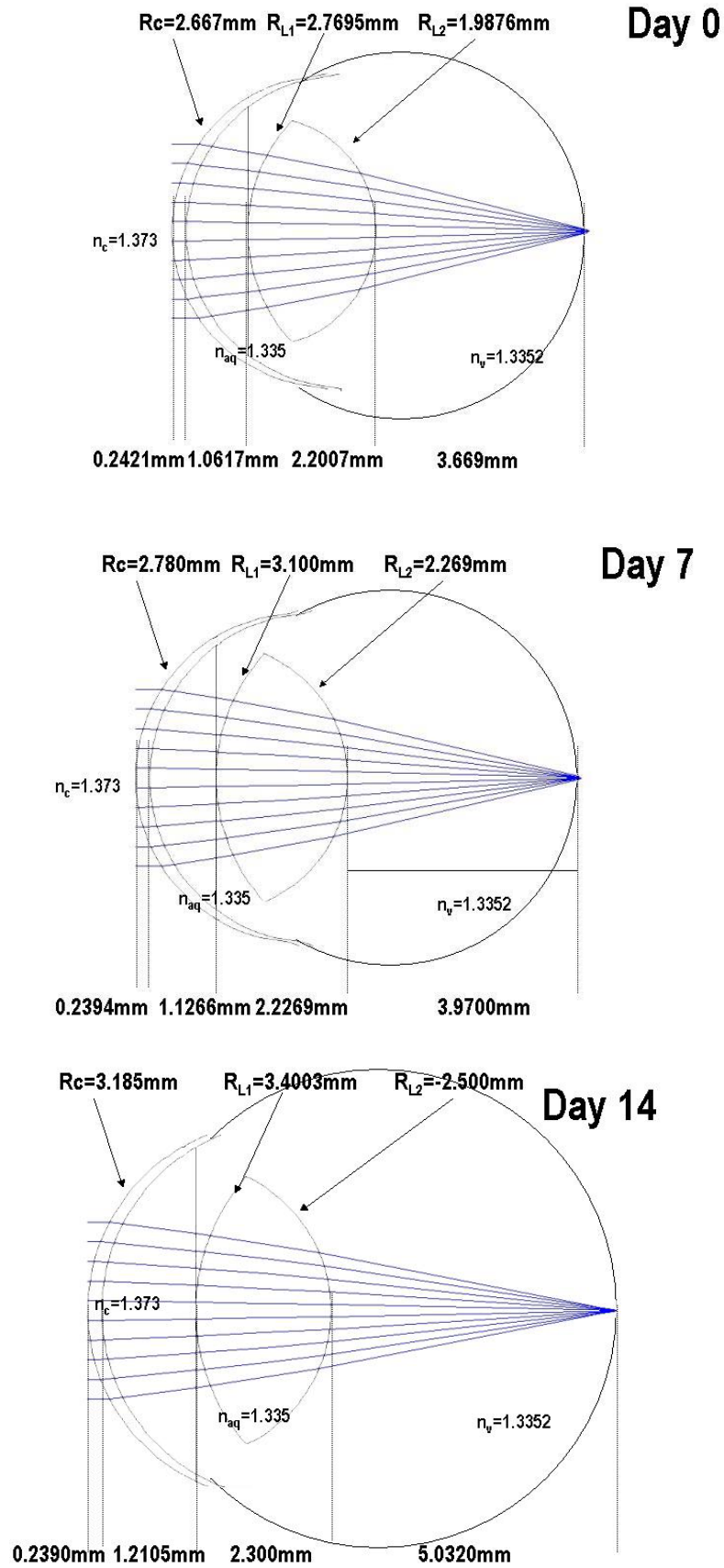


Figure 6.8 Schematic diagrams of chick eye models for days 0,7 and 14

Simulations were performed for three days during the measurement period of the experiments of Chapter 3 (0, 7 and 14days), for both normal eyes and myopia-developing eyes. Some parameters (refractive index of the cornea and humors) were kept constant with time and refractive error. Other parameters (corneal and lens radius, anterior and posterior chamber depth, lens thickness and index refractive lens) were allowed to vary with time according to the patterns described in the literature (and explained in detail in Section 6.2.1., while distribution of the index refractive lens was allowed to vary to optimize the match between simulated and measured aberrations. Simulation diagrams of chick eye for 0, 7 and 14days are in Figure 6.8.

The best fits of the model, obtained with the parameters shown in yellow circle symbols in Figures 6.1-6.7., will be shown in graphical form as a function of age in comparison with linear fits of the experimental values of defocus and spherical aberration from Chapter 3.

6.3.2. Computer model for the mouse eye

Using similar procedures as those described for the chick eye, we simulated the mouse model eye in Zemax, and the spherical error and spherical

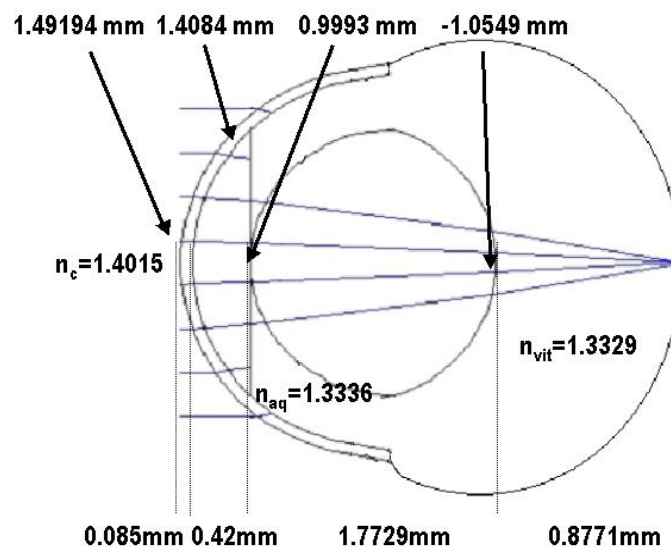


Figure 6.9 4-week old mouse schematic eye. Axial dimensions, radii and refractive indices are shown.

aberration were simulated using ray tracing. Figure 6.9 shows the mouse schematic eye (wild-type, 4-week old). The only variable in this model was the lens refractive index distribution.

6.4. Results

6.4.1. Chick eye model

Figure 6.10 shows simulated defocus (from Z_{20} Zernike term) for days 0, 7 and 14 and a linear regression to the retinoscopy experimental data of Chapter 3 for emmetropic eye (A) and axial elongated myopic eye (B).

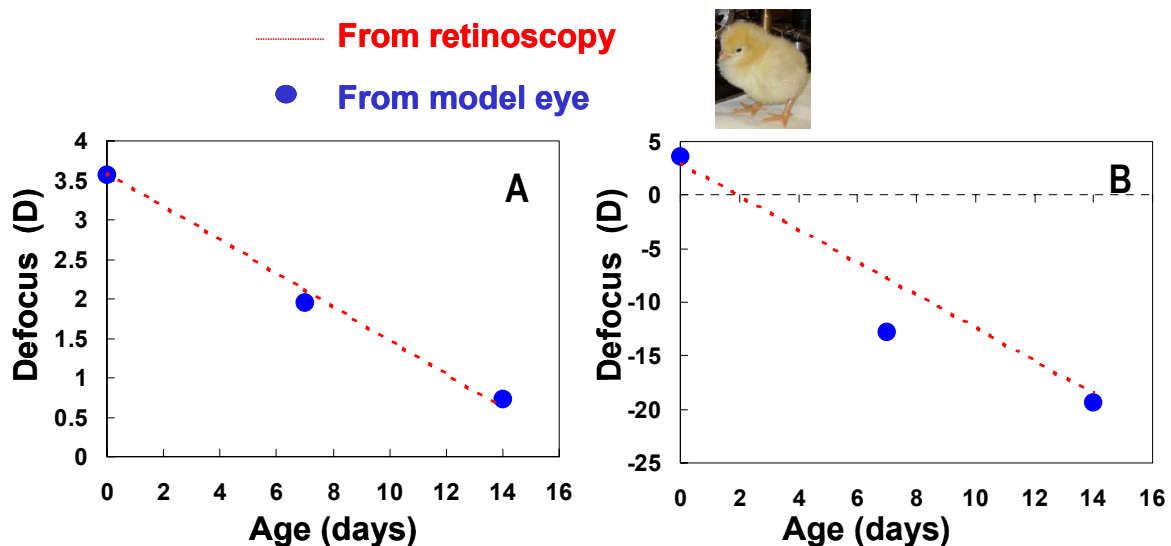


Figure 6.10 Longitudinal values of defocus obtained from Z_{20} Zernike coefficients from retinoscopy (see Chapter 3) and computer eye model for the chick eye: (A) Emmetropic eye (B) Myopic eye where only axial elongation has been modified.

Figure 6.11 shows simulated spherical aberration (from Z_{40}) for days 0, 7 and 14 and a linear regression to the Hartmann-Shack experimental spherical aberration of Chapter 3 for emmetropic eye (A) and axial elongated myopic eye (B).

We have found that the model predicts accurately the amounts of refractive error, and the rate of change of refractive error in normal and form-deprived chick eyes. Most interestingly, the model is able to predict the

decrease of spherical aberration with age in normal eyes, and the increase of spherical aberration in emmetropic eyes. While the trends are well reproduced, the model fails at reproducing the exact amounts of spherical aberration (although it should be noted that in all cases the values are very small, and trends seem more important than the actual amount).

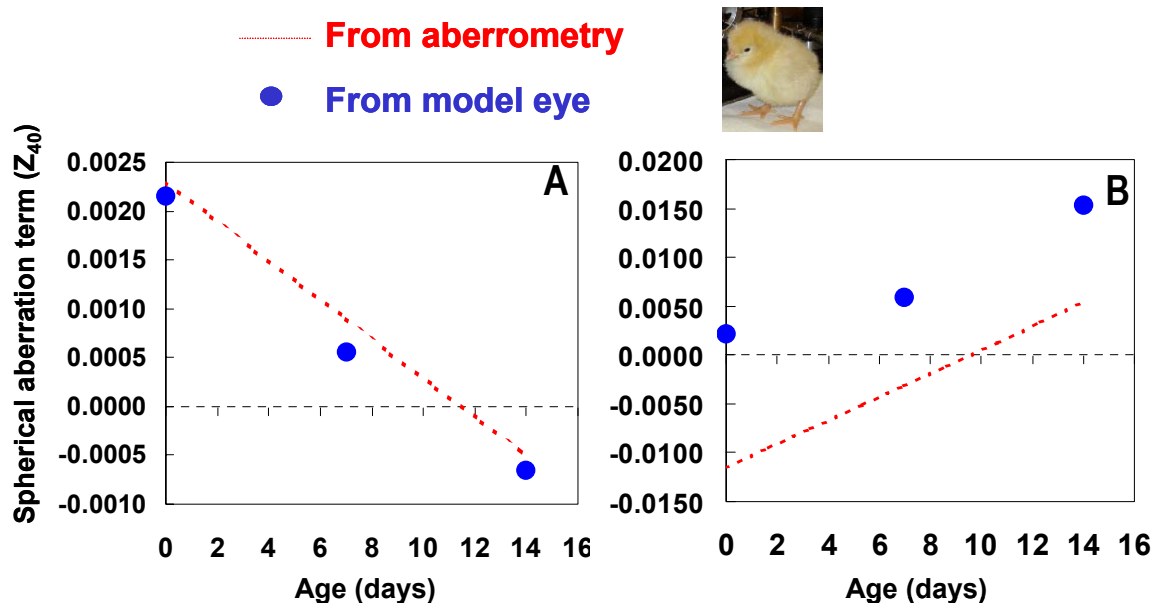


Figure 6.11 Spherical aberration term (Z_{40} Zernike coefficient) from aberrometry (see Chapter 3) and computer eye model for the chick eye: (A) Emmetropic eye (B) Myopic eye where only axial elongation has been modified.

We found that the best fits (simultaneously for defocus and spherical aberration) and trends were obtained when the only different parameter between emmetropic and myopic chick eyes is axial length. The use of steeper corneal radii of curvature in myopic chicks (Gottlieb et al. 1987; Schaeffel and Howland 1988; Irving et al. 1992) resulted in excessive myopia (for the axial lengths under consideration), and larger amounts of spherical aberration than those observed experimentally. The same effect has an increase of the anterior chamber depth.

Also, we found that the best simultaneous fits were obtained using a gradient index profile for the lens. When a homogeneous lens refractive index is kept constant with increasing age (for example, the effective index reported by Schaeffel & Howland (1988) 1.455), refractive error tends toward hyperopia in

the normal eye from -3.351 microns in day 0 to -8.6 microns in day 14, and the ocular spherical aberration tends toward more negative values (from $Z_{40} = +1.17$ microns to $Z_{40} = -0.08$ microns). To account for the measured changes in defocus, the effective index of the lens each should increase with age from 1.467 to 1.518 between day 0 and 14. In this chick model with a homogeneous lens the spherical aberration in the normal eye decreased from 1.17 microns (3.6 D) to 0.034 microns (0.5 D). In myopic eyes when effective index (1.455) is constant with age the experimental rate of increase of myopia is not well reproduced, and the spherical aberration decreases.

The gradient index distribution that best reproduces the experimental data consists of a constant value in lens core (1.3947), and an age-dependent index in the periphery of the lens (day 0: 1.3710; day 7: 1.3722; day 14: 1.3786). This is also anatomically plausible, consistent with lens fibers growing from the center to the cortex

These results indicate that changes in the refractive lens are essential to account for fine tuning of axial length to optical power, and that a gradient index profile would account for the fine tuning of the spherical aberration and its disruption in myopia development.

In human eyes, the asphericity of the cornea, and presumably the asphericity of the lens plays a major role in determining the total spherical aberration of the eye (to the extent that newer generations of intraocular lenses are designed with aspherical surfaces so that they produce negative spherical aberration to compensate the spherical aberration of the cornea (Marcos et al. 2005). We modeled corneal asphericity, according to, to our knowledge, the only value reported in the literature on a single chick.

When the corneal asphericity reported by Schaeffel & Howland (1988) (-1.12) is considered, a larger hyperopic values and more negative spherical aberration is obtained. In general, we were not able to reproduce refractive and spherical aberration trends with aging and refractive error only adjusting surface asphericities.

In summary, the most plausible model, in accordance to most reported anatomical parameters and observations, differences in elongation can explain the differences in the change rate of both refraction and spherical aberration between normal and myopia-developing form-deprived eye. Other structural differences appear to have minor contribution. A gradient index model is needed to explain the low amounts of spherical aberration present (both the fine-tuning in emmetropic eyes and the slight increase with age in myopic eyes).

6.4.2. Mouse eye model

Defocus and spherical aberration have been simulated using Ray tracing in Zemax on the schematic model of Fig. 6.8. A comparison of a aberration map obtained from Zernike coefficients of the computer model and from aberrometry in a real mouse are plotted in Figure 6.12. The best fit to the experimental data of refraction and spherical aberration have been obtained using a spherical gradient index model in the crystalline lens, with $n=1.4295$ and 1.373 in the core and the periphery, and $\alpha=-0.12747476$, $\beta=-0.07190183$ in equation 6.1. With these data $Z_{20}=-0.82$ microns (average experimental $Z_{20}=-0.81$ microns –or $+2.48$ D- and $Z_{40}=0.14$ microns (average experimental $Z_{40}=0.1445$). For a homogeneous lens, we computed that for an effective index of 1.44465 , the defocus term is well reproduced ($Z_{20}=-0.8$ microns), but the simulated spherical aberration ($Z_{40}=5.2$ microns) is 5.06 microns, much higher than the experimental value.

As a centered, rotationally symmetric model has been assumed, and no attempt has been made to reproduce the relatively high amounts of coma found experimentally in Chapter 5. A further refinement of the model incorporates biconic surfaces (ellipse), where the radius is modified toward periphery, we found that a conic constant $k_x=-0.005$ reproduced the astigmatism data measured in 4-week old chicks ($Z_{2-2}=-0.12$ microns).

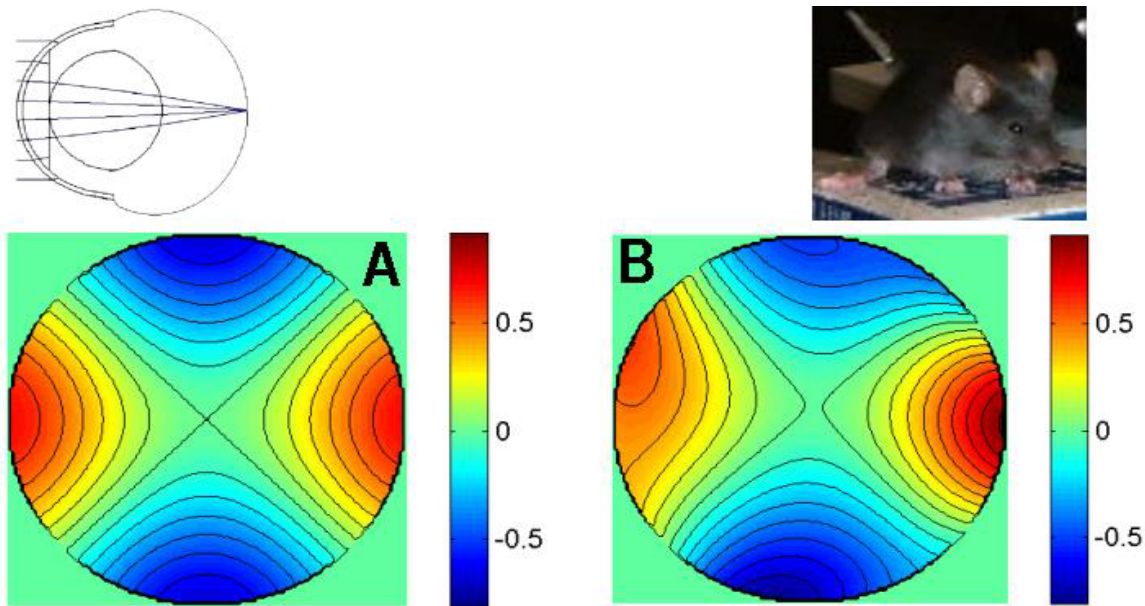


Figure 6.12 Aberration maps for a 4-week old mouse (A) Hartmann-Shack experimental measurement. (B) simulated by ray tracing on a model eye (with a biconic corneal surface).

6.5. Discussion

6.5.1. Chick eye model

We have shown that an eye model with geometrically consistent with the literature is able to reproduce: 1) the shift toward emetropia from 0-14 days in normal chick eyes, and the rate of myopia development in form-deprived eyes. 2) the decrease of spherical aberration from day 0, and relative low values of spherical aberration in both normal and form-deprived myopic chick eyes. 3) the slightly higher amounts of spherical aberration in myopic chick eyes. We found that the differences between emmetropic and myopic eyes are primarily explained by differences in the posterior chamber depth. We also found that a gradient index distribution in the crystalline lens (a simple parabolic model, consistent with measurements of the index of refraction at the lens core and surface) was necessary to explain the low amounts of spherical aberration found in chick eyes.

Previous computer eye models (with cornea and crystalline lens) aimed primarily at predictions of the refractive state. In most cases an effective index of refraction is used in the lens, rather than a gradient index distribution. A

model using an onion-like structure in the crystalline lens had been previously used to explain spherical aberration in a 30-day old chick eye, but accuracies higher than 0.5 D and explanation of longitudinal changes were not attempted (Schaeffel and Howland 1988).

Previous attempts to explain higher order aberrations, and particularly their relative change with development (i.e. increasing size of the globe) were based on very simple models, namely with only one surface and functional expressions for eye growth. Howland (Howland 2005) proposed that for a growing eye with an increase factor of k , the RMS for a constant pupil size, should decrease by a factor of $1/k^{n-1}$, with $n=3.9$ and k a 2nd order polynomial of age as reported by Mihashi et al 2004 (Mihashi et al. 2004). Despite its simplicity, this model is able to predict surprisingly well the general trend of our experimental data (decrease of high order aberrations for a constant pupil size), but it fails at reproducing the actual amounts of aberrations, and at capturing the differences between myopic and emmetropic eyes (i.e. the fact that axial elongation can be associated to larger amounts of spherical aberration).

While our model represents a significant sophistication over existing chick model eyes, the fact that the model is based on rotationally symmetric surfaces prevents it from reproducing the significant amounts of coma and other high order asymmetric aberrations found in the chick eye, which may arise from corneal irregularities and ocular surface misalignments. Also, as any other schematic model, it is only able to capture average trends and magnitudes, and not individual differences which were significant in experimentally measured aberrations.

6.5.2. Mouse eye model

We found that a model using reported biometric data and spherical gradient index model is able to capture the refractive state and amount of spherical aberration in a 4-week old wild type mouse. A gradient index distribution in the lens was necessary to account for the lower values of

spherical aberration (compared to a homogeneous lens), although the indices in the lens core and periphery were lower than those reported by Hughes (Hughes 1979) (1.5 and 1.39 respectively) in the adult rat, as these values resulted in high amounts of myopia when used in the mouse. The equivalent effective index that reproduced accurately the measured refractive error (assuming the geometrical parameters of Fig. 6.9) was 1.44465, much similar to that proposed by Schmucker and Schaeffel 2004a) (Schmucker and Schaeffel 2004), 1.433, than that reported by Retmulla & Hallet (Remtulla and Hallett 1985) 1.659, which would result in high amounts of myopia.

Artal et al.(Artal et al. 1998) developed an optical model of the rat eye. They found that in a small eye, the steeper surfaces result in high amount of aberrations, but the corresponding simulated MTFs were still higher than the experimental double-pass MTFs. This is in contrast to our finding, that, despite the highly degraded optics in the mouse, there seems to be still some compensation (most likely in the form of gradient index distribution in the lens) that prevents for even higher amounts of spherical aberration predicted from geometry (and constant index). The higher optical degradation found in double-pass experiments (higher than from Hartmann-Shack measurements and from computer eye model simulations) could have arisen from intraocular or retinal scattering.

Chapter 7: Conclusions

Conclusiones:

1. Hemos desarrollado tecnología para medir las propiedades óptica in modelos animales. En particular, hemos desarrollado un sensor de onda Hartmann-Shack para medir las aberraciones oculares y un queratómetro para medir radios corneales de curvatura en pollos (miopes, emétopes y tras tratamiento con cirugía refractiva láser) y ratones, desarrollando protocolos para medir la longitud axial y el error refractivo de estos animales. Hemos descrito los primeros resultados en la literatura de aberraciones ópticas “in vivo”, sin anestesia ni retractores de párpado, en dichas especies.
2. La óptica del ojo del pollo no está limitada por difracción.
3. La calidad óptica del pollo mejora durante su desarrollo (es decir, las aberraciones ópticas disminuyen para un tamaño de pupila constante), y esta mejora no parece ser dirigida por estímulos visuales, esto ocurre incluso cuando el ojo está sujeto a una gran degradación de la imagen retiniana (por ejemplo, con difusores).
4. En pollos con un incremento de aberraciones al nacer no ve interferido su proceso de emetropización.
5. Los cambios geométricos resultante de un excesivo alargamiento ocular del ojo del pollo tratado con difusores afectan a la calidad óptica de los componentes oculares. Los ojos miopes muestran mayores cantidades de desenfoque producido por las aberraciones, pero esto es mínimo comparado con la degradación óptica producido por difusores o lo desarrollado por el propio error refractivo. En otras palabras, el aumento de aberraciones parece ser una consecuencia los cambios estructurales

del ojo producidos durante el alargamiento del ojo mas que ser una causa de la miopía (en este modelo la degradación viene impuesta por el difusor y el desenfoque inducido, mucho mayor que la degradación de la imagen retiniana impuesta por aberraciones).

6. Si hay un proceso activo de desarrollo de los componentes ópticos y un ajuste de las aberraciones ópticas de las distintas estructuras oculares, este es seguramente el resultado de un proceso preprogramado o simplemente es debido al escalamiento geométrico, pero no parece estar relacionado con la experiencia visual, al menos en gran medida.
7. La cirugía refractiva no es un método eficiente para inducir alargamiento ocular in el pollo. Una semana después del tratamiento de miopía con PRK, la cornea no presentaba alteraciones en su curvatura.
8. Los ojos de los pollos tratados con cirugía refractiva mostraban de forma significativa mayores cantidades de aberraciones de alto orden que los ojos sin tratar contralaterales. Además, el modelo de cirugía refractiva no afecta al proceso de emetropización, indicando que el aumento de aberraciones no inducen necesariamente miopía.
9. La calidad óptica del ratón es mucho peor que el pollo que el ojo de un primate.
10. Los valores de hipermetropía encontrados con aberrometría Hartmann-Shack en el ojo del ratón son consistentes con los datos previos en la literatura.
11. Las aberraciones de alto orden son la mayor fuente de degradación de la calidad óptica del ojo del ratón, indicando que la presencia de estas aberraciones no generan necesariamente miopía.
12. La gran profundidad de foco en el ratón puede ser la responsable de la alta tolerancia que tiene al desenfoque, y por tanto su baja respuesta a los

diferentes tratamientos para desarrollar miopía, comparada con otros modelos animales. En cualquier caso, la resolución espacial y la profundidad de foco no parece estar limitadas por las aberraciones ópticas.

13. El trazado de rayos de modelos de ojos diseñados a partir de datos biométricos pueden predecir el error refractivo medido y la aberración esférica en el ojo del pollo y ratón, así como cambios longitudinales con la edad y diferencias entre ojos de pollo emétopes y miopes. Se hace necesaria la introducción en el modelo un cristalino con gradiente de índice para reproducir los valores de aberración esférica observada, la cual era menor que los valores reproducidos con un modelo con índice homogéneo. Esto sugiere la existencia de un efecto compensatorio del cristalino de pollo y ratón, tal y como se ha descrito en otras especies.

Conclusions

1. We have implemented technology to measure optical properties in animal models. In particular, we have developed a Hartmann-Shack wavefront sensor for measuring ocular aberrations and a keratometer to measure corneal radius of curvature in chicks (normal, developing myopia and after refractive surgery) and wild type mice, and developed protocols to measure axial length and refractive error in these animals. We have provided among the first results in the literature of optical aberrations (in vivo, without anaesthesia nor retractors) in these species.
2. The optics of the eye in chicks is not limiting spatial resolution.
3. Optical quality in chicks improves during development (i.e. optical aberrations decrease, for a constant pupil size), but this improvement does not seem to be visually guided, since it occurs even when the eye is subject to dramatic retinal image quality degradation (such as diffusers).
4. Chick eyes with higher amounts of aberrations at birth do not emmetropize less efficiently.
5. The geometrical changes resulting from excessive ocular axial growth in the chick eye treated with diffusers affect, the optical quality of the ocular components. Myopic eyes show higher amount of blur produced by aberrations, but this is minimal compared to the optical degradation produced by the diffuser or the developed refractive error. In other words, increased aberrations seem to be a consequence of the structural changes occurring in the excessively elongated eye rather than a cause of myopia (which in this model is induced by the degradation imposed by the diffuser and the induced defocus, much higher than the retinal image degradation imposed by aberrations).

6. If there is an active process for the development of optical components and a tuning of optical aberrations of ocular components this is likely the result of a pre-programmed process or just geometrical scaling but it does not seem to rely on visual experience to occur, at least to a great extent.
7. Corneal refractive surgery is not an efficient method to induce axial elongation in the chick eye. One week following surgery, the corneal curvature eyes treated with myopic PRK did not appear altered.
8. Chick eyes treated with myopic refractive surgery exhibited significantly higher amounts of high order aberrations than the untreated contralateral eyes. However, refractive surgery chick model did not alter the emmetropization process, indicating that increased amounts of aberrations do not necessarily induce myopia.
9. The optical quality in the mouse is much poorer than chick or primates.
10. The hyperopic errors found using Hartmann-Shack aberrometry in the mouse eye are consistent with previous refractive errors in the literature.
11. Higher order aberrations are major sources of optical quality degradation in the mouse eye, indicating that the presence of high amounts of optical aberrations is not necessarily related with myopia.
12. Increased optical depth of focus in mice may be responsible to a higher tolerance to defocus, and therefore for a less efficient response to different treatments to develop myopia, compared to other animal models. In any case, the spatial resolution and behavioural depth of focus does not seem to be limited by the optical aberrations.
13. Ray tracing on schematic eye models designed using known biometrical data can predict the measured refractive error and spherical aberration in the chick eye and mouse eye, as well as longitudinal changes with age and differences between emmetropic and myopic chick eyes. A gradient

index crystalline lens model needed to be assumed to match the amounts of observed spherical aberration, which was systematically higher than when purely geometrical parameters and a constant index were used. This suggests the presence of a compensatory effect in the lens of chicks and mice, as previously reported in other species.

This thesis has resulted in the following peer-reviewed publications:

E. García de la Cera, G. Rodríguez and S. Marcos. “Longitudinal changes and optical aberrations in normal and form-deprived myopic chicks” . Vision Research (2006)46, 579-589

E. García de la Cera, G. Rodríguez, L. Llorente, F. Schaeffel, S. Marcos. “Optical aberrations in the mouse eye” .Vision Research 46 (2006), 2546-2553

E. García de la Cera, G. Rodríguez, A. de Castro, J. Merayo, S. Marcos “Emmetropization and optical aberrations in a myopic corneal refractive surgery chick model “. Vision Research,47, 2465-2472 (2007).

E. García de la Cera, S. Marcos. “Matching ocular biometry to optical aberrations I: Developing normal and myopic chick computer eye model”. (In preparation).

E. García de la Cera, S. Marcos. “Matching ocular biometry to optical aberrations II: 4-week old mouse computer eye model”. (In preparation).

References

References

- Anera, R. G., J. R. Jimenez, et al. (2006). "Prevalence of refractive errors in school-age children in Burkina Faso." Japanese Journal of Ophthalmology **50**(5): 483-484.
- Angle, J. and D. A. Wissmann (1980). "Myopia and Corrective Lenses." Social Science & Medicine Part a-Medical Sociology **14**(6A): 473-479.
- Applegate, R. (1991). Monochromatic wavefront aberrations in myopia. Noninvasive Assessment of the Visual System. Washington, DC, Optical Society of America. **1**: 234-237.
- Artal, P., A. Benito, et al. (2006). "The human eye is an example of robust optical design." Journal of Vision **6**(1): 1-7.
- Artal, P., E. Berrio, et al. (2002). "Contribution of the cornea and internal surfaces to the change of ocular aberrations with age." J. Opt. Soc. Am. A **19**: 137-143.
- Artal, P. and A. Guirao (1998). "Contributions of the cornea and the lens to the aberrations of the human eye." Optics Letters **23**(21): 1713-1715.
- Artal, P., A. Guirao, et al. (2001). "Compensation of corneal aberrations by the internal optics in the human eye." J Vis **1**(1): 1-8.
- Artal, P., P. Herreros de Tejada, et al. (1998). "Retinal image quality in the rodent eye." Visual Neuroscience **15**: 597-605.
- Atchison, D., M. Collins, et al. (1995). "Measurement of monochromatic ocular aberrations of human eyes as a function of accommodation by the Howland aberroscope technique." Vision Research **35**: 313-323.
- Atchison, D. A., C. E. Jones, et al. (2004). "Eye shape in emmetropia and myopia." Investigative Ophthalmology & Visual Science **45**(10): 3380-3386.
- Atchison, D. A. and G. Smith (2000). Optics of the Human Eye. Oxford, Butterworth-Heinemann.
- Barbero, S. (2006). "Refractive power of a multilayer rotationally symmetric model of the human cornea and tear film." Journal of the Optical Society of America a-Optics Image Science and Vision **23**(7): 1578-1585.
- Barbero, S., S. Marcos, et al. (2002). "Validation of the estimation of corneal aberrations from videokeratography in keratoconus." Journal of Refractive Surgery **18**: 263-270.
- Barbero, S., Marcos, S., & Jimenez-Alfaro, I (2003). "Optical aberrations of intraocular lenses measured in vivo and in vitro." Journal of the Optical Society of America A. **20**: 1841-1851.
- Barlow, H. B. and T. J. Ostwald (1972). "Pecten of Pigeons Eye as an Inter-Ocular Eye Shade." Nature-New Biology **236**(64): 88-&.
- Bartmann, M. and F. Schaeffel (1994). "A simple mechanism for emmetropization without cues from accommodation or colour." Vision Research **34**(7): 873-876.
- Bassnett, S. and P. A. Winzenburger (2003). "Morphometric analysis of fibre cell growth in the developing chicken lens." Experimental Eye Research **76**(3): 291-302.

- Beresford, J. A., S. G. Crewther, et al. (2001). "Comparison of refractive state and circumferential morphology of retina, choroid, and sclera in chick models of experimentally induced ametropia." Optometry and Vision Science **78**(1): 40-49.
- Beuerman, R. W., A. Barathi, et al. (2003). "Two Models of Experimental Myopia in the Mouse." Invest. Ophthalmol. Vis. Sci. **44**(5): 4338-.
- Biss, D. P., D. Sumorok, et al. (2007). "In vivo fluorescent imaging of the mouse retina using adaptive optics." Optics Letters **32**(6): 659-661.
- Blaker, J. W. (1980). "Toward an Adaptive Model of the Human-Eye." Journal of the Optical Society of America **70**(2): 220-223.
- Brach, V. (1975). "Effect of Intraocular Ablation of Pecten Oculi of Chicken." Investigative Ophthalmology **14**(2): 166-168.
- Bruhn, S. L. and C. L. Cepko (1996). "Development of the pattern of photoreceptors in the chick retina." Journal of Neuroscience **16**(4): 1430-1439.
- Brunette, I., J. M. Bueno, et al. (2003). "Monochromatic aberrations as a function of age, from childhood to advanced age." Investigative Ophthalmology & Visual Science **44**(12): 5438-5446.
- Bryant, M. R., J. Kampmeier, et al. (1999). "PRK-induced anisometropia in the rabbit as a model of myopia." Graefes Archive for Clinical and Experimental Ophthalmology **237**(2): 161-165.
- Buehren, T., M. J. Collins, et al. (2003). "Corneal aberrations and reading." Optometry and Vision Science **80**(2): 159-166.
- Bullimore, M., B. Gilmartin, et al. (1992). "Steady-state accommodation and ocular biometry in late-onset myopia." Doc Ophthalmol. **80**: 143-155.
- Burns, S. and S. Marcos (2001). Measurement of image quality with the spatially resolved refractometer. Customized corneal ablation: The quest for super vision. R. Applegate, Stack publishing: 203-209.
- Burns, S. A. and S. Marcos (2000). Measurement of the image quality of the eye with the spatially resolved refractometer. Customized Corneal Ablations. R. Applegate. Thorofare, NJ, Slack. In press.
- Burns, S. A., S. Marcos, et al. (2002). "Contrast improvement for confocal retinal imaging using phase correcting plates." Optics Letters **27**: 400-402.
- Calderone, L., P. Grimes, et al. (1986). "Acute Reversible Cataract Induced by Xylazine and by Ketamine-Xylazine Anesthesia in Rats and Mice." Experimental Eye Research **42**(4): 331-337.
- Calver, R., M. Cox, et al. (1999). "Effect of aging on the monochromatic aberrations of the human eye." J Opt Soc Am A **16**: 2069-2078.
- Campbell, C. E. (2005). "A test eye for wavefront eye refractors." Journal of Refractive Surgery **21**(2): 127-140.
- Campbell, M. C. W., J. J. Hunter, et al. (2003). "Image quality on the retina of the chick eye during emmetropization: Goggled vs control eyes." Investigative Ophthalmology & Visual Science **44**: U325-U325.
- Campbell, M. W., H. Haman, et al. (1999). "Dependence of optical image quality on refractive error: eyes after excimer laser photorefractive keratectomy (PRK) versus controls." Investigative Ophthalmology and Visual Science **40 (Suppl.)**(4): 7.

- Cano, D., B. Barbero, et al. (2004). "Comparison of real and computer-simulated outcomes of LASIK refractive surgery." Journal of the Optical Society of America A **21**: 926-936.
- Carkeet, A., H. Luo, et al. (2002). "Refractive error and monochromatic aberrations in Singaporean children." Vision Res. **42**(14): 1809-24.
- Carney, L., J. Mainstone, et al. (1997). "Corneal topography and myopia. A cross-sectional study." Invest Ophthalmol Vis Sci. **38**(2): 311-20.
- Castejon-Mochon, F. J., N. Lopez-Gil, et al. (2002). "Ocular wave-front aberration statistics in a normal young population." Vision Research **42**: 1611-1617.
- Chan, O. Y. C. and M. Edwards (1993). "Refractive Errors in Hong-Kong Chinese Preschool-Children." Optometry and Vision Science **70**(6): 501-505.
- Chang, B., N. Hawes, et al. (2002). "Retinal degeneration mutants in the mouse." Vision Res **42**: 517-525.
- Chen, C. J., B. H. Cohen, et al. (1985). "Genetic and Environmental-Effects on the Development of Myopia in Chinese Twin Children." Ophthalmic Paediatrics and Genetics **6**(1-2): 113-119.
- Chen, L., P. B. Kruger, et al. (2006). "Accommodation with higher-order monochromatic aberrations corrected with adaptive optics." Journal of the Optical Society of America a-Optics Image Science and Vision **23**(1): 1-8.
- Cheng, X., A. Bradley, et al. (2003). "Relationship between refractive error and monochromatic aberrations of the eye." Optom Vis Sci. **80**: 43-49.
- Cheng, X., A. Bradley, et al. (2004). "Related Articles. Predicting subjective judgment of best focus with objective image quality metrics." Journal of Vision **23**(4): 310-321.
- Choh, V., M. J. Y. Lew, et al. (2006). "Effects of interchanging hyperopic defocus and form deprivation stimuli in normal and optic nerve-sectioned chicks." Vision Research **46**(6-7): 1070-1079.
- Choh, V. and J. G. Sivak (2005). "Lenticular accommodation in relation to ametropia: The chick model." Journal of Vision **5**(3): 165-176.
- Choh, V., J. G. Sivak, et al. (2002). "Ultrasound biomicroscopy segment of the enucleated of the anterior chicken eye during accommodation." Ophthalmic and Physiological Optics **22**(5): 401-408.
- Choh, V., J. G. Sivak, et al. (2002). "A physiological model to measure effects of age on lenticular accommodation and spherical aberration in chickens." Investigative Ophthalmology & Visual Science **43**(1): 92-98.
- Ciuffreda, K. J., B. Wang, et al. (2007). "Conceptual model of human blur perception." Vision Res. **47**: 1245-1252.
- Coletta, N., S. Marcos, et al. (2003). "Double-pass measurement of retinal image quality in the chicken eye." Optom Vis Sci **80**: 50-57.
- Coletta, N. J., S. Marcos, et al. (2000). "Optical quality of the chicken eye." Investigative Ophthalmology and Visual Science (Suppl.) **41**: 738.
- Coletta, N. J., D. Troilo, et al. (2001). "Optical quality in the common marmoset eye." Investigative Ophthalmology and Visual Science, (Suppl.) **42**: 37.

- Coletta, N. J., D. Troilo, et al. (2003). "Wavefront aberrations of the marmoset eye." Investigative Ophthalmology & Visual Science **44**: U324-U324.
- Coletta, N. J., D. Troilo, et al. (2004). "Ocular wavefront aberrations in the awake marmoset." Investigative Ophthalmology & Visual Science **45**: U417-U417.
- Collins, M. J., C. F. Wildsoet, et al. (1995). "Monochromatic Aberrations and Myopia." Vision Research **35**(9): 1157-1163.
- Curtin, B. (1985). The Myopias: Basic Science and Clinical Management. Philadelphia, Harper & Row.
- Curtin, B. J. (1985). "Severe Bilateral Myopia." Jama-Journal of the American Medical Association **253**(22): 3316-3316.
- del Val, J. A., S. Barrero, et al. (2001). "Experimental measurement of corneal haze after excimer laser keratectomy." Applied Optics **40**(10): 1727-1734.
- Diether, S. and F. Schaeffel (1997). "Local changes in eye growth induced by imposed local refractive error despite active accommodation." Vision Research **37**(6): 659-668.
- Diether, S. and C. F. Wildsoet (2005). "Stimulus requirements for the decoding of myopic and hyperopic defocus under single and competing defocus conditions in the chicken." Investigative Ophthalmology & Visual Science **46**(7): 2242-2252.
- Donders, F. C. (1864). On the Anomalies of Accommodation and Refraction of the Eye. London, Trar Moore. The New Sydenham Society.
- Dorrnsoro, C., S. Barbero, et al. (2003). "On-eye measurement of optical performance of Rigid Gas Permeable contact lenses based on ocular and corneal aberrometry." Optometry and Vision Science. **80**: 115-125.
- Drexler, W., O. Findl, et al. (1998). "Eye elongation during accommodation in humans: Differences between emmetropes and myopes." Investigative Ophthalmology & Visual Science **39**(11): 2140-2147.
- Dubbelman, M. and G. L. Van der Heijde (2004). "Radius, astigmatism and asphericity of the posterior corneal surface." Investigative Ophthalmology & Visual Science **45**: U24-U24.
- Feldkämper, M. and F. Schaeffel (2003). "Interactions of Genes and Environment in Myopia." Dev Ophthalmol **37**: 34-49.
- Fledelius, H. C. (1981). "Myopia of Prematurity." Acta Ophthalmologica **59**(3): 435-435.
- Fletcher, M. C. (1955). "Myopia of Prematurity." American Journal of Ophthalmology **40**(4): 474-481.
- Flitcroft, D. I. (1998). "A model of the contribution of oculomotor and optical factors to emmetropization and myopia." Vision Research **38**(19): 2869-2879.
- Fujikado, T., T. Kuroda, et al. (2004). "Age-related changes in ocular and corneal aberrations." American Journal of Ophthalmology **138**(1): 143-146.
- Fulk, G. W., L. A. Cyert, et al. (2000). "A randomized trial of the effect of single-vision vs. bifocal lenses on myopia progression in children

- with esophoria - Response." Optometry and Vision Science **77**(12): 631-632.
- García de la Cera, E., G. Rodriguez, et al. (2007). "Emmetropization and optical aberrations in a myopic corneal refractive surgery chick model." Vision Research **47**(18): 2465-2472.
- García de la Cera, E., G. Rodriguez, et al. (2006). "Optical aberrations in the mouse eye." Vision Research **46**(16): 2546-2553.
- García de la Cera, E., G. Rodriguez, et al. (2006). "Longitudinal changes of optical aberrations in normal and form-deprived myopic chick eyes." Vision Research **46**(4): 579-589.
- Garner, L. F., G. Smith, et al. (2001). "Gradient refractive index of the crystalline lens of the Black Oreo Dory (*Allocyttus Niger*): comparison of magnetic resonance imaging (MRI) and laser ray-trace methods." Vision Research **41**(8): 973-979.
- Gee, S. and K. Tabbara (1988). "Increase of ocular axial length in patients with corneal opacification." Ophthalmology **1988**(95): 1276-1278.
- Gianfranceschi, L., A. Fiorentini, et al. (1999). "Behavioural visual acuity of wild type and bcl2 transgenic mouse." Vision Research **39**(3): 569-574.
- Gilmartin, B. (2004). "Myopia: precedents for research in the twenty-first century." Clinical and Experimental Ophthalmology **32**(3): 305-324.
- Gilmartin, B. (2006). "Imaging the myopic eye." Acta Ophthalmologica Scandinavica **84**(Supplement 239).
- Glasser, A., C. J. Murphy, et al. (1995). "The Mechanism of Lenticular Accommodation in Chicks." Vision Research **35**(11): 1525-1540.
- Glasser, A., D. Troilo, et al. (1994). "The Mechanism of Corneal Accommodation in Chicks." Vision Research **34**(12): 1549-1566.
- Glickstein, M. and M. Millidot (1970). "Retinoscopy and eye size." Science **168**: 605-606.
- Goldschmith, E. (1968). "On Etiology of Myopia - an Epidemiological Study." Acta Ophthalmologica **5**: U11-&.
- Goss, D. (2000). "Nearwork and myopia." Lancet. **356**: 1456-1457.
- Goss, D. A. and T. W. Caffey (1999). "Clinical findings before the onset of myopia in youth: 5. Intraocular pressure." Optometry and Vision Science **76**(5): 286-291.
- Goss, D. A. and T. W. Jackson (1996). "Clinical findings before the onset of myopia in youth .4. Parental history of myopia." Optometry and Vision Science **73**(4): 279-282.
- Gottlieb, M. D., L. A. Fugate-Wentzek, et al. (1987). "Different visual deprivations produce different ametropias and different eye shapes." Investigative of Ophthalmology and Visual Science **28**: 1225-1235.
- Green, D., M. Powers, et al. (1980). "Depth of focus, eye size and visual acuity." Vision Research **20**: 827-835.
- Greene, P. R. (1980). "Mechanical Considerations in Myopia - Relative Effects of Accommodation, Convergence, Intraocular-Pressure, and the Extra-Ocular Muscles." American Journal of Optometry and Physiological Optics **57**(12): 902-914.
- Grice, K., J. Bauer, et al. (1997). "Myopic progression differs between children in Boston and Singapore." Investigative Ophthalmology & Visual Science **38**(4): 4539-4539.

- Grosvenor, T. (1987). "A Review and a Suggested Classification-System for Myopia on the Basis of Age-Related Prevalence and Age of Onset." American Journal of Optometry and Physiological Optics **64**(7): 545-554.
- Grosvenor, T. and D. A. Goss (1999). Clinical Management of Myopia, Butterworth-Heinemann.
- Grosvenor, T., D. M. Perrigin, et al. (1987). "Houston Myopia Control Study - a Randomized Clinical-Trial .2. Final Report by the Patient-Care Team." American Journal of Optometry and Physiological Optics **64**(7): 482-498.
- Guggenheim, J. A., J. T. Erichsen, et al. (2002). "Similar genetic susceptibility to form-deprivation myopia in three strains of chicken." Vision Research **42**(25): 2747-2756.
- Guirao, A. and P. Artal (1999). "Corneal aberrations as a function of age." Investigative Ophthalmology & Visual Science **40**(4): S535-S535.
- Guirao, A. and D. Williams (2003). "A method to predict refractive errors from wave aberration data." Optom Vis Sci. **80**: 36-42.
- Gwiazda, J., L. Hyman, et al. (2003). "A randomized clinical trial of progressive addition lenses versus single vision lenses on the progression of myopia in children." Investigative Ophthalmology & Visual Science **44**(4): 1492-1500.
- Gwiazda, J., F. Thorn, et al. (2005). "Accommodation, accommodative convergence, and response AC/A ratios before and at the onset of myopia in children." Optometry and Vision Science **82**(4): 273-278.
- Hammond, C. J., H. Snieder, et al. (2001). "Genes and environment in refractive error: The twin eye study." Investigative Ophthalmology & Visual Science **42**(6): 1232-1236.
- Hayes, B. P., F. W. Fitzke, et al. (1986). "A morphological analysis of experimental myopia in young chickens." Investigative of Ophthalmology and Visual Science **27**: 981-991.
- He, J. C., S. A. Burns, et al. (2000). "Monochromatic aberrations in the accommodated human eye." Vision Research **40**: 41-48.
- He, J. C., J. Gwiazda, et al. (2005). "The association of wavefront aberration and accommodative lag in myopes." Vision Research **45**(3): 285-290.
- He, J. C., S. Marcos, et al. (1998). "Measurement of the wave-front aberration of the eye by a fast psychophysical procedure." Journal of the Optical Society of America A **15**: 2449-2456.
- He, J. C., P. Sun, et al. (2002). "Wavefront aberrations in eyes of emmetropic and moderately myopic school children and young adults." Vision Research **42**(8): 1063-1070.
- Hegde, K., M. Henein, et al. (2003). "Establishment of the mouse as a model animal for the study of diabetic cataracts." Ophthalmic Res.: 12-18.
- Hemminki, E. and O. Parssinen (1987). "Prevention of Myopic Progress by Glasses - Study Design and the 1st-Year Results of a Randomized Trial among Schoolchildren." American Journal of Optometry and Physiological Optics **64**(8): 611-616.

- Hodos, W. and W. J. Kuenzel (1984). "Retinal-image degradation produces ocular enlargement in chicks." Investigative Ophthalmology and Visual Science: 652-659.
- Horner, D. G., P. S. Soni, et al. (2000). "Longitudinal changes in corneal asphericity in myopia." Optometry and Vision Science **77**: 198-203.
- Howland, H. C. (2005). "Allometry and scaling of wave aberration of eyes." Vision Research **45**(9): 1091-1093.
- Hoyt, C. S., R. D. Stone, et al. (1981). "Monocular Axial Myopia Associated with Neonatal Eyelid Closure in Human Infants." American Journal of Ophthalmology **91**(2): 197-200.
- Hughes, A. (1979). "Schematic Eye for the Rat." Vision Research **19**(5): 569-&.
- Hughes, A. and H. Wassle (1979). "Estimate of Image Quality in the Rat Eye." Investigative Ophthalmology & Visual Science **18**(8): 878-881.
- Hung, L. F., M. L. Crawford, et al. (1995). "Spectacle lenses alter eye growth and the refractive status of young monkeys." Nature Medicine **1**: 761-765.
- Huxlin, K. R., G. Yoon, et al. (2004). "Monochromatic ocular wavefront aberrations in the awake-behaving cat." Vision Research **44**(18): 2159-2169.
- Hyman, L., J. Gwiazda, et al. (2005). "Relationship of age, sex, and ethnicity with myopia progression and axial elongation in the correction of myopia evaluation trial." Archives of Ophthalmology **123**(7): 977-987.
- Ibay, G., B. Doan, et al. (2004). "Candidate high myopia loci on chromosomes 18p and 12q do not play a major role in susceptibility to common myopia."
- Iribarren, R., A. Balsa, et al. (2005). "Family history of myopia is not related to the final amount of refractive error in low and moderate myopia." Clinical and Experimental Ophthalmology **33**(3): 274-278.
- Iribarren, R., G. Iribarren, et al. (2002). "Family history and reading habits in adult-onset myopia." Current Eye Research **25**(5): 309-315.
- Irving, E. L., M. G. Callender, et al. (1995). "Inducing ametropias in hatchling chicks by defocus aperture effects and cylindrical lenses." Vision Research **35**(9): 1165-1174.
- Irving, E. L., M. L. Ksilak, et al. (2005). "Refractive Error and Optical Image Quality in Three Strains of Albino Rats." Invest. Ophthalmol. Vis. Sci. **46**: E-Abstract 4334.
- Irving, E. L., J. G. Sivak, et al. (1992). "Refractive Plasticity of the Developing Chick Eye." Ophthalmic and Physiological Optics **12**(4): 448-456.
- Irving, E. L., J. G. Sivak, et al. (1996). "Chick eye optics: Zero to fourteen days." Journal of Comparative Physiology a-Sensory Neural and Behavioral Physiology **179**(2): 185-194.
- Jagger, W. S. (1990). "The Refractive Structure and Optical-Properties of the Isolated Crystalline Lens of the Cat." Vision Research **30**(5): 723-&.
- Jiang, B.-C. (2000). VIII International Conference on Myopia 2000. Myopia 2000, Boston.

- Jorge, J., J. B. Almeida, et al. (2007). "Refractive, biometric and topographic changes among Portuguese university science students: a 3-year longitudinal study." Ophthalm. Physiol. Opt. **27**(3): 287-294.
- Kee, C. S., D. Marzani, et al. (2001). "Differences in time course and visual requirements of ocular responses to lenses and diffusers." Investigative Ophthalmology & Visual Science **42**(3): 575-583.
- Kelly, J. E., T. Mihashi, et al. (2004). "Compensation of corneal horizontal/vertical astigmatism, lateral coma, and spherical aberration by internal optics of the eye." Journal of Vision **4**(4): 262-271.
- Kempen, A. H., P. Mitchell, et al. (2004). "The prevalence of refractive errors among adults in the United States, Western Europe, and Australia." Archives of Ophthalmology **122**(4): 495-505.
- Kern, T. and R. Engerman (1996). "A mouse model of diabetic retinopathy." Arch Ophthalmol. **114**: 986-990.
- Khandekar, R., S. Al Harby, et al. (2005). "Determinants of myopia among omani school children: A case-control study." Ophthalmic Epidemiology **12**(3): 207-213.
- Khoo, C., J. Chong, et al. (1999). "A 3-year study on the effect of RGP contact lenses on myopic children." Singapore Med J **40**: 230-237.
- Kiama, S. G., J. Bhattacharjee, et al. (1997). "Surface specialization of the capillary endothelium in the pecten oculi of the chicken, and their overt roles in pectineal haemodynamics and nutrient transfer to the inner neural retina." Acta Biologica Hungarica **48**(4): 473-483.
- Kinge, B. and A. Midelfart (1999). "Refractive changes among Norwegian university students - A three-year longitudinal study." Acta Ophthalmologica Scandinavica **77**(3): 302-305.
- Kinge, B., A. Midelfart, et al. (1999). "Biometric changes in the eyes of Norwegian university students - A three-year longitudinal study." Acta Ophthalmologica Scandinavica **77**(6): 648-652.
- Kisilak, M. L., M. C. W. Campbell, et al. (2006). "Aberrations of chick eyes during normal growth and lens induction of myopia." Journal of Comparative Physiology a-Neuroethology Sensory Neural and Behavioral Physiology **192**(8): 845-855.
- Kisilak, M. L., M. C. W. Campbell, et al. (2002). "Hartmann-Shack measurement of the monochromatic image quality in the chick eye during emmetropization." Investigative Ophthalmology & Visual Science **43**: U825-U825.
- Kleinstei, R. N., L. A. Jones, et al. (2003). "Refractive error and ethnicity in children." Archives of Ophthalmology **121**(8): 1141-1147.
- Krause, U., K. Krause, et al. (1982). "Sex-Differences in Refraction Errors up to the Age of 15." Acta Ophthalmologica **60**(6): 917-926.
- Kroger, R., M. Campbell, et al. (1999). "Multifocal lenses compensate for chromatic defocus in vertebrate eyes." J Comp Physiol [A]. **184**.
- Kroger, R. H. H. and H. J. Wagner (1996). "Emmetropization in fish: Results from rearing in monochromatic lights." Investigative Ophthalmology & Visual Science **37**(3): 4599-4599.
- Kurtz, D., L. Hyman, et al. (2007). "Role of parental myopia in the progression of myopia and its interaction with treatment in COMET

- children." Investigative Ophthalmology & Visual Science **48**(2): 562-570.
- Lapuerta, P. and J. Schein (1995). "A four-surface schematic eye of macaque monkey obtained by an optical method." Vision research **35**(16): 2245-2254.
- Larsson, E. K., A. C. Rydberg, et al. (2003). "A population-based study of the refractive outcome in 10-year-old preterm and full-term children." Archives of Ophthalmology **121**(10): 1430-1436.
- Li, T., H. C. Howland, et al. (2000). "Diurnal illumination patterns affect the development of the chick eye." Vision Research **40**(18): 2387-2393.
- Liang, J., B. Grimm, et al. (1994). "Objective measurement of wave aberrations of the human eye with the use of a Hartmann-Shack wave-front sensor." Journal of the Optical Society of America A **11**: 1949-1957.
- Liang, J. and D. R. Williams (1997). "Aberrations and retinal image quality of the normal human eye." Journal of the Optical Society of America A **14**: 2873-2883.
- Lin, C. P., C. Alt, et al. (2004). "Mouse Eye Parameters by Optical Coherence Tomography (OCT)." Invest. Ophthalmol. Vis. Sci. **45**: E-Abstract 2786.
- Lin, L. L. K., Y. F. Shih, et al. (1996). "Changes in ocular refraction and its components among medical students - A 5-year longitudinal study." Optometry and Vision Science **73**(7): 495-498.
- Lin, L. L. K., Y. F. Shih, et al. (1999). "Epidemiologic study of ocular refraction among schoolchildren in Taiwan in 1995." Optometry and Vision Science **76**(5): 275-281.
- Lindsey, J. and R. Weinreb (2005). "Elevated intraocular pressure and transgenic applications in the mouse." J Glaucoma. **14**: 318-320.
- Llorente, L., B. Barbero, et al. (2004). "Changes in corneal and total aberrations induced by LASIK surgery for hyperopia." Journal of Refractive Surgery **20**: 203-216.
- Llorente, L., S. Barbero, et al. (2004). "Myopic versus hyperopic eyes: axial length, corneal shape and optical aberrations." <http://journalofvision.org/4/4/5/>. " Journal of Vision **4**: 288.
- Llorente, L., L. Diaz-Santana, et al. (2003). "Aberrations of the human eye in visible and near infrared illumination." Optometry and Vision Science **80**: 26-35.
- Marcos, S. (2001). "Aberrations and Visual Performance following standard laser vision correction." J. Refract. Surgery **17**: 596-601.
- Marcos, S. (2001). "Refractive Surgery and Optical Aberrations." Optics and Photonics News **12**(12): 22-25.
- Marcos, S., B. Barbero, et al. (2001). "Optical response to LASIK for myopia from total and corneal aberration measurements." Investigative Ophthalmology and Visual Science. **42**: 3349-3356.
- Marcos, S., B. Barbero, et al. (2001). "Optical response to LASIK for myopia from total and corneal aberrations." Investigative Ophthalmology and Visual Science. **42**: 3349-3356.
- Marcos, S., S. Barbero, et al. (2005). "Optical quality and depth-of-field of eyes implanted with spherical and aspheric intraocular lenses." Journal of Refractive Surgery **21**: 223-235.

- Marcos, S., S. Barbero, et al. (2001). Why high myopic eyes tend to be more aberrated? Optical Society of America Technical Digest, Long Beach, CA.
- Marcos, S., S. Barbero, et al. (2002). "The sources of optical aberrations in myopic eyes." 2002 Annual Meeting Abstract and Program Planner accessed at www.arvo.org. Association for Research in Vision and Ophthalmology. Abstract 1510.
- Marcos, S., S. Barbero, et al. (2004). Optical quality of the eye and aging. Custom Corneal Ablation: the quest for supervision. In press. R. K. a. R. A. A. S. MacRae, Slack.
- Marcos, S., S. Barbero, et al. (2001). "Total and corneal aberrations before and after standard LASIK refractive surgery." Investigative Ophthalmology and Visual Science **42 (Suppl.)**: 529.
- Marcos, S., S. A. Burns, et al. (2001). "Investigating sources of variability of monochromatic and transverse chromatic aberrations across eyes." Vision Research **41**: 3861-3871.
- Marcos, S., L. Díaz-Santana, et al. (2002). "Ocular aberrations with ray tracing and Shack-Hartmann wavefront sensors: does polarization play a role?" Journal of the Optical Society of America A. **19**: 1063-1072.
- Marcos, S., E. Moreno, et al. (1999). "The depth-of-field of the human eye from objective and subjective measurements." Vision Research **39**: 2039-2049.
- Marcos, S., E. Moreno-Barriuso, et al. (2000). Do myopic eyes suffer from larger amount of aberrations? Myopia 200. Proceedings of the 8th International Conference on Myopia, Boston, International Conference on Myopia 2000 Press.
- Marcos, S., P. Rosales, et al. (2008). "Balance of corneal horizontal coma by internal optics in eyes with intraocular artificial lenses: Evidence of a passive mechanism." Vision Res **48**: 70-79.
- Marcos, S., P. Rosales, et al. (2007). "Change in corneal aberrations after cataract surgery with 2 types of aspherical intraocular lenses." Journal of Cataract and Refractive Surgery **33(2)**: 217-226.
- Maul, E., S. Barroso, et al. (2000). "Refractive Error Study in Children: Results from La Florida, Chile." American Journal of Ophthalmology **129(4)**: 445-454.
- McBrien, N. and D. Adams (1997). "A longitudinal investigation of adult-onset and adult-progression of myopia in an occupational group. Refractive and biometric findings." Invest Ophthalmol Vis Sci. **38**: 321-333.
- McBrien, N. A. (1998). "Regulation of scleral extracellular matrix metabolism in a mammalian model of axial myopia." Experimental Eye Research **67(Suppl.1)** S263).
- McBrien, N. A. and A. Gentle (2003). "Role of the sclera in the development and pathological complications of myopia." Progress in Retinal and Eye Research **22(3)**: 307-338.
- McKanna, J. A. and V. A. Casagrande (1978). "Reduced Lens Development in Lid-Suture Myopia." Experimental Eye Research **26(6)**: 715-723.

- McLellan, J., S. Marcos, et al. (2001). "Age-related changes in monochromatic wave aberrations in the human eye." Investigative Ophthalmology and Visual Science: 1390-1395.
- McLellan, J. S., S. Marcos, et al. (1999). "The change of the aberrations of the eye with age." Investigative Ophthalmology and Visual Science (Suppl.) **40**: 36.
- Merayo-Llodes, J., B. Yañez, et al. (2001). "Experimental model of Corneal Haze." J. Refractive Surgery **17**: 696-699.
- Mihashi, T., T. Li, et al. (2004). "Constant light produces more optical aberration especially overcorrected spherical aberrations in chickens." Investigative Ophthalmology & Visual Science **45**: U417-U417.
- Miles, F. A. and J. Wallman (1990). "Local Ocular Compensation for Imposed Local Refractive Error." Vision Research **30**(3): 339-349.
- Montés-Micó, R. and T. Ferrer-Blasco (2000). "Distribution of refractive errors in Spain." Documenta Ophthalmologica **101**: 25-33.
- Montiani-Ferreira, F., F. Cardoso, et al. (2004). "Postnatal development of central corneal thickness in chicks of Gallus gallus domesticus." Veterinary Ophthalmology **7**(1): 37-39.
- Montiani-Ferreira, F., S. Petersen-Jones, et al. (2003). "Early postnatal development of central corneal thickness in dogs." Veterinary Ophthalmology **6**(1): 19-22.
- Moreno-Barriuso, E., S. Marcos, et al. (2001). "Comparing Laser Ray Tracing, Spatially Resolved Refractometer and Hartmann-Shack sensor to measure the ocular wavefront aberration." Optometry and Vision Science **78**: 152 - 156.
- Moreno-Barriuso, E., J. Merayo-Llodes, et al. (2001). "Ocular aberrations before and after myopic corneal refractive surgery: LASIK-induced changes measured with Laser Ray Tracing." Investigative Ophthalmology and Visual Science **42**: 1396-1403.
- Moreno-Barriuso, E., J. M. Merayo-Llodes, et al. (2000). "Ocular aberrations after refractive surgery measured with a laser ray tracing technique." Investigative Ophthalmology and Visual Science (Suppl.) **41**: 303.
- Morgan, I. and K. Rose (2005). "How genetic is school myopia?" Progress in Retinal and Eye Research **24**(1): 1-38.
- Morris, V. B. (1982). "An Afoveate Area Centralis in the Chick Retina." Journal of Comparative Neurology **210**(2): 198-203.
- Murphy, C. J., A. Glasser, et al. (1995). "The Anatomy of the Ciliary Region of the Chicken Eye." Investigative Ophthalmology & Visual Science **36**(5): 889-896.
- Mutti, D., K. Zadnik, et al. (1992). "A video technique for phakometry of the human crystalline lens." Invest Ophthalmol Vis Sci. **33**: 1771-1782.
- Mutti, D., K. Zadnik, et al. (1996). "Myopia. The nature versus nurture debate goes on." Invest Ophthalmol Vis Sci. **37**: 952-957.
- Mutti, D. O., L. A. Jones, et al. (2002). "Excess accommodative lag accompanies but does not precede the onset of myopia." Investigative Ophthalmology & Visual Science **43**: U337-U337.

- Mutti, D. O., L. A. Jones, et al. (2000). "AC/A ratio, age, and refractive error in children." Investigative Ophthalmology & Visual Science **41**(9): 2469-2478.
- Mutti, D. O., G. L. Mitchell, et al. (2002). "Parental myopia, near work, school achievement, and children's refractive error." Investigative Ophthalmology & Visual Science **43**(12): 3633-3640.
- Mutti, D. O., E. Semina, et al. (2002). "Genetic loci for pathological myopia are not associated with juvenile myopia." American Journal of Medical Genetics **112**(4): 355-360.
- Mutti, D. O., J. N. VerHoeve, et al. (1997). "The artifact of retinoscopy revisited: Comparison of refractive error measured by retinoscopy and visual evoked potential in the rat." Optometry and Vision Science **74**(7): 483-488.
- Naiglin, L., C. Gazagne, et al. (2002). "A genome wide scan for familial high myopia suggests a novel locus on chromosome 7q36." Journal of Medical Genetics **39**(2): 118-124.
- Nakao, S., S. Fujimoto, et al. (1968). "Model of Refractive-Index Distribution in Rabbit Crystalline Lens." Journal of the Optical Society of America **58**(8): 1125-&.
- Nakao, S., T. Ono, et al. (1963). "The distribution of refractive indices in the human crystalline lens." Japanese Journal of Ophthalmology **58**: 1125-1130.
- Ni, J. and E. L. Smith (1989). "Effects of chronic optical defocus on the kitten's refractive status." Vision Research **29**(8): 929-938.
- Nickla, D. L. (2006). "The phase relationships between the diurnal rhythms in axial length and choroidal thickness and the association with ocular growth rate in chicks." Journal of Comparative Physiology a-Neuroethology Sensory Neural and Behavioral Physiology **192**(4): 399-407.
- Nickla, D. L., C. Wildsoet, et al. (1998). "Visual influences on diurnal rhythms in ocular length and choroidal thickness in chick eyes." Experimental Eye Research **66**(2): 163-181.
- Nickla, D. L., C. F. Wildsoet, et al. (2001). "Endogenous rhythms in axial length and choroidal thickness in chicks: Implications for ocular growth regulation." Investigative Ophthalmology & Visual Science **42**(3): 584-588.
- Norton, T. T. (1990). "Experimental Myopia in Tree Shrews." Ciba Foundation Symposia **155**: 178-199.
- Norton, T. T. (1999). "Animal Models of Myopia: Learning How Vision Controls the Size of the Eye." ILAR Journal **40**(2).
- Norton, T. T. and N. A. McBrien (1992). "Normal Development of Refractive State and Ocular Component Dimensions in the Tree Shrew (Tupaia-Belangeri)." Vision Research **32**(5): 833-842.
- Norton, T. T. and J. A. Rada (1995). "Reduced Extracellular-Matrix in Mammalian Sclera with Induced Myopia." Vision Research **35**(9): 1271-1281.
- Ong, E. and K. J. Ciuffreda (1995). "Nearwork-induced transient myopia - A critical review." Documenta Ophthalmologica **91**(1): 57-85.
- Over, R. and D. Moore (1981). "Spatial acuity of the chicken." Brain Research **211**: 424-426.

- Pacella, R., J. McLellan, et al. (1999). "Role of genetic factors in the etiology of juvenile-onset myopia based on a longitudinal study of refractive error." Optometry and Vision Science **76**: 381-386.
- Paluru, P., S. M. Ronan, et al. (2003). "New locus for autosomal dominant high myopia maps to the long arm of chromosome 17." Investigative Ophthalmology & Visual Science **44**(5): 1830-1836.
- Paquin, M. P., H. Hamam, et al. (2002). "Objective measurement of optical aberrations in myopic eyes." Optometry and Vision Science **79**(5): 285-291.
- Park, T. W., J. Winawer, et al. (2003). "Further evidence that chick eyes use the sign of blur in spectacle lens compensation." Vision Research **43**(14): 1519-1531.
- Parssinen, O., E. Hemminki, et al. (1989). "Effect of Spectacle Use and Accommodation on Myopic Progression - Final Results of a 3-Year Randomized Clinical-Trial among Schoolchildren." British Journal of Ophthalmology **73**(7): 547-551.
- Pennie, F. C., I. C. J. Wood, et al. (2001). "A longitudinal study of the biometric and refractive changes in full-term infants during the first year of life." Vision Research **41**(21): 2799-2810.
- Perrigin, J., D. Perrigin, et al. (1990). "Silicone-acrylate contact lenses for myopia control: 3-year results." Optom Vis Sci. **67**: 764-769.
- Phillips, J. R., M. Khalaj, et al. (2000). "Induced myopia associated with increased scleral creep in chick and tree shrew eyes." Investigative Ophthalmology & Visual Science **41**(8): 2028-2034.
- Pickett-Seltner, R. L., J. G. Sivak, et al. (1988). "Experimentally induced myopia in chicks: morphometric and biochemical analysis during the first 14 days after hatching." Vision Research **28**: 323-328.
- Pickettseltner, R. L., J. Weerheim, et al. (1987). "Experimentally Induced Myopia Does Not Affect Posthatching Development of the Chick Lens." Vision Research **27**(10): 1779-1782.
- Pierscionek, B. K. and D. Y. C. Chan (1989). "Refractive-Index Gradient of Human Lenses." Optometry and Vision Science **66**(12): 822-829.
- Plainis, S., H. S. Ginis, et al. (2005). "The effect of ocular aberrations on steady-state errors of accommodative response." Journal of Vision **5**(5): 466-477.
- Porciatti, V., T. Pizzorusso, et al. (1999). "The visual physiology of the wild type mouse determined with pattern VEPs." Vision Research **39**(18): 3071-3081.
- Portellinha, W. and R. Belfort (1991). "Central and Peripheral Corneal Thickness in Newborns." Acta Ophthalmologica **69**(2): 247-250.
- Porter, J., A. Guirao, et al. (2001). "Monochromatic aberrations of the human eye in a large population." J Opt Soc Am A **18**(8): 1793-803.
- Priolo, S., J. G. Sivak, et al. (2000). "Effects of experimentally induced ametropia on the morphology and optical quality of the avian crystalline lens." Investigative Ophthalmology & Visual Science **41**(11): 3516-3522.
- Prusky, G. T., N. M. Alam, et al. (2004). "Rapid Quantification of Adult and Developing Mouse Spatial Vision Using a Virtual Optomotor System 10.1167/iovs.04-0541." Invest. Ophthalmol. Vis. Sci. **45**(12): 4611-4616.

- Quek, T. P. L., C. G. Chua, et al. (2004). "Prevalence of refractive errors in teenage high school students in Singapore." Ophthalmic and Physiological Optics **24**(1): 47-55.
- Rabin, J., R. C. Van Sluyters, et al. (1981). "Emmetropization: a vision-dependent phenomenon." Investigative Ophthalmology and Visual Science: 561-564.
- Ramamirtham, R., C. S. Kee, et al. (2006). "Monochromatic ocular wave aberrations in young monkeys." Vision Research **46**(21): 3616-3633.
- Ramamirtham, T., C.-S. Kee, et al. (2004). "Wave aberrations in rhesus monkeys with vision-induced ametropias." Invest Ophthalmol Vis Sci. : **45**.
- Remtulla, S. and P. E. Hallett (1985). "A Schematic Eye for the Mouse, and Comparisons with the Rat." Vision Research **25**(1): 21-31.
- Ritter, M., E. Aguilar, et al. (2005). "Three-Dimensional In Vivo Imaging of the Mouse Intraocular Vasculature during Development and Disease." Invest Ophthalmol Vis Sci. **46**: 3021-3026.
- Robb, R. M. (1977). "Refractive Errors Associated with Hemangiomas of Eyelids and Orbit in Infancy." American Journal of Ophthalmology **83**(1): 52-58.
- Roorda, A. and D. Williams (2001). Retinal imaging using adaptive optics. Customized corneal ablation: The quest for super vision. R. Applegate, Stack publishing: 42-48.
- Rosales, P. and S. Marcos (2006). "Phakometry and lens tilt and decentration using a custom-developed Purkinje imaging apparatus: validation and measurements." Journal of the Optical Society of America a-Optics Image Science and Vision **23**(3): 509-520.
- Rosales, P. and S. Marcos (2007). "Customized computer models of eyes with intraocular lenses." Optics Express **15**(5): 2204-2218.
- Rosales, P., W. Wendt, et al. (2008). "Changes in crystalline lens radii of curvature and lens tilt and decentration during dynamic accommodation in Rhesus Monkeys." Journal of Vision **8**(18): 1-12.
- Rosenfield, M. (1998). Accommodation and myopia. Myopia and nearwork. B. Gilmartin. Oxford, Butterworth-Heinemann: 91-116.
- Rosner, M. and M. Belkin (1987). "Intelligence, Education, and Myopia in Males." Archives of Ophthalmology **105**(11): 1508-1511.
- Saw, S. M. (2003). "A synopsis of the prevalence rates and environmental risk factors for myopia." Clin Exp Optom. **86**(5): 289-294.
- Saw, S. M., A. Cheng, et al. (2007). "School grades and myopia." Ophthalmic and Physiological Optics **27**(2): 126-129.
- Saw, S. M., W. H. Chua, et al. (2005). "Eye growth changes in myopic children in Singapore." British Journal of Ophthalmology **89**(11): 1489-1494.
- Saw, S. M., W. H. Chua, et al. (2002). "Nearwork in early-onset myopia." Investigative Ophthalmology & Visual Science **43**(2): 332-339.
- Saw, S. M., E. C. Shih-Yen, et al. (2002). "Interventions to retard myopia progression in children - An evidence-based update." Ophthalmology **109**(3): 415-421.
- Schaeffel, F. and E. Burkhardt (2002). "Measurement of Refractive State and Deprivation Myopia in a Black Wildtype Mouse." Invest. Ophthalmol. Vis. Sci. **43**(12): 182-.

- Schaeffel, F., E. Burkhardt, et al. (2004). "Measurement of refractive state and deprivation myopia in two strains of mice." Optometry and Vision Science **81**(2): 99-110.
- Schaeffel, F. and S. Diether (1999). "The growing eye: an autofocus system that works on very poor images." Vision Research **39**: 1585-1589.
- Schaeffel, F., A. Glasser, et al. (1988). "Accommodation, refractive error and eye growth in chickens." Vision Research **28**: 639-657.
- Schaeffel, F. and H. Howland (1988). "Visual optics in normal and ametropic chickens." Vision Science **3**: 83-98.
- Schaeffel, F. and H. C. Howland (1987). "Corneal Accommodation in Chick and Pigeon." Journal of Comparative Physiology a-Sensory Neural and Behavioral Physiology **160**(3): 375-384.
- Schaeffel, F. and H. C. Howland (1988). "Mathematical-Model of Emmetropization in the Chicken." Journal of the Optical Society of America a-Optics Image Science and Vision **5**(12): 2080-2086.
- Schaeffel, F. and H. C. Howland (1991). "Properties of the feedback loops controlling eye growth and refractive state in the chicken." Vision Research **31**: 717-34.
- Schaeffel, F. and H. C. Howland (2003). "Letter to editor. Axial length changes in the mouse eye." Invest Ophthalmol Vis Sci **2003**.
- Schaeffel, F., H. C. Howland, et al. (1986). "Natural Accommodation in the Growing Chicken." Vision Research **26**(12): 1977-1993.
- Schaeffel, F., P. Simon, et al. (2003). "Molecular biology of myopia." Clin Exp Optom. **85**(5): 295-307.
- Schaeffel, F., D. Troilo, et al. (1990). "Developing eyes that lack accommodation grow to compensate for imposed defocus." Vision Neuroscience **4**: 177-183.
- Schipper, I., P. Senn, et al. (1995). "Intraocular-Pressure after Excimer-Laser Photorefractive Keratectomy for Myopia." Journal of Refractive Surgery **11**(5): 366-370.
- Schippert, R. and F. Schaeffel (2006). "Peripheral defocus does not necessarily affect central refractive development." Vision Research **46**(22): 3935-3940.
- Schmid, K. L., T. Hills, et al. (2003). "Relationship between intraocular pressure and eye growth in chick." Ophthalmic and Physiological Optics **23**(1): 25-33.
- Schmid, K. L. and C. F. Wildsoet (1996). "Effects on the compensatory responses to positive and negative lenses of intermittent lens wear and ciliary nerve section in chicks." Vision Research **36**(7): 1023-1036.
- Schmid, K. L. and C. F. Wildsoet (1997). "Contrast and spatial-frequency requirements for emmetropization in chicks." Vision Research **37**(15): 2011-2021.
- Schmid, K. L. and C. F. Wildsoet (1998). "Assessment of visual acuity and contrast sensitivity in the chick using an optokinetic nystagmus paradigm." Vision Research **38**(17): 2629-2634.
- Schmucker, C. and F. Schaeffel (2004). "In vivo biometry in the mouse eye with low coherence interferometry." Vision Research **44**(21): 2445-2456.

- Schmucker, C. and F. Schaeffel (2004). "A paraxial schematic eye model for the growing C57BL/6 mouse." Vision Research **44**(16): 1857-1867.
- Schmucker, C., M. Seeliger, et al. (2005). "Grating acuity at different luminances in wild-type mice and in mice lacking rod or cone function." Invest Ophthalmol Vis Sci. **46**: 398-407.
- Schuck, J., H. Gerhardt, et al. (2000). "The peripapillary glia of the optic nerve head in the chicken retina." Anatomical Record **259**(3): 263-275.
- Seaman, A. R. and Himelfar.Tm (1963). "Correlated Ultrafine Structural Changes of Avian Pecten Oculi and Ciliary Body of Gallus Domesticus - Preliminary Observations on Physiology .1. Effects of Decreased Intraocular Pressure Induced by Intravenous Injection of Acetazo Lamide (Diamox)." American Journal of Ophthalmology **56**(2): 278-&.
- Shen, W., M. Vijayan, et al. (2005). "Inducing form-deprivation myopia in fish." Investigative Ophthalmology & Visual Science **46**(5): 1797-1803.
- Sherman, S. M., T. T. Norton, et al. (1977). "Myopia in the lid sutured tree shrew." Brain Research **124**: 154-157.
- Simensen, B. and L. O. Thorud (1994). "Adult-Onset Myopia and Occupation." Acta Ophthalmologica **72**(4): 469-471.
- Singh, K. D., N. S. Logan, et al. (2006). "Three-dimensional modeling of the human eye based on magnetic resonance imaging." Investigative Ophthalmology & Visual Science **47**(6): 2272-2279.
- Sivak, J. G. and T. Mandelman (1982). "Chromatic Dispersion of the Ocular Media." Vision Research **22**(8): 997-1003.
- Sivak, J. G., L. A. Ryall, et al. (1989). "Optical Constancy of the Chick Lens During Pre-Hatching and Post-Hatching Ocular Development." Investigative Ophthalmology & Visual Science **30**(5): 967-974.
- Smith, E., III (1998). "Environmentally induced refractive errors in animals." Myopia and Nearwork. Butterworth Heinemann Oxford.: 57-90.
- Smith, E. L. and L. F. Hung (2000). "Form-deprivation myopia in monkeys is a graded phenomenon." Vision Research **40**(4): 371-381.
- Smith, E. L., C. S. Kee, et al. (2005). "Peripheral vision can influence eye growth and refractive development in infant monkeys." Investigative Ophthalmology & Visual Science **46**(11): 3965-3972.
- Smith, E. L., H. Patsy, et al. (2006). Methods and apparatuses for altering relative curvature of field and positions of peripheral, off-axis focal positions. United States, The Vision CRC Limited (Sydney, AU).
- Smith, G. (2003). "The optical properties of the crystalline lens and their significance." Clin Exp Optom. **86**(1): 3-18.
- Sperduto, R. D., D. Seigel, et al. (1983). "Prevalence of Myopia in the United-States." Archives of Ophthalmology **101**(3): 405-407.
- Straznicky, C. and M. Chehade (1987). "The Formation of the Area Centralis of the Retinal Ganglion-Cell Layer in the Chick." Development **100**(3): 411-420.
- Taberner, J., P. Piers, et al. (2007). "Intraocular lens to correct corneal coma." Optics Letters **32**(4): 406-408.

- Tejedor, J. and P. de la Villa (2003). "Refractive changes induced by form deprivation the mouse eye." Investigative Ophthalmology & Visual Science **44**(1): 32-36.
- Thibos, L., X. Hong, et al. (2002). "Statistical variation of aberration structure and image quality in a normal population of healthy eyes." J Opt Soc Am A **19**: 2329-2348.
- Thibos, L. N., R. A. Applegate, et al. (2000). "Standards for reporting the optical aberrations of eyes." Vision Science and its Applications, OSA Trends in Optics & Photonics **35**: 110-130.
- Thibos, L. N., X. Cheng, et al. (2002). "Optical aberrations of chick eyes." Investigative Ophthalmology & Visual Science **43**: U33-U33.
- Thibos, L. N., P. Faao, et al. (1999). "Clinical applications of the Shack-Hartmann aberrometer." Optometry and Vision Science **76**: 817-825.
- Thorn, F., A. A. V. Cruz, et al. (2005). "Refractive status of indigenous people in the northwestern Amazon region of Brazil." Optometry and Vision Science **82**(4): 267-272.
- Thorn, F., K. Grice, et al. (1999). "Myopia: The blur hypothesis links nature & nurture." Investigative Ophthalmology & Visual Science **40**(4): S448-S448.
- Tian, Y. B. and C. F. Wildsoet (2006). "Diurnal fluctuations and developmental changes in ocular dimensions and optical aberrations in young chicks." Investigative Ophthalmology & Visual Science **47**(9): 4168-4178.
- Tokoro, T. (1988). "Effect of visual display terminal (VDT) work on myopia progression." Acta Ophthalmologica Suppl. **185**: 172-174.
- Tokoro, T. (1988). "On the definition of pathologic myopia in group studies." Acta Ophthalmol. Suppl. **185**: 107-108.
- Troilo, D. (1990). "Experimental Studies of Emmetropization in the Chick." Ciba Foundation Symposia **155**: 89-114.
- Troilo, D., M. D. Gottlieb, et al. (1987). "Visual deprivation causes myopia in chicks with optic nerve section." Curr Eye Research **6**: 993-999.
- Troilo, D. and S. J. Judge (1993). "Ocular development and visual deprivation myopia in the common marmoset (*Callithrix jacchus*)." Vision Research **33**: 1311-1324.
- Troilo, D., T. Li, et al. (1995). "Differences in Eye Growth and the Response to Visual Deprivation in Different Strains of Chicken." Vision Research **35**(9): 1211-1216.
- Troilo, D. and D. L. Nickla (2002). "The response to form deprivation by occluder in the marmoset differs with age of onset." Investigative Ophthalmology & Visual Science **43**: U34-U34.
- Troilo, D., D. L. Nickla, et al. (2000). "Form deprivation myopia in mature common marmosets (*Callithrix jacchus*)." Investigative Ophthalmology & Visual Science **41**(8): 2043-2049.
- Troilo, D. and J. Wallman (1987). "Changes in Corneal Curvature During Accommodation in Chicks." Vision Research **27**(2): 241-247.
- Troilo, D. and J. Wallman (1991). "The regulation of eye growth and refractive state: an experimental study of emmetropization." Vision Research **31**: 1237-50.

- Tuunanen, T. H. and T. T. Tervo (1998). "Results of photorefractive keratectomy for low, moderate, and high myopia." Journal of Refractive Surgery **14**(4): 437-446.
- Ursekar, A. (1983). "Classification, etiology and pathology of myopia." Indian Journal of Ophthalmology **31**(6): 709-711.
- Van Alphen, G. (1961). "On emmetropia and ametropia." Opt Acta (Lond) **142 (Suppl.)**: 1-92.
- Varughese, S., R. M. Varghese, et al. (2005). "Refractive error at birth and its relation to gestational age." Current Eye Research **30**(6): 423-428.
- Vilupuru, A. S., A. Roorda, et al. (2004). "Spatially variant changes in lens power during ocular accommodation in a rhesus monkey eye." Journal of Vision **4**(4): 299-309.
- Wallman, J. (1993). "Retinal Control of Eye Growth and Refraction." Progress in Retinal Research **12**: 133-153.
- Wallman, J. and J. I. Adams (1987). "Developmental Aspects of Experimental Myopia in Chicks - Susceptibility, Recovery and Relation to Emmetropization." Vision Research **27**(7): 1139-1163.
- Wallman, J. and J. I. Adams (1987). "Developmental aspects of experimental myopia in chicks: susceptibility, recovery and relation to emmetropization." Vision Research **27**: 1139-1163.
- Wallman, J., J. I. Adams, et al. (1981). "The Eyes of Young Chickens Grow toward Emmetropia." Investigative Ophthalmology & Visual Science **20**(4): 557-561.
- Wallman, J., J. Turkel, et al. (1978). "Extreme myopia produced by modest change in early visual experience." Science **20**: 1249-1251.
- Wallman, J., C. Wildsoet, et al. (1995). "Moving the retina: choroidal modulation of refractive state." Vision Research **35**: 37-50.
- Wallman, J. and J. Winawer (2004). "Homeostasis of eye growth and the question of myopia." Neuron **43**(4): 447-468.
- Wang, J. Y. and T. R. Candy (2005). "Higher order monochromatic aberrations of the human infant eye." Journal of Vision **5**(6): 543-555.
- Wang, L. and D. D. Koch (2004). "Age-related changes in corneal and ocular higher-order aberrations." American Journal of Ophthalmology **138**(5): 897-897.
- Weisel, T. N. and E. Raviola (1977). "Myopia and eye enlargement after neonatal lid fusion in monkeys." Nature **266**: 66-68.
- Whatham, A. R. and S. J. Judge (2001). "Compensatory changes in eye growth and refraction induced by daily wear of soft contact lenses in young marmosets." Vision Research **41**(3): 267-273.
- Wickremasinghe, S., P. J. Foster, et al. (2004). "Ocular biometry and refraction in mongolian adults." Investigative Ophthalmology & Visual Science **45**(3): 776-783.
- Wiesel, T. N. and E. Raviola (1977). "Myopia and Eye Enlargement after Neonatal Lid Fusion in Monkeys." Nature **266**(5597): 66-68.
- Wildsoet, C. and J. Wallman (1995). "Choroidal and scleral mechanisms of compensation for spectacle lenses in chicks." Vision Research(35): 1175-1194.

- Wildsoet, C. F. (1997). "Active emmetropization - Evidence for its existence and ramifications for clinical practice." Ophthalmic and Physiological Optics **17**(4): 279-290.
- Wilson, B. J., K. E. Decker, et al. (2002). "Monochromatic aberrations provide an odd-error cue to focus direction." Journal of the Optical Society of America a-Optics Image Science and Vision **19**(5): 833-839.
- Winawer, J. and J. Wallman (2002). "Temporal constraints on lens compensation in chicks." Vision Research **42**(24): 2651-2668.
- Wolburg, H., S. Liebner, et al. (1999). The pecten oculi of the chicken: A model system for vascular differentiation and barrier maturation. International Review of Cytology - a Survey of Cell Biology, Vol 187. **187**: 111-159.
- Yinon, U. (1984). "Myopia induction in animals following alteration of visual input during development: a review." Curr. Eye Res. **3**: 677-690.
- Yinon, U., L. Rose, et al. (1980). "Myopia in the Eye of Developing Chicks Following Monocular and Binocular Lid Closure." Vision Research **20**(2): 137-&.
- Young, F. A., G. A. Leary, et al. (1969). "Transmission of Refractive Errors within Eskimo Families." American Journal of Optometry and Archives of American Academy of Optometry **46**(9): 676-&.
- Young, T., P. Paluru, et al. (2001). "A new locus for autosomal dominant high myopia maps to chromosome 17q21-23." American Journal of Human Genetics **69**(4): 526-526.
- Young, T. L., P. C. Palura, et al. (2005). "Mutation screening of 6 positional candidate genes for the autosomal dominant high-grade myopia 5 locus." Investigative Ophthalmology & Visual Science **46**.
- Young, T. L., S. M. Ronan, et al. (1998). "Evidence that a locus for familial high myopia maps to chromosome 18p." American Journal of Human Genetics **63**(1): 109-119.
- Zadnik, K. and D. O. Mutti (1987). "Refractive Error Changes in Law Students." American Journal of Optometry and Physiological Optics **64**(7): 558-561.
- Zadnik, K., W. A. Satariano, et al. (1994). "The Effect of Parental History of Myopia on Childrens Eye Size." Jama-Journal of the American Medical Association **271**(17): 1323-1327.
- Zhao, J. L., X. J. Pan, et al. (2000). "Refractive Error Study in Children: Results from Shunyi District, China." American Journal of Ophthalmology **129**(4): 427-435.
- Zhong, X. W., J. Ge, et al. (2004). "Effects of photorefractive keratectomy-induced defocus on emmetropization of infant rhesus monkeys." Investigative Ophthalmology & Visual Science **45**(10): 3806-3811.
- Zhu, X. S., T. Lin, et al. (1995). "Sex-Differences in Chick Eye Growth and Experimental Myopia." Experimental Eye Research **61**(2): 173-179.
- Zhu, X. Y., J. A. Winawer, et al. (2003). "Potency of myopic defocus in spectacle lens compensation." Investigative Ophthalmology & Visual Science **44**(7): 2818-2827.
- Ziylan, S., D. Serin, et al. (2006). "Myopia in preterm children at 12 to 24 months of age." Journal of Pediatric Ophthalmology & Strabismus **43**(3): 152-156.

Zylbermann, R., D. Landau, et al. (1993). "The Influence of Study Habits on Myopia in Jewish Teenagers." Journal of Pediatric Ophthalmology & Strabismus **30**(5): 319-322.